Springer Hydrogeology

Majid Hosseini
Muhammad Aqeel Ashraf

Application of the SWAT Model for Water Components Separation in Iran

Springer

Springer Hydrogeology

More information about this series at http://www.springer.com/series/10174

Majid Hosseini · Muhammad Aqeel Ashraf

Application of the SWAT Model for Water Components Separation in Iran

Springer

Majid Hosseini
Soil Conservation and Watershed
Management Research Institute
(SCWMRI)
Tehran
Iran

Muhammad Aqeel Ashraf
Department of Geology
University of Malaya
Kuala Lumpur
Malaysia

Springer Hydrogeology
ISBN 978-4-431-55563-6 ISBN 978-4-431-55564-3 (eBook)
DOI 10.1007/978-4-431-55564-3

Library of Congress Control Number: 2015938316

Springer Tokyo Heidelberg New York Dordrecht London

Printed on acid-free paper

Springer Japan KK is part of Springer Science+Business Media (www.springer.com)

Preface

This current book is an attempt to reveal some aspects of hydrologic processes affected in water components separation in a water supply catchment by the application of soil and water assessment tools (SWATs) in Iran. The SWAT model is a continuation of nearly 30 years of modeling efforts conducted by the USDA Agricultural Research Service. Modeling is the main approach to the separation of water components' in catchment outlets with diverse soils, land use, and slopes. Most models are not useful for this purpose. The utilized empirical model performs successfully only within a calibrated range. Lumped conceptual models cannot also be used to predict the impacts of land use change on catchment hydrology. Because these models treat the catchment as a single unit, they ignore the tremendous heterogeneity of hydrological responses resulting from the spatial and temporal variability of climate, topography, soils, and vegetation.

One of the principal motivations for the development of distributed, physically based models was to predict the impacts of land use change. Physically based models can, in principle, overcome many of the deficiencies associated with lumped conceptual models through their use of parameters that have a physical interpretation and through their representation of spatial variability in the parameter values. Therefore, a simple GIS interface physically based and computationally efficient distributed model needs to be chosen for the evaluation of the effects of land use change on water components' separation on catchment hydrology and water balance. It has been found that most of the distributed or physically based hydrological and water quality models from developed countries are not suitable to be directly used in developing countries due to both a lack of data and different climatic conditions. The SWAT model is utilized extensively in advanced countries for investigating the impacts of land use change on water balance but has not yet been widely adopted in Iran despite being regarded as having a very good potential for such a purpose. The successful application of this model to this particular catchment will highlight the potential success of its application to other catchments in Iran.

Contents

Abbreviations

%	Percent
°C	Degree Celsius
^{137}Cs	Cesiun One Thirty Seven
A_d	Catchment Area
A_f	Flood Plain Area
AI	Dryness Coefficient
CSDR	Channel Sediment Delivery Ratio
DEM	Digital Elevation Model
DF	Dry Farming
Dv	Deviance
EPM	Erosion Potential Method
ER	Erosion Rate
ET	Evapotranspiration
GDP	Gross Domestic Product
GIS	Geographic Information System
Gs	Average Yearly Sediment Amount
HSDR	Hillslope Sediment Delivery Ratio
IDF	Inactive Dry Farming
km^2	Kilometer Square
$km^3\ year^{-1}$	Kilometer Cube Per Year
$kt\ year^{-1}$	Kilo Ton Per Year
LLNP	Lore Lindu National Park
LUCK	Land Use Change Modeling Kit
LULC	Land Use and Land Cover
MARE	Mean Absolute Error
$mg\ L^{-1}$	Milligram Per Litter
MLC	Maximum Likelihood
mm	Millimeter
MR	Moderate
NO_3^-	Nitrate
P	Precipitation

PR	Poor
Q	Observed Streamflow
Q	Streamflow Out of the Basin
Q′	Simulated Streamflow
Qb	Base Flow
QMLE	Quasi-Maximum-Likelihood Estimator
Qs	Stormflow
RUSLE	Revised Universal Soil Loss Equation
SC	Sediment Concentration
SDR	Sediment Delivery Ratio
SSY	Specific Sediment Yield
SWAT	Soil and Water Assessment Tools
SY	Sediment Yield
t ha^{-1} yr^{-1}	Ton Per Hectare Per Year
UMR	Upper Mississippi River
USLE	Universal Soil Loss Equation
X	Observed Value
X′	Simulated Value

Chapter 1
Application of Hydrological Models Related to Land Use Land Cover Change

Abstract Anthropogenic activities such a clearing tropical forests, adapting subsistence in agriculture, escalating farmland production or growing urban areas and infrastructure change worlds landscape in ubiquitous ways. For the purpose of obtaining fresh water for irrigation, industry and domestic consumption, human activities have changed the natural hydrological cycle. Fertilizers and chemicals directly entering the environment, putting effect on water quality and ecological units. Worldwide water withdrawal is nearly 3900 km^3 $year^{-1}$. Agriculture contributes 85 % of world wide consumption decreasing water table in various regions causing water balance fluctuation. Upper Mississippi River (UMR) basin and river basin in Lowa suggest ancient LULC changes compressed basin scale water balance. Cumulative stream flow trends found better than cumulative precipitation alone. Disturbance in water balance causes the transfer of pollutants to streams and finally to Gulf of Mexico. Influence of land use changes on storm runoff comprised three parts (i) generation of spatially explicit land use scenario (ii) generation of spatially distributed and process based runoff hydrological models (iii) interpretation, demonstration and dissemination of results.

Keywords Land use activities · Evapotranspiration · Sediment flux · Suspended sediment budget

1.1 Response of Water Balance to Land Use Changes

Land-use activities whether converting natural landscapes for human use or altering management practices on human-dominated lands, have transmuted a large fraction of the earth, acreage surface. Anthropogenic activities such as clearing tropical forests, adapting subsistence agriculture, escalating farmland production or growing urban areas and infrastructure, are shifting the world, s landscapes in ubiquitous ways (Fig. 1.1) (DeFries et al. 2004). Though land-use activities differ significantly across the world, their ultimate consequence is mostly the same, the attainment of natural resources for instant human requirements, normally at the

M. Hosseini and M.A. Ashraf, *Application of the SWAT Model for Water Components Separation in Iran*, Springer Hydrogeology,
DOI 10.1007/978-4-431-55564-3_1

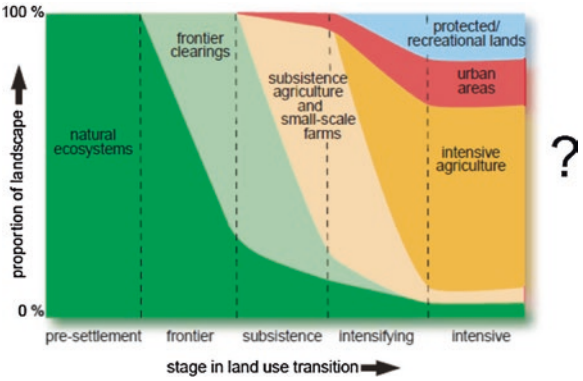

Fig. 1.1 Land use alteration

outlay of disturbing environmental conditions. Land-cover changes also disturb the water balance and surface energy in turn modifying the local climates (Pielke 2001; Kalnay and Cai 2003).

The hydrologic cycle has been altered by human activities to make available freshwater for irrigation, industry, and domestic consumption (Postel et al. 1996; Vörösmarty et al. 2000). Moreover, anthropogenic chemicals enter the environment from fertilizers and atmospheric contaminants exceeding the natural sources and have pervasive effects on water quality and coastal and freshwater ecological units (Matson et al. 1997; Bennett et al. 2001). Land use can disturb the surface water balance and the partitioning of precipitation into evapotranspiration, runoff, and groundwater flow. Surface runoff and river discharge usually upsurge when natural vegetation (particularly forest) is cleared (Sahin et al. 1996; Costa et al. 2003). For example the Tocantins River basin in Brazil presented a ~25 % upsurge in river discharge between 1960 and 1995, coincident with intensifying agriculture but no prominent variation in precipitation (Costa et al. 2003).

Supply of fresh water is openly influenced by water demand related with land-use activities, particularly irrigation through water extractions and alterations. Nowadays, worldwide water withdrawals is total ~3900 km^3 $year^{-1}$, or ~10 % of the entire worldwide renewable resource, and the consumptive use of water (not resumed to the watershed) is assessed to be ~1800–2300 km^3 $year^{-1}$ (Gleick 2003; Shiklomanov 1998). Only agriculture contributes ~85 % of worldwide consumptive use (Gleick 2003). The end result is that several large rivers, particularly in semiarid areas, have significantly reduced flows, and some routinely dry up (Rosegrant et al. 2002; Postel 1999). Furthermore, the withdrawal of groundwater reserves is nearly collectively unsustainable and has caused the decreasing water tables in various regions (Rosegrant et al. 2002; Postel 1999).

A number of studies conducted by Turkelboom et al. (2008); Wijesekara et al. (2010); Mawardi (2010) have manifested that the land changes triggered by the growth of urbanization, agricultural practices and distressed forests region are origin of water balance fluctuations. The term of water balance refers to "the balance between input and output of water from precipitation and the outflow of water by evapotranspiration, groundwater recharge and stream flow".

Land use and land cover (LULC) change is possibly the maximum perceptible response of the agriculture sector to these exterior elements such as developments in technology, better-quality fertilizer and pest management, and fluctuating market forces. Farmers acclimatize to changing environments by exploiting their land in a manner which produces the highest return on their investment of time, energy and money. In the past, the effects of LULC changes on water resources were generally ignored or considered a side effect of development (i.e., "not planned" (Scanlon et al. 2005), however nowadays it is accepted that an assessment of historical influences may be used to comprehend our existing condition and predict concerns of future LULC change on water resources. Exterior aspects that subsidized to the modification in LULC change in the past continue to shape the direction of LULC change in the future.

Indication from the Upper Mississippi River (UMR) basin and river basins in Iowa strongly suggest that the ancient LULC change has compressed the basin-scale water balance (Schilling and Libra 2003; Zhang and Schilling 2006). Since the mid-20th century, numerous Iowa rivers have had growing drifts in yearly streamflow, least streamflow, annual base flow and the ratio of yearly base flow to streamflow (Schilling and Libra 2003). The cumulative streamflow trends were found to be better than cumulative precipitation alone could elucidate. Increasing yearly base flow was considerably associated to growing row crop intensity in their watersheds (Schilling 2005). Related investigation extended to the UMR basin specified that streamflow in several large rivers draining row crop-dominated states exhibited indication for increasing trends over the last 60 years (Zhang and Schilling 2006). The detected streamflow changes can be clarified by considering the water balance for a large watershed over a long period of time (several years) when the variation in storage can be ignored (Gupta 1989):

$$P = Q + ET \tag{1.1}$$

where P symbolizes precipitation, Q symbolizes streamflow out of the basin, and ET symbolizes evapotranspiration. Likewise supposed in Eq. (1.1) is that anthropogenic extractions (i.e., pumping) are insignificant. On the basis of Eq. (1.1) and supposing there is no variation in P, Q becomes larger for watersheds dominated by seasonal crops compared to watersheds dominated by perennial vegetation as there is a smaller amount of annual ET loss from seasonal row crops compared to perennial vegetation (Brye et al. 2000; Food and Agriculture Organization of the United Nations 1998). As Q is composed of base flow (Qb) and stormflow (Qs), increasing Q in a watershed may be the outcome of increasing Qb, Qs or both. Hydrograph separation of streamflow records in Iowa and the UMR shows that Qs remains more or less persistent and that the cumulative yearly streamflow was largely due to an upsurge in base flow or groundwater discharge to a river (Schilling and Libra 2003; Zhang and Schilling 2006). A considerable increase of streamflow and base flow can be found to increased groundwater recharge during the spring when seasonal crop fields are freshly cultivated or uncultivated (Zhang and Schilling 2006).

Changing LULC alone that caused in increased water transfer from agricultural watersheds would not be reflected a serious concern. Nevertheless, as water is the

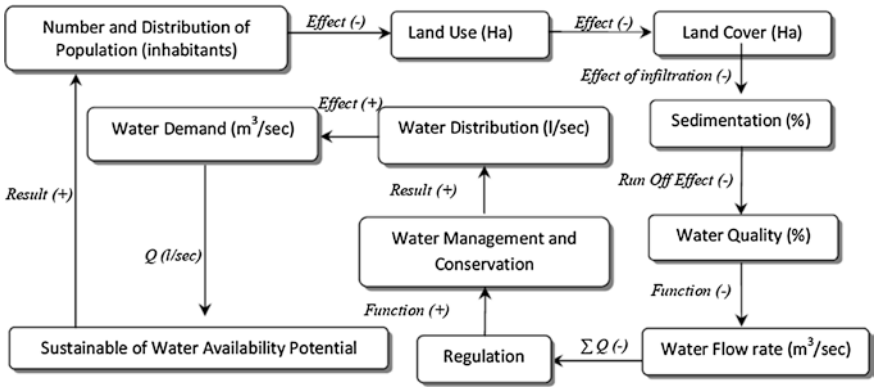

Fig. 1.2 Effect of land use changes on water balance and management cycle in urban watershed

transporter of agricultural contaminants, altering the water balance of a watershed has potential to disturb the pollutant transfer to streams and eventually to the Gulf of Mexico. For instance, nitrate (NO_3^-) is mostly carried to streams through base flow and tile drainage (Hallberg 1987; Schilling and Zhang 2004), so intensification in yearly base flow may account to more nitrate transported to surface water. Twofold and threefold upsurge in nitrate level have been observed in Iowa rivers during the 1940–2000 period (National Agricultural Statistics Service, Quick Stats 2006, http://www.nass.usda.gov/QuickStats/Create_County_All.jsp). A change in the annual water balance to more surface water runoff would cause an increasing phosphorus transfer from a watershed (Steegen et al. 2001; McDowell et al. 2001). Extreme delivery of nitrate and phosphorus to the Mississippi River from the agricultural Midwest have been involved in subsidizing to Gulf of Mexico hypoxia (Goolsby et al. 1999; Rabalais et al. 2002). Figure 1.2 represents the overall effects of land use changes on water quality and water balance, and management strategies in urban watershed.

1.1.1 Response of Runoff Generation and Flood to Land Use Changes

One requirement for the evaluation of the impacts of predicted changes in land use and/or land cover on runoff generation is application of one land use scenario or more. A modeling kit known as land use change modeling kit (LUCK) is a source of spatial conversion of the whole trends in land uses into spatially-distributed scenarios of land use patterns, taking into consideration their topology in a true position mode. The assignment of land use classes to each grid cells is comprehended in a spatially categorical way, reliant on an estimation of the characteristics of the location as well as of its interactions with its neighborhood.

The influences of land use changes on storm runoff generation, regarding quantity and quality, in Southwest Germany was explored by (Niehoff et al. 2001). Their outcomes were deliberated in light of a simulation study that was comprised of three parts (1) generation of spatially explicit land-use scenarios; (2) generation of spatially distributed and process-based runoff hydrological models; (3) interpretation, demonstration, and dissemination of results. They addressed the main questions which nearly constantly contribute for the boundary conditions of land use dynamics as well as for the spatial and temporal scale of the hydrological and meteorological processes elaborated:

1. What kinds of land use changes have been described in the past? What kind of land use changes can be anticipated in the future? And what possible spatial distributions of these deviations in the landscape will these variations have?
2. Which runoff generation mechanisms (i.e., infiltration excess, overland flow, saturation excess, subsurface storm flow, and quick groundwater outflow) will possibly be influenced by land use and land cover changes? And how hydrological model can exemplify them?
3. How are the effects of land use and land cover changes on storm-runoff generation interrelated to features of rainfall events and temporal trends? And what is the relative importance of catchment characteristics and its spatial scale?

Incited by looking for an answer to these critical questions, on the one hand, and in order to achieve the objectives of study, on the other, Ashraf et al. (2014) selected three dissimilar catchments within the Rhine basin. Their size was in range of 100–500 km^2. One catchment area was representing a different features of land use pattern; primarily urban, agricultural, or forested. Their outcomes reveal that the impact of land use conditions on storm runoff generation to a large extent relies on the features of related rainfall events and on the corresponding spatial scale. In other words, high precipitation intensities with convective storm events have strong impacts as compared to low precipitation intensities with long-lasting adjective storm events. Nonetheless, formation of floods in large river basins is slightly dependent on convective events and accordingly land use conditions therefore this type of rainfall events is usually restricted to small scale incidents.

Subsequent modeling of land use change effects on runoff generation of a river basin was employed by Hundecha and Bardossy (2004), and it was examined that growth of urbanization increases the lower peak runoff resulting from summer storms, on the contrary higher peaks have very little response to winter rainfall. Outcomes of this investigation display a significant decrease both in peak runoff and total runoff volumes as a consequence of intensified afforestation.

Long-lasting influences of land use change on catchment runoff in semi-arid Zimbabwe was investigated by Kristian et al. (1998), on the basis of evaluation of long hydrological time series ranging from 25 to 50 years from six non-experimental catchments located in countryside and 200–1000 km^2 in size range. A methodology was implemented by coupling common statistical methods with hydrological modeling to discriminate between the impacts of climate changeability and those of land use change. Generally the hydrological model NAM had

potential to simulate the detected hydrographs in a good manner throughout the reference period, hence providing a source to contribute to the impacts of climate changeability and then make stronger the effects of following statistical tests. An authorized model was employed to make available the runoff record during the test period which would have happened in the nonappearance of land use change. The investigation specified a decline in the yearly runoff for most of the six catchments, with the major variations taking place for catchments found within public acreage where a significant intensification in agriculture and growth of population had occurred. Nevertheless, only in the case of one catchment, the decline was merely statistically significant at the 5 % level.

De Roo et al. (2001) explored the origins of the flooding and the impacts of land use changes, soil features and predecessor catchment moisture conditions on flooding, and then generated a model LISFLOOD for disturbed catchment. Runoff in large river basins is triggered by LISFLOOD. The model was implemented on two transnational European river basins in order to certify it: the Meuse catchment (France, Belgium, Germany and The Netherlands) and the Oder basin (The Czech Republic, Poland and Germany). Land use change facts over the past 200 years were administered at the instant of model testing in both catchments. In order to trigger the impacts of these land use changes on floods, the LISFLOOD model is implemented.

1.1.2 Response of Evapotranspiration to Land Use Changes

Impacts of land use changes on hydrology have been comprehensively described by Calder (1993). The key deviations in land uses such as afforestation, deforestation, intensification of agriculture, drainage of wetlands, construction of roads, and urbanization impose strong impacts on the catchment hydrology. Though, the most prominent impact imposed by land use changes on the water balance of the river catchment is evapotranspiration process (Calder 1993). In addition, evapotranspiration rates vary with land covers. Dissimilar crops having diverse leaf area indices, vegetation covers, albedo and root depths, and may contribute to this point.

In Indonesia, Olchev et al. (2008) manifested the influence of deforestation and land use changes on evapotranspiration process of mountainous tropical rain forest zone situated in the northern part of the Lore-Lindu National Park (LLNP) in Central Sulawesi (Indonesia). By implementing a regional process-based SVAT model "SVAT-Regio", they computed above constituents. The outcomes specified a deforestation scenario (allowing for mainly anthropogenic impacts) which was employed assumes a comparatively significant decline of the zones covered by tropical rain forests, i.e. about 15 %, and an intensification of agricultural (coffee plantations, corn and rice fields) and urban areas. Furthermore, a little upsurge of grassland zone is also considered by scenario. The consequences of modeling experiments display that 15 % deforestation of the study zone results in comparatively a slight reduction of monthly evapotranspiration by about 2 %, transpiration by about 6 % and interception evaporation by about 5 %, along with a rise of

soil evaporation by about 21 %. The maximum decline in evapotranspiration was found in cloudy days and rainy weather conditions; on the contrary, it was found minimum in dry and sunny and days.

Equally important, the relevant interception rates during storms vary with nature of land cover to another. Although it is well-established that interception losses specify a substantial net increase in evaporative losses of catchment (Ward and Robinson 1990), the stated impacts of interception only influence surface run-off rates and are only perceptible during small storms; in the case of largest storms and food events, they pose non-significant impacts (Calder 1993). Land uses also disturb the infiltration and soil water redistribution processes as particularly the saturated hydraulic conductivity is affected by plant roots and pores resulting from soil fauna (Ragab and Cooper 1993). The effects of urban areas and roads construction on overland flow stands as a patent model on such impacts of land cover types on the infiltration and soil water redistribution processes. Lastly, land use affects roughness of surface and in turn velocity of overland flow and flow rates of floodplain are controlled by it.

Several impacts of land use and vegetation on the water balance have been explained, for instance those of the shifting vegetation cover (leaf area index) which will affect evapotranspiration. But not so much is clear about the impacts of vegetation on soil characteristics, which affects infiltration and soil water redistribution through flow and groundwater recharge. Even though the exact influences of deforestation on catchment water balance is quiet unclear (Bonell and Gilmour 1978), there appears to be no uncertainty that land uses affect the hydraulic cycles. Definitely, not so much is clear about the computable effects of vegetation on the aforementioned processes. One of the main questions is how flora affects the evapotranspiration, infiltration, soil water redistribution and their controlling parameters as well.

It is verified that a non-significant difference exists between physical characteristics of soils of different areas selected for study (Cernusca et al. 1999). The noticeably complex organic perspectives of abandoned zones and a large amount of water can be retained by forestry as compared to that of intensively managed hay meadows; in contrast opposite is proved for the mineral soil perspective. In the upmost section of the mineral soil perspective, wide pores and infiltration rates together upsurge from intensively managed hay meadows to forests. It may be attributed to the alterations in litter configuration and quantity, rise of root biomass and subsequent alterations in humus content. Conversely, field capacity declines with the proliferation of wide pores. Soil of similar properties subjected to intensively managed hay meadows consequently represents the higher water retaining capacity and more plan-available water than under cheap management. Overall, these dissimilarities in soil physical characteristics don not considerably influence the soil water balance. Nevertheless, discrete dissimilarities are visible in evapotranspiration rates of the selected land use types; ample amount of water is transpired into atmosphere by forests and hay meadows than e.g. grasslands and unplanted fields. Rates of evapotranspiration were found in range of 38–58 % of precipitation across all land-use type. The water left behind infiltrates the soils or, to a minor extent, runs off the surface to finally enter the watercourses (Bakar

et al. 2015). The consequences of fluctuations in evapotranspiration rates become apparent in area water balance models of the smallest watersheds; the end result of the entire reforestation of previously cultivated zones would be decrease in run-off of 7–52 % (Bou-Vinals unpublished), hence there is a remarkable risk of flooding because of fluctuations in forest cover.

1.2 Response of Sediment Yield to Land Use Changes

Increased sediment yields from river basins as a consequence of accelerated erosion triggered by reduction of vegetation cover, agricultural activities, land use change, and other forms of catchment disturbance have been increasingly documented as a serious environmental concern in several areas of the world (Gellis et al. 2006). The suspended sediment load is a water quality component with two aspects. Its elimination from the soil in surplus amounts might be harmful to the soil productivity. In contrast, the suspended sediment in a watercourse is a form of a pollutant, by itself and by being a transporter of adsorbed elements such as metals and organics. Thus, not only the enhancement of water quality, but also the eradication of erosion is of equal importance to control the suspended sediment in a watercourse and on a watershed. Nevertheless, two main advantageous aspects of suspended sediment are unnoticed. Suspended sediment can be utilized as a fertilizer when applied on land contiguous to the watercourse during floods as well as a vital source of sediment to coastal zones with beaches (Albek and Albek 2003).

The outcomes of investigations related to erosion plot and catchment experiments studies in several diverse zones of the world offer a clear indication of a significant association of soil erosion rates to land use and correlated anthropogenic activities. It is illustrated by Table 1.1 that the transformation of natural vegetation to cultivation can accelerate rates of soil erosion by an order of magnitude or more. Accelerated soil erosion rates can be predictable to give rise to enhanced sediment transportation by indigenous watercourses and findings of many previous experiments of catchment have proved that reduction of vegetation cover or land

Table 1.1 A contrast of soil erosion rates under natural uninterrupted conditions and under farming in particular regions of the world

Region	Land use changes	Increase in sediment yield	Reference
Zulkifley et al. (2014) NewZealand	Clearfelling	X8	O'Loughlin et al.
Oregon, U.S.A.	Clearfelling	X39	Bakar et al. (2015)
Northern England	Afforestation (ditching and ploughing)	X100	Painter et al. (1974)
Texas, U.S.A.	Forest clearance and cultivation	X310	Chang et al. (1982)
Maryland, U.S.A.	Building construction	X126-375	Wolman and Schick (1967)

Table 1.2 Selected outcomes from investigational basin studies of the effects of land use variations on sediment yield

Country	Natural (kg m^{-2} $year^{-1}$)	Cultivated (kg m^{-2} $year^{-1}$)
China	<0.20	15.00–20.00
U.S.A.	0.003–0.30	0.50–17.00
Ivory coast	0.003–0.02	0.01–9.00
Nigeria	0.05–0.10	0.01–3.50
India	0.05–0.10	0.03–2.00
Belgium	0.01–0.05	0.30–3.00
U.K.	0.01–0.05	0.01–0.30

use change can again cause upsurges in sediment yield of an order of magnitude or more (Table 1.2). According to Abernethy (1990) who conducted the experiments over many small reservoir catchments in Southeast Asia then suggested that throughout the current century yearly sediment yields have successively enhanced by 2.5–6 % $year^{-1}$ as a consequence of reduction of vegetation cover and consequent increase of land use (Fig. 1.3). Abernethy found that the ratio of the intensification in sediment yield to that for population was larger than unity and averaged 1.6:1 accompanying these changes to manipulation rate of population. Based on these outcomes he stated that yearly suspended sediment yields from river basins in many unindustrialized states could be likely to twofold within almost 20 years. If the aforementioned overviews are combined with evidence on intensification of world population and the overall degree of reduction of vegetation cover on land and increase of land use, which specifies, for instance, that the zone of the earth, s surface rendered crop yield and livestock grazing has enhanced by more than five times over the past 200 years (Buringh and Dudal 1987), key enhancements in the sediment loads of the world's rivers could be incidental (Douglas 1967). The existing confirmation concerning the influences of anthropogenic activities and land use change on the sediment loads of the world's rivers, is still less clear-cut. Prevailing assessments of the overall transmission of sediment from the land surface of the globe to the oceans proves that existing flux is around 20–109 tons $year^{-1}$ (Milliman and Syvitski 1992; Walling and Webb 1996), nonetheless, the degree to which this value has amplified over and above the 'natural value' remains undefined.

Sedimentation decreases the storage capacity of reservoirs worldwide (Gharibreza et al. 2014; Palmeiri et al. 2001; Nagle et al. 1999). White (2001) and Mahmood (1987) determined that the global rate of sedimentation in reservoirs is 1 % $year^{-1}$. Most reservoirs are constructed to be operational for 50–100 years, before sedimentation makes them useless (Gharibreza et al. 2013a). The study of impact of reservoir sedimentation has been conducted in detail in Africa (Ward 1980; Jordan 1989; Shahin 1993), Asia (Ongkosongo et al. 1992), Australia (Gharibreza et al. 2013b), and the United Kingdom (Gharibreza et al. 2013c). Figure 1.3 shows trends of growing sediment yield in numerous reservoir catchments in Southeast Asia (Abernethy 1990).

Anthropogenic activities and their effects on reservoirs can enhance the sedimentation rate (Ongkosongo et al. 1992; Renwick 1996). The implementation of effective

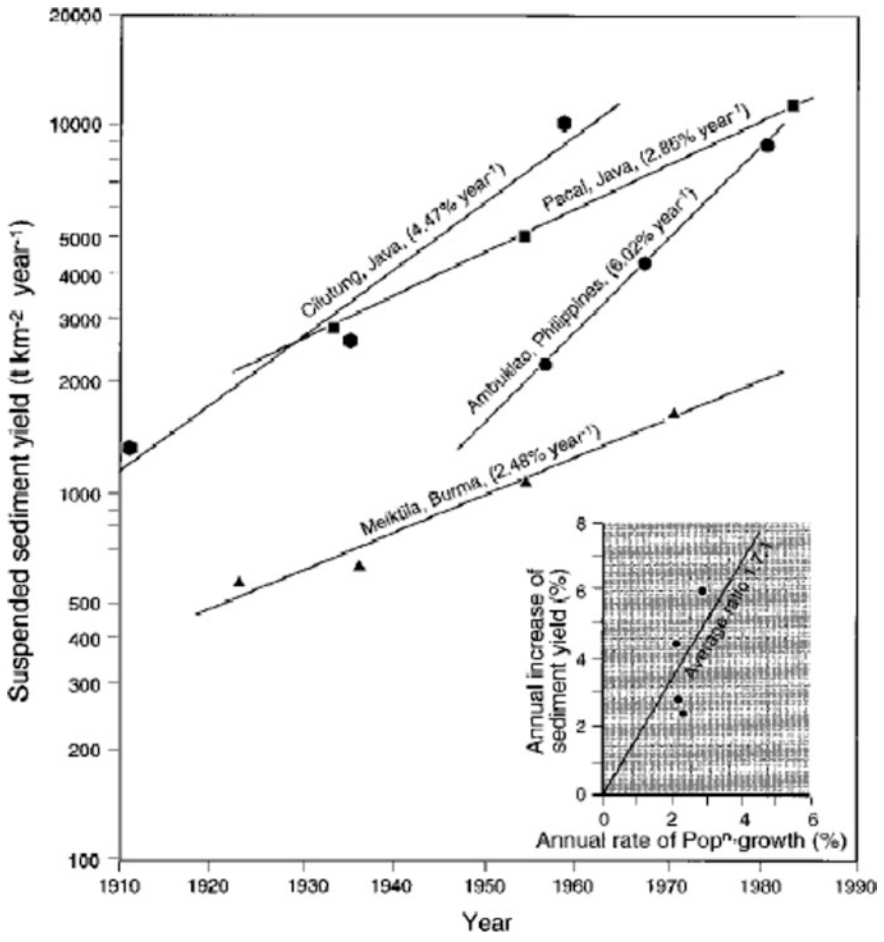

Fig. 1.3 Trends of growing sediment yield in numerous reservoir catchments in Southeast Asia (Abernethy 1990)

approaches to decrease sedimentation rates involves distinction between erosion rates in unaffected reservoirs and man induced erosion in effected reservoirs (Ongkosongo et al. 1992; Palmeiri et al. 2001; Nagle et al. 1999). First project related to sedimentation of reservoir initiated in Puerto Rico in the 1940s and two-third of 65 reservoirs was involved in study in the United States (Fig. 1.4) (Nevares and Dunlop 1948). The sedimentation rates were found highest for three reservoirs, Puerto Rico-Comerío, Coamo, and Guayabal. Geologic conditions, deforestation, and intensive cultivation of steep slopes were contributed to the maximum erosion rates.

According to Gharibreza et al. (2013d), who observed the effects of land use change on sediment yield in the Zagbo River Catchment in Southern Benin. It was reported that 59 % increase in cultivated surface from 1,080,000 ha in 1962 to 1,717,000 ha in 1994 (FAO 1997). Land was not adequate because of dense

Fig. 1.4 Photograph presenting complete sedimentation in Comerío Reservoir in 1989. The reservoir was built in 1914 with a storage capacity of 6.06 × 106 m^3 and by 1935, was almost 70 % filled with sediment (Nevares and Dunlop 1948)

population and immigration and as a consequence, cultivation of crops intensified and the crop-free period shortened. With this dense population and intensified cropping system, farming practices were transforming from semi-permanent to constant cropping practices consequently making the outdated ways of reestablishing soil fertility via fallow unviable. Eventually, this leads to drop in agricultural yield. The trial was to bring to pause the negative trend in agricultural yield because of soil erosion and soil degradation, and to reverse the drop of the healthy base (soil). The Soil and Water Assessment Tool (SWAT) was employed to predict the impacts of different land management scenarios on sediment yield in this zone. The outcomes of SWAT model simulation in this project manifested the sensitivity of subbasins to develop sediment yield (eight subbasins extracted from a topographic map).

1.2.1 Response of Sediment Flux to Land Use Changes

Indications from previous long-term records of sediment load suggest that river sediment fluxes are sensitive to various impacts, comprising reservoir construction, reduction of vegetation cover and land use change, other types of land disturbance, involving mining activity, soil and water conservation measures and sediment management practices and climatic changes. Some of these impacts are source of accelerated sediment loads, while others, specifically soil and water storage and sediment management practices, and reservoir construction reduced the sediment fluxes. In various cases, it is hard to unravel the impacts of climate variation from that of other variation in catchment condition. Even though there is clear confirmation that the sediment loads of some rivers are fluctuating, others exhibit little

confirmation of any major temporal trend. This could reveal either shortage of variation in the controlling elements or the buffering of any variation by the river basin. In order to evaluate the existing trends in the sediment loads of the world's rivers, 145 large rivers were selected and their yearly runoff and sediment load were calculated. Based on investigation of 50 % of the sediment load data proved to be statistically significant increasing or decreasing trends, mostly indicating decreasing loads. When yearly runoff series considered, statistically significant trends were followed by a small number of rivers i.e. 30 %. From many previous studies it is proved that reservoir construction is possibly the greatest significant impact on land-ocean sediment fluxes; however the influence of other factors causing increase of sediment loads could be identified as well. A long-term and larger record however, is requisite to make available more perfect evaluation of existing trends in land-ocean sediment transport by the world's rivers (Walling and Fang 2003).

A study was conducted by Gharibreza et al. (2013e) to investigate the strong impacts of variations in climate and land use on the mobilization of fine sediment and the net transfer of wash load from the upstream basin to the lower Rhine delta. Geographical information system-embedded models was employed to simulate the yield, and transfer of wash load through the drainage network and settlement on floodplains along the lower river beaches. The outcomes of model show that if climate changes in accordance with the UKHI climate-change scenario, coupled with land use changes, rates of erosion will be accelerated in the Alps and reduced in the German part of the basin. In the case of whole basin, erosion will enhance by almost 12 %. Nevertheless due to ineffective sediment discharge, accelerated erosion in the Alps will pose little impacts on the sediment load further downstream. In the delta zone, sediment loads are predicted to decline by 13 %. When variations in river release are considered, it seems that, though highly significant discharges are predicted to take place more commonly, sedimentation on floodplains inclines to reduce. This is primarily triggered by decreased sediment loads at discharges during which the floodplains are just flooded and trapping proficiencies are maximum.

The Goodwin Creek Research Watershed 21.3 km^2 in size and is located in the north central part of Mississippi in the bluff mountains just east of the Mississippi River floodplain. Surveys have been conducted annually regarding land use on the watershed and the percentage of cultivated land has reduced from 26 to 12 % from 1982 to 1990, respectively. In Goodwin Creek throughout the period of 9 years the level of fines (<0.062 mm), sand (0.062–2.0 mm) and gravel (>2.0 mm) have declined by 62, 66 and 39 %, respectively. The decline in the percentage of cultivated land disturbs the sediment budget of the watershed in two ways. A source of readily eroded sediment has been eliminated, and the energy of the flowing water available to erode and transfer of sediment has been decreased. The lower flow in the channels from the less cultivated land in the watershed was possibly the key source for the lesser rates of transport of sand and gravel (Zulkifley et al. 2014).

Spatially distributed soil erosion and sediment delivery model (WATEM/SEDEM) employed by Ward et al. (2008) in order to simulate sediment yield in Meuse basin for three time-periods: 4000–3000 BP (slight anthropogenic impacts); 1000–2000 AD (involves land use and climate variation); and the 21st Century. Climatic

variations are based on climate model output (ECBilt-CLIO-VECODE). For the 21st Century the model is forced according to two emission scenarios of the Intergovernmental Panel on Climate Change (IPCC), i.e. the SRES scenarios A2 and B1. These scenarios are assigned towards the upper and lower end of the entire IPCC scenario range correspondingly. For 4000–3000 BP the basin is supposed to be nearly completely forested; for 1000–2000 AD land use is restored by means of CORINE data, ancient sources and land use modelling; and for the 21st Century land use is constructed on the European land use change project EURURALIS. At the same time as rainfall erosivity is enhanced by merely 3 % between 4000–3000 BP and 1000–2000 AD, sediment yield rises from 92,000 to 306,000 Mg a^{-1}. This simulation study proves that almost entire upsurge is just because of the transformation of forest to agricultural land. Throughout the period from 1000 to 1900 AD, sediment yield increased continuously, with a peak of 388,000 Mg a^{-1} in the 19th Century (because of permanent deforestation). In the 20th Century, reforestation and rapid development caused the decline to 281,000 Mg a^{-1}. Although land use change is considered as the key factor for long lasting variations in sediment yield, the sensitivity of sediment yield to climatic variations increases as the proportion of deforested land rises. For the 21st Century the outcomes are extremely sensitive to the scenarios applied. Because of rather significant rise in rainfall erosivity, sediment yield rises by 12 and 8 % related to the 20th Century according to scenario A2 and B1 respectively. Conversely, the related land use change scenarios are the source to decline in sediment yield by 26 and 46 % (A2 and B1, respectively). Hence, the overall impact is the decline of sediment yield. This investigation manifests the potentially remarkable efficiency of land use planning as a tool to alleviate the adverse influences of soil erosion and sediment transport to watercourses.

1.2.2 Response of Suspended Sediment Budget to Land Use Changes

Sediment budgets are used by geomorphologists to refer to the main origins, transport pathways and sinks of sediment in a catchment. They have been practiced for usual resource evaluation problems, addressing questions for instance; which sub-catchments are the prevailing origin of sediment; where is sediment deposited (which often specifies an influence); which practices are the main source of the maximum sediment; and, if land use is altered in a fraction of the catchment how will that change downstream yield (Prosser et al. 2001). In several developing states, the management of sediment-related environmental issue is strictly hindered due to absence of data on sediment mobilization and transfer in river basins. The sediment budget perception signifies a valuable framework for accumulating such data, which can, sequentially, be applied to contribution with the design and employment of soil erosion and sediment control strategies (Walling et al. 2001). A sediment budget deals with a number of benefits as a modeling framework. The clear association of source, to sink, to export can strictly restrain the predictions.

It lets information on one facet, for instance export rates, to be used to limit other facets, for example the potential of sources. Information on the bases of fluxes in diverse constituents of a budget offers further limitations (Gharibreza et al. 2013a).

The information required to build a catchment sediment budget is hard to accumulate. Against this background, a combined methodology to establish a catchment suspended sediment budget, including a river monitoring station, the application of ^{137}Cs measurements to evaluate soil erosion and deposition and floodplain accumulation rates within the catchment, and sediment source fingerprinting, has been established and verified in the 63 km^2 catchment of the upper Kaleya River in southern Zambia. This methodology delivers comprehensive information on discrete modules of the suspended sediment delivery system, as well as documents the establishment of the total catchment sediment budget (Walling et al. 2001).

In order to assess the river health, a model of river sediment budgets was developed to predict the spatial patterns of transport and deposition of suspended load and bedload. The model reflects spatial patterns of three types of sediment source: sheetwash, gully and streambank erosion sediment is channeled through river system, integrating modest physical conceptualization of suspended load and bedload deposition. A unique aspect of the model is the knack of clearly relate sites of sediment source in a catchment to their involvement to downstream export. Figure 1.5 represents the conceptualization of the suspended sediment budget for a river link. Generally, the best method to represent the dissimilarity between plot and hillslope sediment yields and delivery to streams is to relate a hillslope sediment delivery ratio (HSDR) to Revised Universal Soil Loss Equation (RUSLE) (Gharibreza et al. 2013a).

Dense population size (3900 km^2) causing agricultural intensification is a serious aspect, with hillslope erosion because of forest removal a prevailing concern for the two sub-catchments of Mae Chaem Rive (3900 km^2), Thailand (Merritt 2002) (Fig. 1.6). A sediment source, transport, and deposition model known as SedNet has been employed to two sub-catchments, the Mae Suk (95 km^2) and the Mae Kong Kha (91 km^2). SedNet models predict the river sediment loads by assembling material budgets that contribute to the key origins and deposits of sediment. SedNet models use a simple mean annual conceptualisation of transport

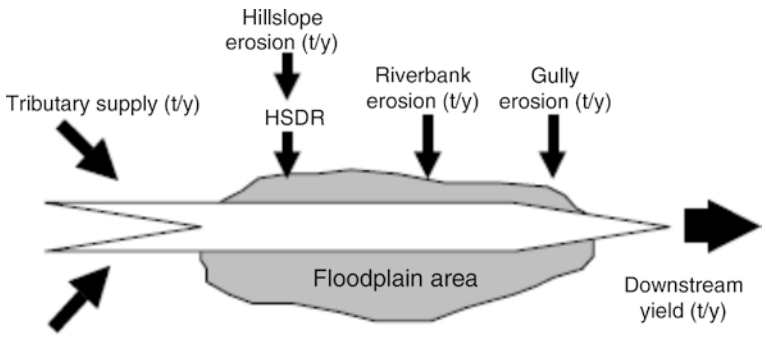

Fig. 1.5 Conceptualization of suspended sediment budget for a river tank

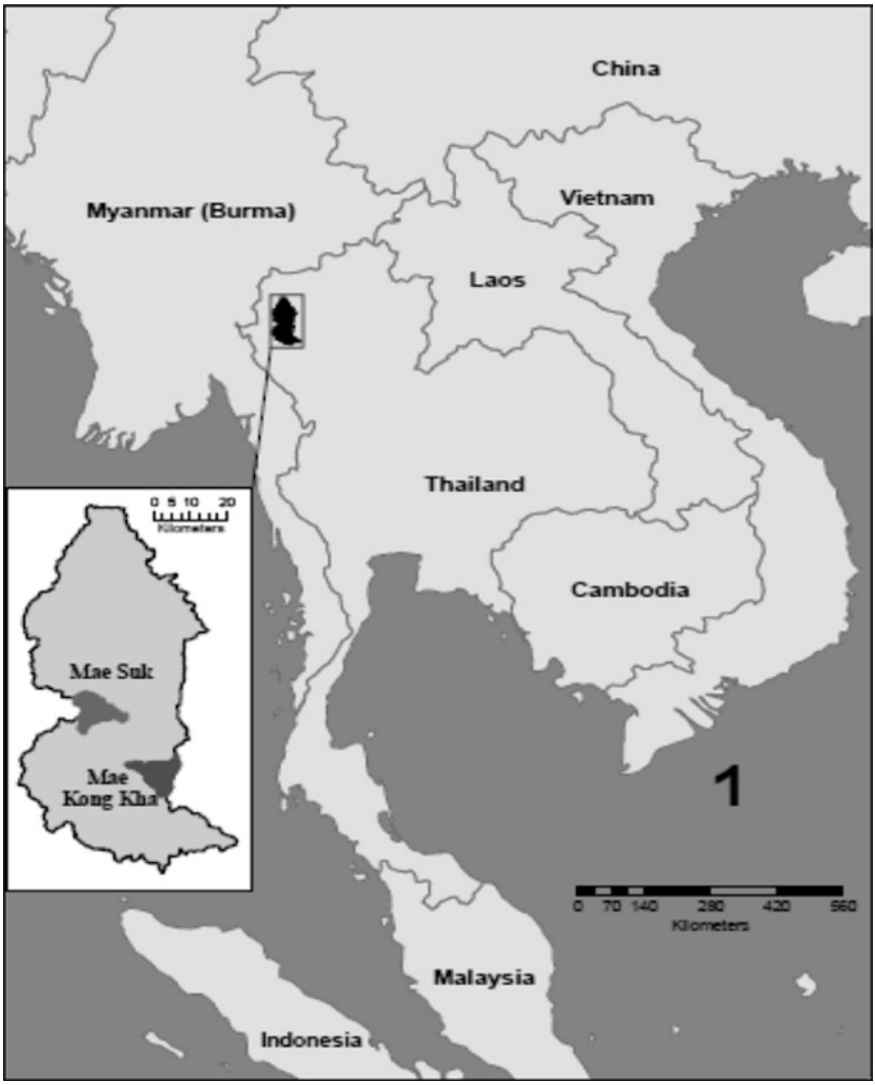

Fig. 1.6 Location of two sub-catchments Mae Suk and Mae Kong Kha within Mae Chaem

and deposition processes in streams and is represented in Fig. 1.7. It is now being applied at regional scales such as river catchments, using more detailed inputs (DeRose 2002; Bakar et al. 2015; Hartcher et al. 2005).

The source areas of suspended sediment altered considerably between 1995 and 2003. Mapping of better quality and improved classification of land use (dividing forest types into evergreen, deciduous, and pine plantations) contribute to the variations in source areas. Because of land use classification, the uncertainty in suspended sediment export decreased by 23 and 17 % with the forest reduction

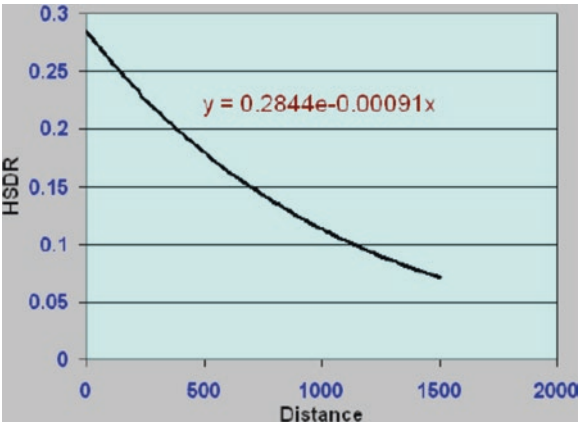

Fig. 1.7 The supposed relationship concerning HSDR and distance from stream

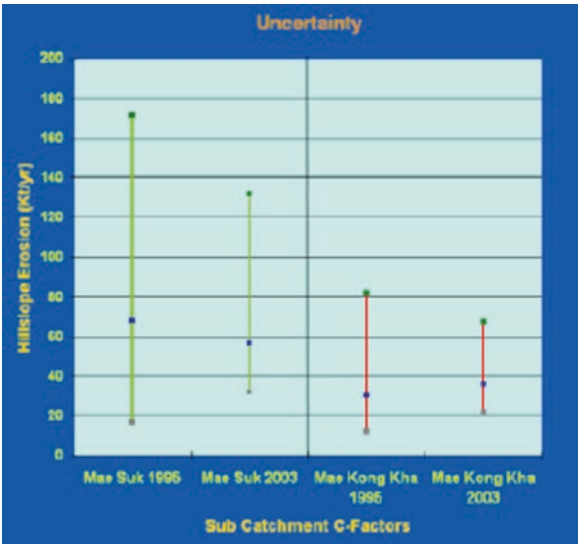

Fig. 1.8 Reductions in uncertainty with improved landuse classification in the Mae Suk and Mae Kong Kha sub-catchments

28.99–12.92 kt year^{-1} and 26.91–11.44 kt year^{-1} for the Mae Suk and Mae Kong Kha catchments, respectively (Fig. 1.8). More advancement will best be attained by upgraded land use coverage which specifies the type of crop being cultivated since these crops subsidize a main fraction of sediment yield. It will drop the range of possible C-factors as well as develop a considerable decrease in uncertainty, and will then let us to concentrate on the main source areas of hillslope erosion and sediment yield.

Hillslope erosion can be calculated using the Revised Universal Soil Loss Equation (RUSLE) represented by Eq. (1.2) where:

$$Soil\ Loss\left(\text{t ha}^{-1}\ \text{year}^{-1}\right) = R \times K \times L \times S \times C \times P \tag{1.2}$$

R rainfall erosivity factor
K soil erodibility factor
$L\,S$ hill length/slope factor
C vegetation cover factor
P Land Use Practice Factor (not used)

Another term, the hillslope delivery ratio (HSDR) is also applied to account for redeposition of hillslope sediment before it is discharged into a stream. Total sediment discharged to stream can be calculated by Eq. (1.3).

$$\textit{Total sediment delivered to stream} = \textit{Soil Loss} \times \textit{HSDR} \tag{1.3}$$

Total predicted sediment yield (low to high C-factors) for 1995 in Mae Suk was 154.45 kt year^{-1} (16.98–171.43 kt year^{-1}). This range decreased by 35–99.76 kt year^{-1} (31.86–131.62 kt year^{-1}) using the 2003 land use classification (Table 1.3).

Table 1.3 Categorization of vegetation cover categories and C factors for Mae Suk

1995 landuse	Law C-factor	Sediment contribution (kt/year)	High C-factor	Sediment contribution (kt/year)
Forest	0.010	4.07	0.000	33.06
Fallow	0.020	2.75	0.800	110.39
Fieldcrops	0.250	10.31	0.790	32.59
Paddy	0.100	0.28	0.200	0.79
Urban	0.00	0	0.300	0.03
	Total	16.98	Total	171.43

2003 Land use	Law C-factor	Sediment contribution (kt/year)	High C-factor	Sediment contribution (kt/year)
Hill evergreen forest	0.001	2.69	0.003	10.18
Dry deciduous forest	0.001	0.20	0.020	2.32
Mix deciduous forest	0.001	0.38	0.040	2.89
Hill evergreen forest/dry deciduous forest	0.001	0.02	0.020	0.45
Pine forest	0.088	0.41	0.088	0.78
Total forest		(**3.7**)		(**16.62**)
Fallow	0.020	2.83	0.340	38.32
Field crop	0.250	27.1	0.790	85.71
Paddy	0.100	1.99	0.280	6.3
Urban	0.000	0.15	0.300	1.89
Fruit tree	0.150	1.16	0.600	2.31
	Total	31.86	Total	131.62

Table 1.4 Categorization of vegetation cover and C factors for Mae Kong Kha

1995 Landuse	Law C-factor	Sediment contribution (kt/year)	High C-factor	Sediment contribution (kt/year)
Forest	0.010	3.86	0.080	33.77
Fieldcrops	0.250	7.06	0.790	21.91
Fallow	0.020	0.69	0.800	27.11
Paddy	0.100	0.51	0.280	1.40
Urban	0.00	0.00	0.300	0.47
	Total	12.11	Total	81.67

2003 Land use	Law C-factor	Sediment contribution (kt/year)	High C- factor	Sediment contribution (kt/year)
Mix deciduous forest	0.001	0.99	0.040	6.13
Pine forest	0.088	3.59	0.0088	3.60
Hill evergreen forest	0.001	1.17	0.003	3.58
Dry deciduous forest/pine forest	0.001	0.39	0.088	3.91
Dry deciduous forest	0.001	0.07	0.020	0.43
Total forest		(**6.21**)		(**17.65**)
Field crop	0.250	13.87	0.790	43.96
Paddy	0.100	1.49	0.280	4.43
Urban	0.000	0.11	0.300	1.02
Fruit tree	0.150	0.05	0.600	0.20
Wine	0.800	0.19	0.800	0.21
	Total	21.93	Total	67.46

The range of total predicted sediment yield for the 1995 land use in Mae Kong Kha was 69.56 kt year^{-1} (12.11–81.67 kt year^{-1}). This range decreased by 35–45.53 % kt year^{-1} (21.93–67.46 kt year^{-1}) using the 2003 land use classification (Table 1.4). As it is clear from Fig. 1.9 that land use in 2003 has a remarkable impact on the hillslope erosion grid. Only satellite image analysis conducted in 1995 shows usually more even rates of erosion, though it also represented overprinting impacts from hill shadows in the image categorization method. The 2003 categorization consequences in the hillslope erosion categories being more unchanging in particular regions and clearly defining land use changes not recognized in 1995 (Hartcher and Post 2005).

In Lake Asan watershed sediment budget of land use changes was calculated using the Universal Soil Loss Equation (USLE), sediment delivery ratio (SDR), and trap efficiency (TE) coupled with geographic information technology (Kim et al. 2014). Variations in soil erosion were analyzed using Landsat-5 TM images. The sediment yield to Lake Asan was assessed using the SDR and TE. The data obtained related to sediment budget was compared with observed data from the Lake Asan watershed from 1974 to 2003. The overall predictable annual mean

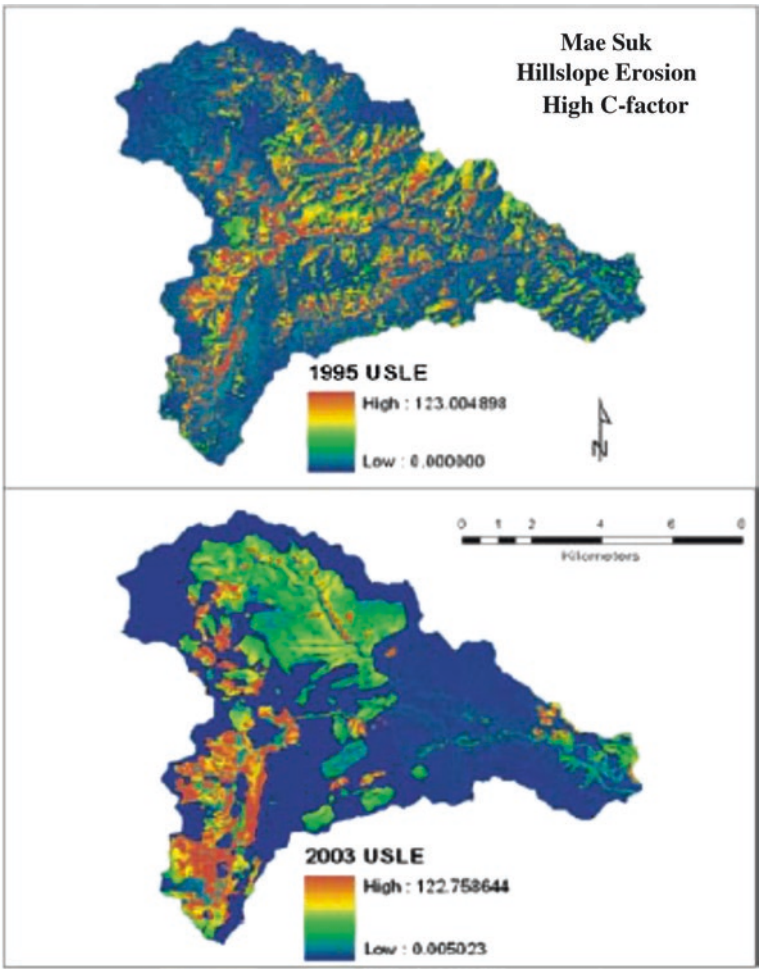

Fig. 1.9 Hillslope erosion grid for Mae Suk using 'best-guess' C-factors

sediment budgets were 0.267, 0.301, and 0.339 Ã-10 ton in 1986, 1992, and 2000, respectively, and its average calculated was 0.302 Ã-10 ton. The average estimated sediment budget was 3.15 Ã-10 ton year. The rate of rise in soil erosion was found to be about 2 % each year from 1986 to 2000 because of land use change. This study was valuable for administrators to recognize reservoir restoration management approaches for constant delivery of water for irrigation purpose.

In the Rhine catchment (Fig. 1.10) under Holocene climate conditions, comparatively fine sediment is generated, deposited and relocated on the hillslopes and then carried to the fluvial system (Fig. 1.11). Sediment discharged in rivers is then transported to downstream within river channels. In this study sediment budgets were estimated by collective measurements of sediment confined in floodplains in the

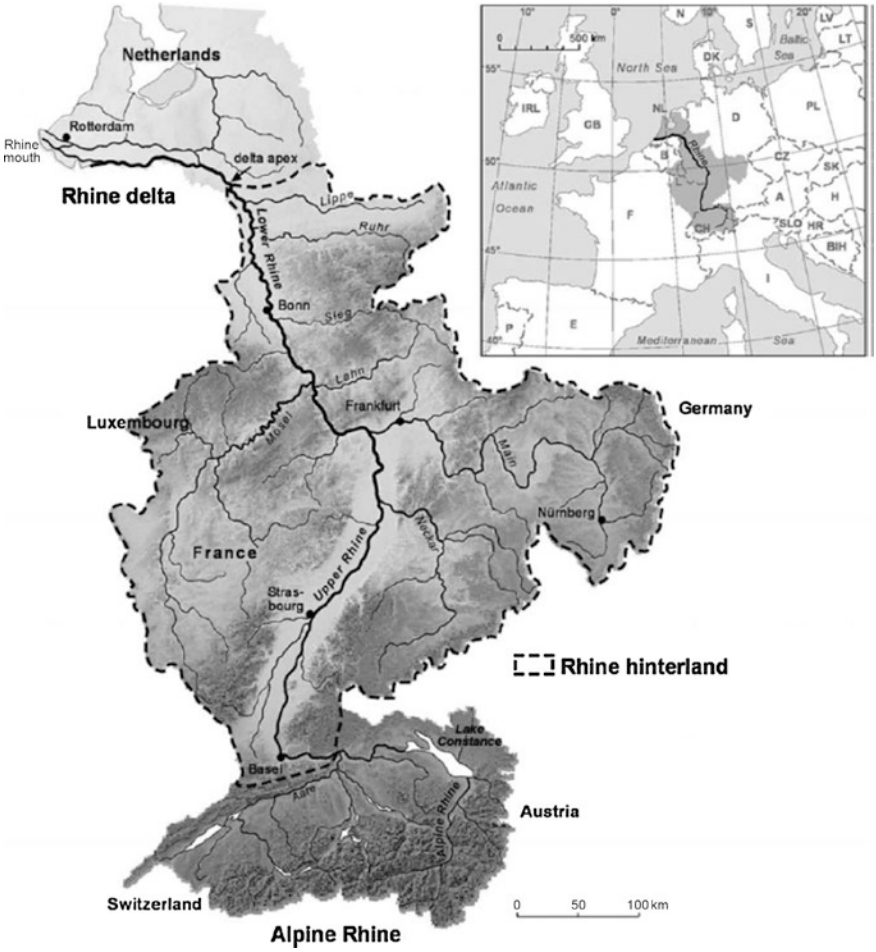

Fig. 1.10 Location of Rhine catchment with main tributaries in Europe

hinterland and in the Rhine delta (Erkens et al. 2006). Sediment delivery ratios (SDR) indicate the fraction of sediment sendoff a region comparative to the quantity of sediment eroded in that region. The fraction of sediment produced by erosion that reaches the river is termed as the hillslope SDR (or HSDR). On the other hand, the fraction of sediment that reaches the outlet compared with the sediment carried to the channel is termed as the channel SDR, or CSDR terminology following Asselman et al. (2003).

The effect of land use and climatic variations on the fluvial system depends on the size of catchment. The size of Rhine catchment is 185,000 km^2. A sediment budget is estimated to specify the concentration of alluvial sediment that was stored throughout the Holocene and to evaluate the rates of longstanding soil erosion. The outcomes prove that 599/14-109 t of Holocene alluvial sediment is deposited in the non-alpine region of the Rhine catchment (South and Central Germany, Eastern France, The

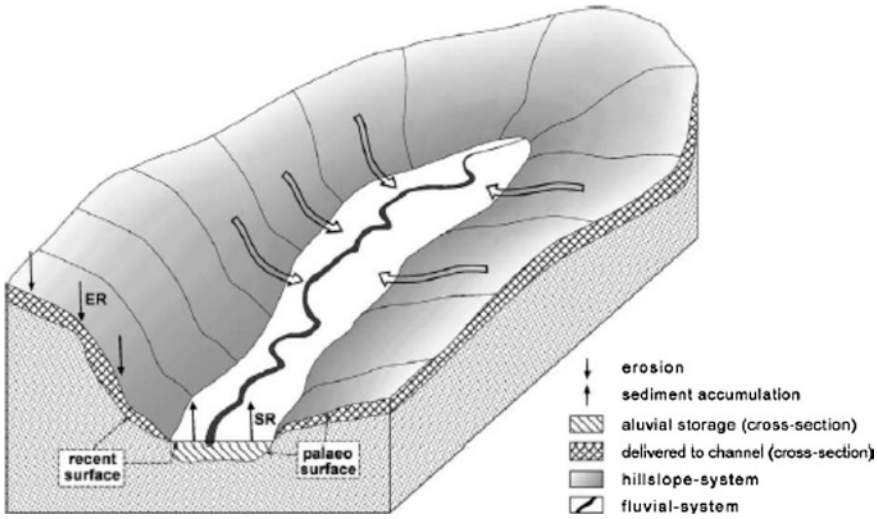

Fig. 1.11 A schematic image for the sediment budget method showing sediment fluxes towards sediment fluxes towards the floodplain storage

Netherlands). Around 50 % of Holocene alluvial sediment is stored along the trunk valley and the delta (Upper Rhine, Lower Rhine, coastal plain), whereas the remaining is deposited along the tributary valleys. The floodplain sediment deposition relates to an average erosion rate of 0.559/0.16 t ha^{-1} $year^{-1}$ (38.59/10.7 mm k^{-1} $year^{-1}$) across the Rhine catchment exterior to the Alps. This is the average estimation for sediments that were transported to the channel network and is at the lower edge of erosion rates than that of other investigations adapting different approach.

Hillslope erosion can be defined as "the amount of material that is delivered to the channel network", and the erosion rate ER can be calculated based on the sediment volume SV deposited on the floodplains in a time interval T.

Based on the work of Gharibreza et al. (2014, 2013b), erosion rates E_R* and E_R (in mm k^{-1} $year^{-1}$ and t ha^{-1} $year^{-1}$, respectively are measured by Eqs. (1.4) and (1.5).

$$E_R{}^* = \frac{S_V}{T \times (A_d - A_f)} \times \frac{1}{1 - \mathrm{CSDR}} (L/T) \tag{1.4}$$

$$E_R = \rho_B \times E_R{}^* (M/L^2/T) \tag{1.5}$$

where A_f symbolizes floodplain area, A_d symbolizes catchment area and $A_d - A_f$ symbolizes erosive area (that is the catchment area without the floodplains) and ρ_B symbolizes bulk density of the alluvial sediment. The channel sediment delivery ratio CSDR in Eq. (1.4) refers to the fraction of the eroded material sendoff the river at the downstream end of the investigated zone.

The summary of deposited alluvial sediment concentrations in the Rhine catchment has been described in Table 1.5. Total 37.69/8.3 km^3 volume, consistent to

Table 1.5 Summary of holocene alluvial sediment storage within the Rhine catchment

Rhine and main tributaries	Catchment area			Larger floodplains Subcatchments >4.11 km^2, GK200-resolved				Smaller floodplains Subcatchments 0.3–4.1 km^2; upscaling approach (Eq. 1.1)				Total floodplain sediment storage			
	Total area	Erosive area		Floodplains area		Sediment volume		Flood plain area		Sediment volume		Sediment volume S_v		Mass	
	A_d (km^2)	$A_d - A_f$ (km^2)	Error	A_f (km^2)	Error	S_v (km^2)	Error	A_f (km^2)	Error	S_v (km^2)	Error	S_v (km^2)	Error	$P_B X\ S_v$ (10^9 t)	Error
Wied	744.9	679.4	18.5	30.6	6.1	0.05	0.02	34.9	17.4	0.06	0.03	0.10	0.03	0.16	0.05
Emscher	806.4	686.3	26.4	77.2	15.4	0.12	0.04	42.9	21.4	0.07	0.04	0.19	0.06	0.29	0.08
Wupper	838.0	761.0	21.5	36.5	7.3	0.06	0.02	40.5	20.3	0.06	0.04	0.12	0.04	0.18	0.06
Ahr	910.7	832.9	23.8	31.9	6.4	0.05	0.02	45.9	22.9	0.07	0.04	0.12	0.04	0.19	0.07
Erft	1818.6	1557.6	58.4	164.5	32.9	0.26	0.08	96.5	48.2	0.15	0.09	0.42	0.12	0.63	0.18
Sieg	2870.1	2567.1	76.2	165.9	33.2	0.27	0.09	137.1	68.5	0.22	0.12	0.48	0.15	0.73	0.22
Nahe	4070.0	3581.2	114.9	290.5	58.1	0.46	0.15	198.2	99.1	0.32	0.18	0.78	0.23	1.17	0.35
Ruhr	4476.8	4018.8	118.4	241.9	48.4	0.39	0.12	216.0	108.0	0.35	0.19	0.73	0.23	1.10	0.34
Lippe	4857.6	4183.9	161.3	391.7	78.3	0.63	0.20	282.0	141.0	0.45	0.25	1.08	0.32	1.62	0.48
Ill	4858.1	2918.3	365.4	1785.6	357.1	2.86	0.91	154.3	77.1	0.25	0.14	3.10	0.93	4.66	1.39
Lahn	5916.4	5260.6	161.5	368.2	73.6	0.59	0.19	287.6	143.8	0.46	0.26	1.05	0.32	1.57	0.48
Neckar	13,970.8	12,223.3	400.4	1070.9	214.2	1.71	0.55	676.6	338.3	1.08	0.61	2.80	0.82	4.19	1.23
Main	27,306.6	24,077.4	776.3	1868.0	373.6	2.99	0.96	1361.1	680.5	2.18	1.22	5.17	1.55	7.75	2.32
Mosel	28,226.6	24,580.9	843.4	2208.9	441.8	3.53	1.13	1436.9	718.4	2.30	1.29	5.83	1.71	8.75	2.57
Lower Rhine	2532.1	21,191.1	76.7	360.6	72.1	0.58	0.18	52.4	26.2	0.08	0.05	0.66	0.19	0.99	0.29
Middle Rhine	2658.4	2383.9	73.9	137.4	27.5	0.22	0.07	137.2	68.6	0.22	0.12	0.44	0.14	0.66	0.21

(continued)

Table 1.5 (continued)

Rhine and main tributaries	Catchment area			Larger floodplains Subcatchments >4.11 km^2, GK200-resolved				Smaller floodplains Subcatchments 0.3–4.1 km^2; upscaling approach (Eq. 1.1)				Total floodplain sediment storage			
	Total area	Erosive area		Floodplains area		Sediment volume		Flood plain area		Sediment volume		Sediment volume S_v		Mass	
	A_d (km^2)	$A_d - A_f$ (km^2)	Error	A_f (km^2)	Error	S_v (km^2)	Error	A_f (km^2)	Error	S_v (km^2)	Error	S_v (km^2)	Error	$P_B X\ S_v$ (10^9 t)	Error
Upper Rhine	18,863.1	14,376.0	833.7	3918.7	783.7	6.27	2.01	568.4	284.2	0.91	0.51	7.18	2.07	10.77	3.11
Hinterland total	125,725.1	107,297.5	3837.8	12,659.3	2531.9	20.25	6.48	5768.3	2884.2	9.23	5.16	29.48	8.29	44.23	12.43
Rhine trunk	24,053.6	18,896.4	958.0	4399.3	879.9	7.04	2.25	758.0	379.0	1.21	0.68	8.25	2.35	12.38	3.53

Catchment area based on DEM calculations. Larger floodplains based on the geological maps (GK200, 1:200 000). Additional area of smaller floodplains based on upscalling approach (see text). Area to volume calculations using mean floodplain thickness Df = 1.6 ± 0.4 m. volume to mass using $\rho_B = 1500$ kg/m^3. Conservation errors assumed for floodplain areas of larger floodplains: ±20 % for smaller floodplains +50 %

entire quantity of 53.59/12.4-109 t is deposited in the Rhine catchment. These concentrations relate to an eroded volume of 41.99/9.3 km^3 (59.59/13.9–109 t), supposing a CSDR at the river mouth of 10 % and T-/10,000 year. The outcomes indicate that deposited Holocene alluvial sediment is 599/14–109 t in the non-alpine area of the Rhine catchment (South and Central Germany, Eastern France, The Netherlands) (Hoffmann et al. 2007).

In order to assess the discrete modules of the sediment budget for two small (<4 km^2) lowland and agricultural catchments using ^{137}Cs measurements, sediment source fingerprinting and other outdated monitoring tools were used by (Walling et al. 2002). This involved an illustrative range of slope angles, slope lengths and land use. To determine the gross and net erosion rates, a simple topographically driven soil erosion model (Terrain-Based GIS, TBGIS) employed on a DEM. The sediment budgets suggested for the catchments point out the significance of subsurface tile drains as a pathway for sediment transport, contributing to 60 and 30 % of the sediment yield from the two catchments. The erosions calculated from channel banks were 10 and 6 % of the sediment yield from the two catchments. Even though the suspended sediment yields from these catchments were crossing the UK standard values (90 t km^{-2} $year^{-1}$), the sediment delivery ratios were found in range of 14–27 %, demonstrating that a major fraction of the mobilized sediment was deposited in the catchments. In-field and field-to-channel depositions were revealed to be of alike concentration; nevertheless deposition of sediment in the channel system and related wetlands was comparatively small, on behalf of <5 % of the annual suspended sediment yield.

1.2.3 Response of Sedimentation Rate to Land Use Changes

Generally the sedimentation rates are estimated based on boreholes for which only one ^{14}C-age is accessible (Table 1.6). In these cases merely an average sedimentation rate subsequently storage of the old sample can be calculated. To analyze the influence of averaging in Rhine catchment (Fig. 1.12), sedimentation rates were modeled on the basis of three different scenarios with altering sedimentation rates $SR_{assumed}(t)$. A persistent sedimentation rate of 0.3 mm a^{-1} was supposed by the 1000 BC scenario during 12000 and 1000 BC and a linear rise from 0.3 to 4 mm a^{-1} from the time when 1000 BC to present. There was similarity between the 500 AD, 1800 AD and 1000 BC scenario, however in the case of 500 AD and at 1800 AD, a linear rise observed later. On the basis of these scenarios, the depth D of subsurface layers with different ages T can be measured by Eq. (1.6).

$$D = \int_0^T \mathrm{SR}_{\mathrm{assumed}}(t)\mathrm{d}t \tag{1.6}$$

Modelled mean sedimentation rate SR_{model} is obtained by D/T ratio, and it was associated to the observed mean sedimentation rates $SR_{mean.obs}$ given by the ^{14}C-date.

Table 1.6 Distribution of ^{14}C-samples in drillings (leftward) and catchments of different sizes (rightward)

#^{14}C-samples per drilling	Number of drillings	Catchment size (km^2)	#^{14}C-samples
1	45	–	12
2	16	<0.1	1
3	4	0.1–10	5
4	5	1–10	27
5	0	10–100	28
6	1	100–1000	35
7		1000–10,000	7

The $SR_{mean.obs}$ of each ^{14}C-age was estimated on the basis of its depth D and its age T by $SR_{mean.obs} = D/T$ self-reliantly of other ^{14}C-dates in the same borehole.

On the basis of a recently piled up ^{14}C-database of alluvial and colluvial samples, floodplain sedimentation rates (SR) were estimated on the basis of ^{14}C-date T_i and its depth D_i below the surface using Eq. (1.7).

$$SR_{i,obs} = (D_i - D_{i-1})/(T_i - T_{i-1}) \tag{1.7}$$

and D_{i-1} and T_{i-1} denotes the depth and age of the following stratigraphic younger ^{14}C-sample. Ti denotes the mean value of the 2σ-age range given by the calibrated age. In the case of the uppermost ^{14}C sample, $i = 1$ and $D_0 = 0$ and $T_0 = 0$.

By using Eq. (1) sedimentation rates are estimated from ^{14}C-samples and found in range of 0.1 and 1 mm a^{-1} previous to 0 BC/AD and illustrate a strong scatter afterward 0 BC/AD (Fig. 1.13a). Though, at numerous sites sedimentation rates keep on persistent after 0 BC/AD, at other sites highest floodplain sedimentation rates accelerate up to 8 mm a^{-1} throughout the past 2000 years. The scatter plot presented in Fig. 1.13a can best be explained by a power law increase with:

$$SR_{max} = 222.5T^{-0.7} \tag{1.8}$$

where SR_{max} = sedimentation rate in mm a^{-1} and T = time in years before 2000 AD (black line in Fig. 1.13a).

Effect of land use change on sedimentation rate was investigated by Godwin et al. (2011) during the 2009–10 rain spell at Chesa Causeway Dam in the Upper Ruya subcatchment of Zimbabwe (Fig. 1.14). Sample collection after storm events enhances the possibility of overlapping with peak sediment levels. By averaging the monthly sedimentation rates the sediment concentration was determined. The sediment quantification was done using the following Eqs. (1.9, 1.10, 1.11, 1.12, and 1.13):

$$MAI = CA * MAR \tag{1.9}$$

where

MAI is the gross mean annual reservoir inflow (m^3 year^{-1})
CA is the catchment area (km^2)
MAR is the mean annual runoff (mm year^{-1})

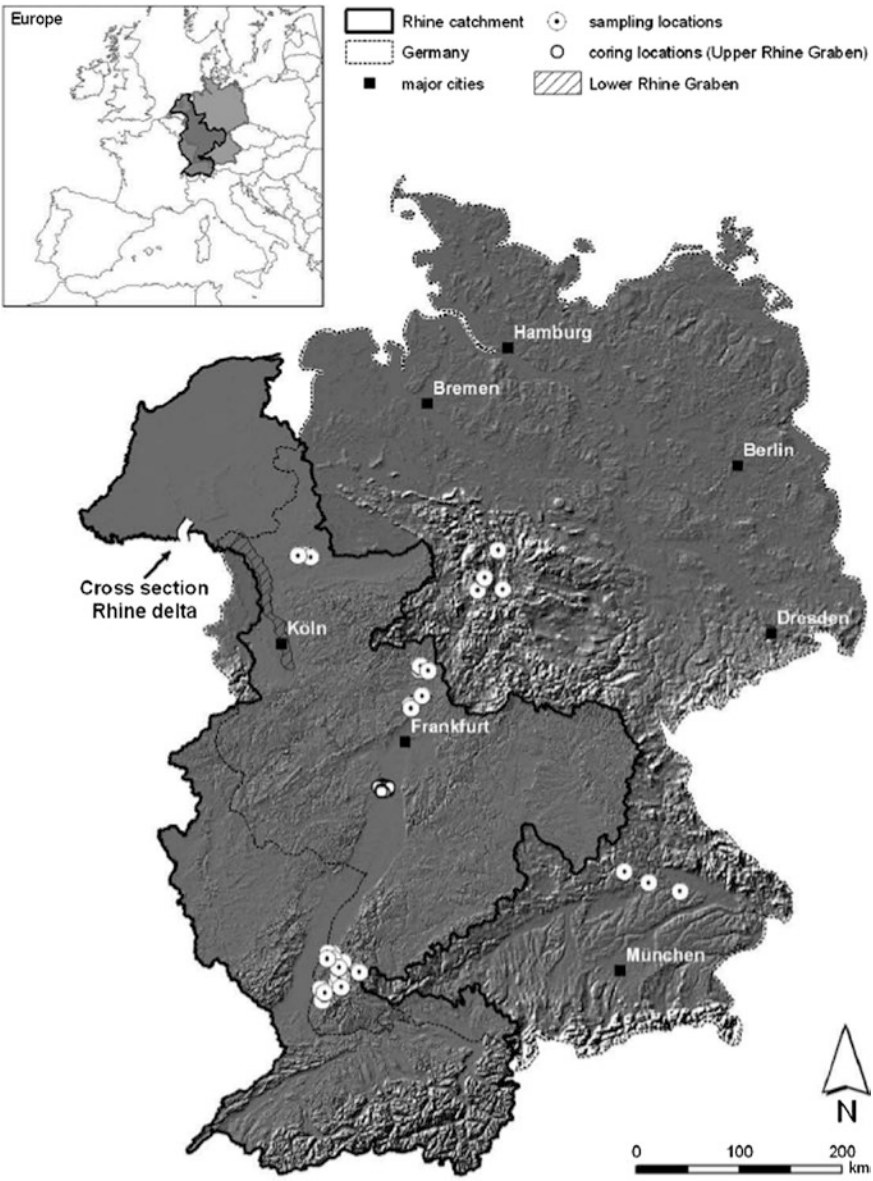

Fig. 1.12 Rhine catchment with citation of corings, cross-sections and ^{14}C-samples

$$SRg = DC/MAI \tag{1.10}$$

where

SRg is the gross storage ratio
DC is the gross dam capacity

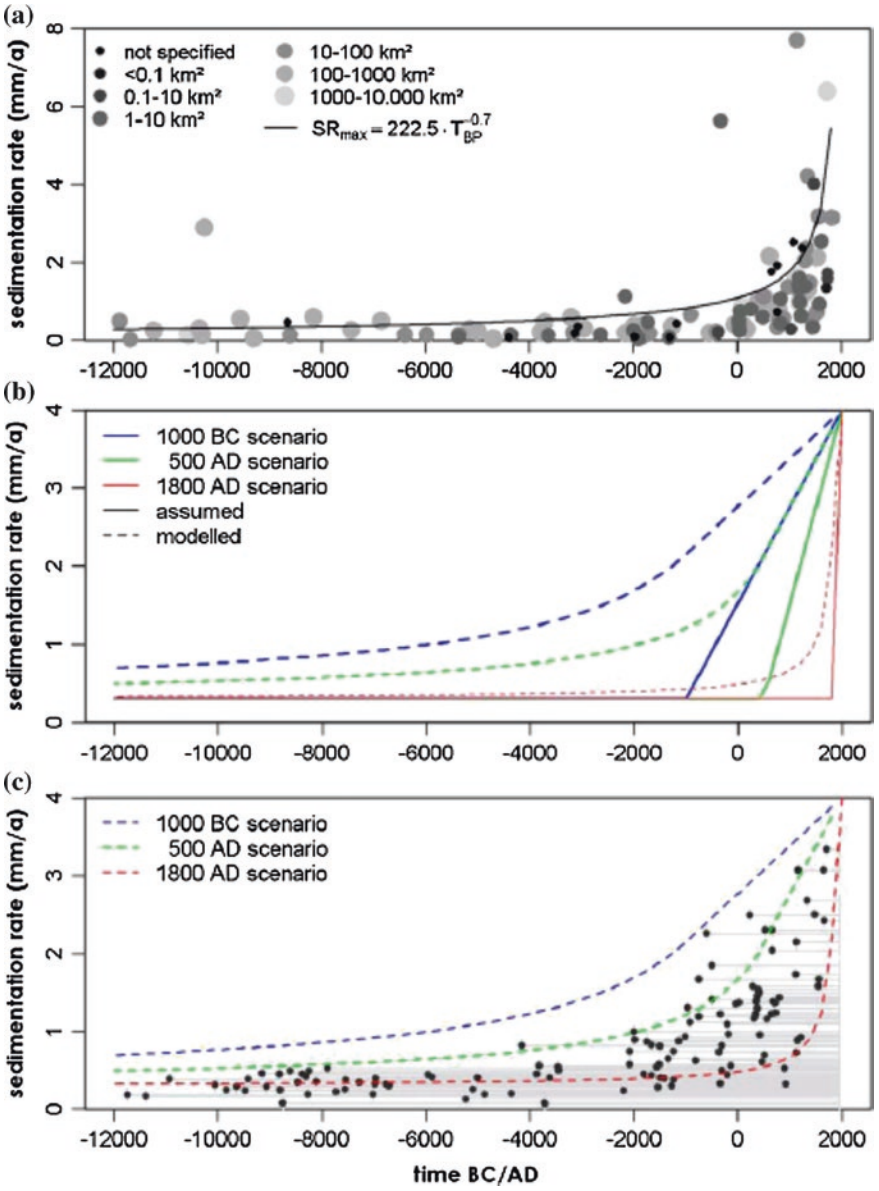

Fig. 1.13 **a** Fluctuating floodplain sedimentation rates based on the basis of ^{14}C-ages from floodplains of German rivers. Signs denote the area of the respective catchment. **b** Impact of averaging because of sedimentation rate measurement employing the ^{14}C-ages and sample depths. The three scenarios vary on the arrival of enhanced sedimentation at 1000 BC represented by *blue line*, 500 AD represented by *green line* and 1800 AD, represented by *red line*. The *wrecked lines* depict the deceptive sedimentation rates for the three scenarios. **c** Comparison of calculated sedimentation rate from the ^{14}C-ages and deceptive sedimentation rates measured from 1000 BC, 500 AD and 1800 AD scenarios (Hoffmann et al. 2008)

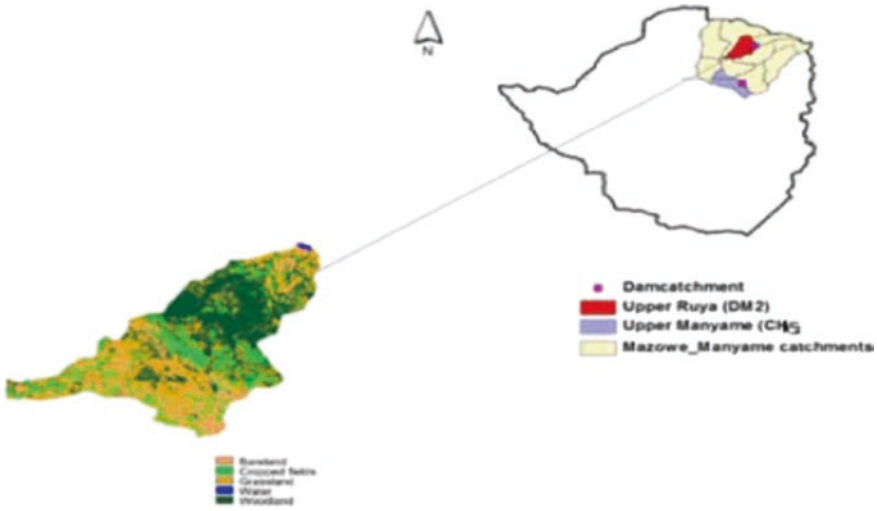

Fig. 1.14 Chesa Causeway Dam in the Upper Ruya sub-catchment of Zimbabwe

$$T_n = (0.1 + 9 * SRg) * 100 \tag{1.11}$$

where T_η is the trap efficiency (%)

On the whole, the trap efficiency is supposed to be 100 % for most reservoirs were the gross storage ratio >0.1

$$SY = MAI * SC/1000 \tag{1.12}$$

where SY is the mass of sediments in the inflowing river in t year^{-1} (Sediment yield), SC is the sediment concentration

$$SSY = SY/A \tag{1.13}$$

where SSY is the specific sediment yield which gives a measure of mass of sediments per unit area per given time (measured in t km^{-2} year^{-1}) and A is the area of the catchment in km^2. Following above procedure sediment investigation exhibited that the sediment specific yields at the dam were 774 t km^{-2} year^{-1} applying the grab sampling method and 503 t km^{-2} year^{-1} calculated from hydrographic survey. It is portrayed from Fig. 1.15 that the reservoir basin has condensed in altitude up to 1 m from the original (where the original initial delineation was 92 m) this can be endorsed to the existing accelerated rates of sediment yields i.e. 503 t km^{-2} year^{-1} being dumped into the reservoir. This has caused the dam capacity falling by 46 % throughout the period of 12 years (1991–2003); there is a 33 % drop throughout the duration of 2003–2010 and the total drop in storage volume over 19 years estimated as 67 %. If no interferences are laid in place to lessen the specific sediment yields supposing persistent rate of dumping the reservoir would be entirely silted up in the subsequent 11 years which is 20 years less the calculated duration.

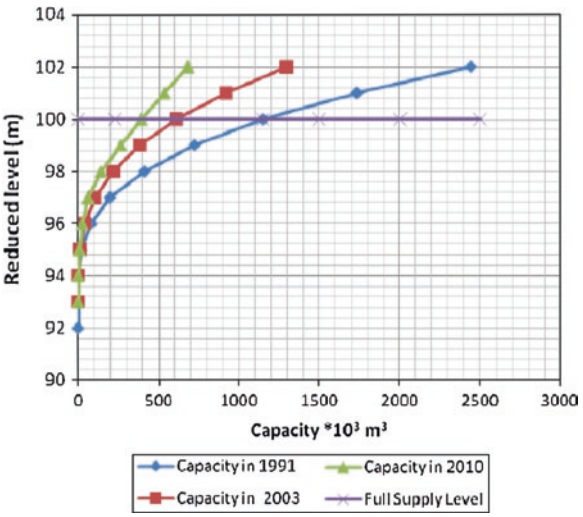

Fig. 1.15 Chesa Causeway Dam capacity assessment over the years

References

Abernethy C (1990) The use of river and reservoir sediment data for the study of regional soil erosion rates and trends. Paper presented at the international symposium on water erosion, sedimentation and resource conservation, pp 93–100

Albek M, Albek E (2003) Predicting the effects of the climate change on the sediment yield of watersheds. Diffuse pollution conference Dublin 3G: Agriculture 3-137

Ashraf MA, Ahmad M, Aqib S, Balkhair KS, Bakar NKA (2014) Chemical species of metallic elements in the aquatic environment of an ex-mining catchment. Water Environ Res 86(8):77–728

Asselman NEM, Middelkoop H, Dijk PM (2003) The impact of changes in climate and land use on soil erosion, transport and deposition of suspended sediment in the River Rhine. Hydrol Process 17:3225–3244. doi:10.1002/hyp.1384

Bakar AFA, Yusoff I, Ng TF, Ashraf MA (2015) Cumulative impacts of dissolved ionic metals on the chemical characteristics of river water affected by alkaline mine drainage from the Kuala Lipis gold mine, Pahang, Malaysia. Chem Ecol 31(1):22–33. doi:10.1080/02757540.2014.950569

Bennett EM, Carpenter SR, Caraco NR (2001) Bioscience 51(227)

Bonell M, Gilmour DA (1978) The development of overland flow in a tropical rainforest catchment. J Hydrol 39:365–382

Brye KR, Norman JM, Bundy LG, Gower ST (2000) Water budget evaluation of prairie and maize ecosystems. Soil Sci Am J 64:715–725

Buringh P, Dudal R (1987) Agricultural land use in space and time. In: Wolman MG, Fournier FGA (eds) Land transformation in agriculture, SCOPE report no, 32. Wiley, Chichester, pp 9–43

Calder IR (1993) Hydrologic effects of land-use change. In: Maidment DR (ed) Handbook of hydrology. McGraw-Hill, New York, p 50

CanberraProsser I, Moran C, Lu H, Scott A, Rustomji P, Stevenson J, Priestley G, Roth C, Post DA (2002) Regional patterns of erosion and sediment transport in the Burdekin River catchment. CSIRO land and water technical report 5/02 http://www.clw.csiro.au/publications/technical2002/tr5-02.pdf

Cernusca A, Tappeiner U, Bayfield N (1999) Land use changes and vegetation changes in sub-alpine areas. In: Bottarin R, Tappeiner U (eds) Interdisciplinary mountain research. Blackwell, Berlin, pp 180–191

Chang M, Roth FA Jr, Hunt EV Jr (1982) Sediment production under various forest-site conditions. In: Walling DE (ed) Recent developments in the explanation and prediction of erosion and sediment yield. IAHS Publ 137:13–22

Costa MH, Botta A, Cardille JA (2003) Effects of large-scale changes in land cover on the discharge of the Tocantins River, Southeastern Amazonia. J Hydrol 283(206)
De Roo A, Odijk M, Schmuck G, Koster E, Lucieer A (2001) Assessing the effects of land use changes on floods in the Meuse and Oder catchment. Phys Gem Earth B 26(7–8):593–599
DeFries RS, Foley JA, Asner GP (2004) Front. Ecol Environ 2(249)
DeRose R, Prosser I, Wilkinson L, Hughes A,Young W (2002) Regional patterns of erosion and sediment and nutrient transport in the Mary River catchment, Queensland." CSIRO land and water technical report 37/02 http://www.clw.csiro.au/publications/technical2002/tr37-02.pdf
Douglas I (1967) Man, vegetation and the sediment yields of rivers. Nature 215:925–928
Erkens G, Cohen KM, Gouw MJP, Middelkoop H, Hoek WZ (2006) Holocene sediment budgets of the Rhine delta (the Netherlands): a record of changing sediment delivery, vol 206. IAHS Publication, Wallingford, pp 406–415
Food and agriculture organization of the United Nations (1998) Crop evapotranspiration: guidelines for computing crop water requirements. Irrig Drain Pap 56, Rome
Gellis AC, Webb RMT, McIntyre SC, Wolfe WJ (2006) LAND-use effects on erosion, sediment yields, and reservoir sedimentation: a case study in the LAGO LOÍZA basin PUERTO RICO. Phys Geogr 27(1):39–69
Gharibreza M, Raj JK, Yusoff I, Ashraf MA, Othman Z, Zakaria W, Tahir WM (2013a) Effects of agricultural projects on nutrient levels in Lake Bera (Tasek Bera). Peninsular Malaysia. Agric Ecosyst Environ 165(1):19–27
Gharibreza M, Raj JK, Yusoff I, Othman Z, Zakaria W, Tahir WM, Ashraf MA (2013b) Historical variations of Bera Lake (Malaysia) sediments geochemistry using radioisotopes and sediment quality indices. J Radioanal Nuclear Chem 295(3):1715–1730
Gharibreza M, Raj JK, Yusoff I (2013c) Sedimentation rates in Bera Lake (Peninsular Malaysia) using 210Pb and 137Cs radioisotopes. Geosciences J 17(2):211–220. doi:10.1007/s12303-013-0013-3
Gharibreza M, Raj JK, Yusoff I, Othman Z, Zakaria W, Tahir WM, Ashraf MA (2013d) Land use changes and soil redistribution estimation using 137Cs in the tropical Bera Lake catchment. Malaysia. Soil Till Res 131(1):1–10
Gharibreza M, Ashraf MA, Yusoff I, Raj JK (2013e) An evaluation of Bera Lake (Malaysia) sediment contamination using quality guidelines. J Chem 2013(13):387035
Gharibreza M, Habibi A, Imamjomeh SR, Ashraf MA (2014) Coastal processes and sedimentary facies in the Zohreh River Delta (Northern Persian Gulf). CATENA 122(1):150–158. doi:10.1016/j.catena.2014.06.010
Gleick PH (2003) Water use: annual review of environment and resources. Environ Resource 28:275–314
Godwin M, Gabriel S, Hodson M, Wellington D (2011) Sedimentation impacts on reservoir as a result of land use on a selected catchment in Zimbabwe. International J Eng Sci Technol 3(8):6599–6608
Goolsby DA, Battaglin WA, Lawrence GB, Artz RS, Aulenbach BT, Hooper RP, Keeney DR, Stensland GJ (1999) Flux and sources of nutrients in the Mississippi-Atchalfalalya River Basin. Decis Anal Ser 17, coastal ocean program, NOAA, Silver Spring, Md
Gupta RS (1989) Hydrology and hydraulic system. Prentice-Hall, Englewood Cliffs
Hallberg GR (1987) Nitrates in ground water in Iowa. In: D'Itri FM, Wolfson LG (eds) Rural ground water contamination, pp 23–68
Hartcher MG, Post DA, Kinsey-Henderson AE (2005) Uncertainty in modelling the sources and sinks of suspended sediment in the Mae Chaem catchment, Thailand. In: SIMMOD conference, Bangkok, Thailand
Hoffmann T, Erkens G, Cohen KM, Houben P, Seidel J, Dikau R (2007) Holocene floodplain sediment storage and hillslope erosion within the Rhine catchment. Holocene 17(1):105–118
Hoffmann T, Erkens G, Gerlach R, Klostermann J, Lang A (2008) Trends and controls of Holocene floodplain sedimentation in the Rhine catchment, Catena
Hundecha Y, Bardossy A (2004) Modeling of the effect of land use changes on the runoff generation of a river basin through parameter regionalization of a watershed model. J Hydrol 292:281–295

Jordan JMJ (1989) The sediment problem in South Africa reservoirs. In: Yang SSY (ed) Sediment transport modeling: proceedings of the international symposium. New Orleans, LA: Hydraulics Division of the American Society of Civil

Kalnay E, Cai M (2003) Impact of urbanization and land-use change on climate. Nature 423(1):528–531

Kim SM, Jang TI, Kang MS, Im SJ, Park SW (2014) Environ Earth Sci. doi:10.1007/s12665-013-2621-7

Kristian J, Lcrup JK, Refsgaard JC, Mazvimavi D (1998) Assessing the effect of land use change on catchment runoff by combined use of statistical tests and hydrological modeling: case studies from Zimbabwe. J Hydrol 205:147–163

Mahmood K (1987) Reservoir sedimentation, impact, extent, and mitigation. World Bank, Washington, DC, World Bank technical paper no. 71

Matson PA, Parton WJ, Power AG, Swift MJ (1997) Agricultural intensification and ecosystem properties. Science 277(5325):504–509

Mawardi I (2010) River basin watershed damage and decrease the carrying capacity of water resources in Java as well as efforts to handle (in Indonesian language). Hidrosfir Indon J 5(3):57–64

McDowell R, Sharpley A, Folmar G (2001) Phosphorus export from an agricultural watershed: Linking source and transport mechanisms. J Environ Qual 30:1587–1595

Merritt WS (2002) Biophysical considerations in integrated catchment management: a modelling system for northern Thailand. PhD Thesis, Australian National University

Milliman JD, Syvitski JPM (1992) Geomorphic/tectonic control of sediment discharge to the ocean: the importance of small mountainous rivers. J Geol 100:325–344

Nagle GN, Fahey TJ, Lassoie JP (1999) Management of sedimentation in tropical watersheds. Environ Manage 23:441–452

Nevares R, Dunlop JC (1948) Some engineering and geological data on reservoir sedimentation in Puerto Rico. Unpublished U.S. geological survey report Nordin JCF, Stevens JC (1991) The silt problem—a review. J Sedim Res 3:1–18

Niehoff D, Fritsc U, Bronstert A (2001) Land-use impacts on storm-runoff generation: scenarios of land-use change and simulation of hydrological response in a meso-scale catchment in SW-Germany. J Hydrol 267:80–93

Olcheve A, Ibrom A, Priess J, Eresmi S, Leemhuis C, Twele A, Radler K, Kreilein H, Panferov O, Gravenhorst G (2008) Effects of land-use changes on evapotranspiration of tropical rain forest margin area in Central Sulawesi (Indonesia): modelling study with a regional SVAT model. Ecol Model 212:131–137

Ongkosongo OSR, Sukardi S, Ilyas MA (1992) Sedimentation in rivers and associated water bodies in Indonesia with a special note on the volcanicdebris deposits. Int J Sedim Res 7:93–103

Painter RB, Blyth K, Mosedale JC, Kelly M (1974) The effect of afforestation on erosion processes and sediment yield. In: Effects of man on the interface of the hydrological cycle with the physical environment. IAHS Publ 113(1):62–68

Palmeiri A, Shah F, Dinar A (2001) Economic reservoir sedimentation and the sustainable management of dams. J Environ Manage 61:149–163

Pielke Sr RA (2001) Infuence of the spatial distribution of vegetation and soils on the prediction of cumulus convective rainfall. Rev Geophys 39(1):151–177

Posser IP, Hughes AO, Rustomji P, Young W, Moran CJ (2001) Assessment of river sediment budgets for the national land and water resources audit, Technical report 15/01, CSIRO land and water

Postel SL (1999) Pillar of sand: can the miracle last?. Norton, New York

Postel SL, Daily GC, Ehrlich PR (1996) Human appropriation of renewable freshwater. Science 271(5250):785–788

Rabalais NN, Turner RE, Scavia D (2002) Beyond science into policy: gulf of Mexico hypoxia and the Mississippi River. BioScience 52:129–142. doi:10.1641/0006-3568(2002)052[0129:BSIPGO]2.0

Ragab R, Cooper JD (1993) Variability of unsaturated zone water transport parameters: implications for hydrological modeling. I. situ measurements. J Hydrol 148:109–131

Renwick WH (1996) Continent-scale reservoir sedimentation patterns in the United States. In: Walling DE, Webb BW (eds) Erosion and sediment river basins, vol 217. International Association of Hydrological Sciences Publication, Wallingford

Rosegrant MW, Cai X, Cline SA (2002) World water and food to 2025. Int Food Policy Res Inst, Washington
Sahin V, Hall MJ (1996) The effects of afforestation and deforestation on water yields. J Hydrol 178(1):293–309
Scanlon BR, Reedy RC, Stonestrom DA, Prudic DE, Dennehy KF (2005) Impact of land use and land cover change on groundwater recharge and quality in the southwestern US. Global Change Biol 11:1577–1593. doi:10.1111/j.1365-2486.2005.01026.x
Schilling KE (2005) Relation of baseflow to row crop intensity in Iowa. Agric Ecosyst Environ 105:433–438. doi:10.1016/j.agee02.008
Schilling KE, Jha MK, Zhang Y, Gassman PW, Schilling KE, Libra RD (2003) Increased baseflow in Iowa over the second half of the 20th century. J Am Water Resour Assoc 39:851–860. doi:10.1111/j.1752-1688.2003.tb04410.x
Schilling KE, Zhang YK (2004) Baseflow contribution to nitratenitrogen export in a large agricultural watershed, USA. J Hydrol 295:305–316. doi:10.1016/j.jhydrol.2004.03.010
Shahin MMA (1993) An overview of reservoir sedimentation in some African river basins sediment problems: strategies for monitoring, prediction and control (Proceedings of the Yokohama Symposium, July 1993). LAHS Publication no. 217, pp 93–100
Shiklomanov IA (1998) UN comprehensive assessment of the freshwater resources of the world. State Hydrol Inst, St. Petersburg
Steegen A, Grovers G, Takken NJ, Poesen J, Merckx R (2001) Factors controlling sediment and phosphorus export from two Belgian agricultural catchments. J Environ Qual 30:1249–1258
Turkelboom FT, Poesen J, Trébuil G (2008) The multiple land degradation effects caused by land-use intensification in tropical steeplands: a catchment study from northern Thailand. Elsevier, Amsterdam
Vörösmarty CJ, Green P, Salisbury J, Lammers RB (2000) Global water resources: vulnerability from climate change and population growth. Science 289(1):284–288
Walling DE, Collins AL, Sichingabula HM, Leeks GJL (2001) Integrated assessment of catchment suspended sediment budgets: a Zambian example. Land degradation and development 12(5)
Walling DE, Fang D (2003) Recent trends in the suspended sediment loads of the world's rivers. Global and planetary change. Hydrol Process 39(1–2):111–126
Walling DE, Russell MA, Hodgkinson RA, Zhang Y (2002) Establishing sediment budgets for two small lowland agricultural catchments in the UK. CATENA 47(4):323–353
Walling DE, Webb BW (1996) Erosion and sediment yield: a global overview. In: Walling DE, Webb BW (eds) Erosion and sediment yield: global and regional perspectives. IAHS Publication, no. 236: 3–19
Ward PRB (1980) Sediment transport and reservoir siltation formula for Zimbabwe-Rhodesia. J S Afr Inst Civil Eng 10:A3034–3035
Ward PJ, Balen RT, Verstraeten G, Renssen H, Vandenberghe J (2008) Holocene and future response of suspended sediment yield to land use and climate change: a case study for the Meuse basin. Geophys Res 10:A3034–A3035
Ward RC, Robinson M (1990) Principles of hydrology. McGraw-Hill, London, p 365
White WR (2001) Evacuation of sediments from reservoirs. Thomas Telford, London, UK
Wijesekara GNW, Gupta A, Valeo C, Hasbani JG, Marceau DJ (2010) Impact of land-use changes on the hydrological processes in the Elbow river watershed in southern Alberta. International Congress on Environmental Modelling and Software Modelling for Environment's Sake. 5th Biennial Meeting, Ottawa, Canada
Wolman MG, Schick AP (1967) Effects of construction on fluvial sediment, urban and suburban areas of Maryland. Water Resour Res 3(1):451–464
Zhang YK, Schilling KE (2006) Increasing streamflow and baseflow in Mississippi River since the 1940s: effect of land use change. J Hydrol 324:412–422. doi:10.1016/j.jhydrol.2005.09.033
Zulkifley MTM, Ng TF, Raj JK, Hashim R, Ashraf MA (2014) The effects of lateral variation in vegetation and basin dome shape on a tropical lowland stabilization in the Kota Samarahan-Asajaya area, West Sarawak, Malaysia. Acta Geol Sin-Eng 88(3):894–914

Chapter 2
Effect of Land Use Changes on Water Balance and Sediment Yield in Iran

Abstract Land use changes in response to water balance in Iran were studied. About 29 % of total land comprise of agriculture and considered one of most significant economic sector. In northern Iran, Gorganrood, a mountainous catchment comprehensively examined by using WetSpa model which comprises of topography, soil and land use maps to predict discharge hydrographs and spatial distribution of hydrological factors. Deliberated hydrological processes in the model are evapotranspiration, precipitation, depression storage, interception, surface runoff, percolation, interflow, infilteration, ground water flow and water balance in each layer of soil. Response of water balance in soil and water in Kanyanrood catchment, Lake Urmia basin, Karkheh catchment, sedimentations, sub-catchments also mitigated. Different models used in the study also discussed.

Keywords Agriculture · Hydrological processes · Interflow

2.1 Response of Water Balance to Land Use Changes in Iran

Iran is in the Middle East with an area of approximately 1.75 million km^2. Almost 510,000 km^2 land of Iran is allotted for the agriculture which indicates the 29 % of the entire land of Iran. The agricultural sector is one of the most significant economic sectors in Iran, and has extensively expanded in the last two decades as very large population is economically reliant on it. In 2007, agricultural yield contributed for 23 % of the Gross Domestic Product (GDP), 9 % higher than that of in 1992 (FAO 2008). Almost 90 % of the water resources are assigned to the agriculture sector (Ardakanian 2005). As it is represented by Fig. 2.1 that in 2004, 92.2 % of entire water withdrawal was supplied to the agriculture sector in Iran. Hence, with the increase in population size and higher demand for food, more land has been used for crop growth and there is a high pressure on natural resources, particularly water. Iran is one of the countries that have to pay grants to utilize resource, mainly water resources which attribute to the poor management in agriculture (FAO 2008).

M. Hosseini and M.A. Ashraf, *Application of the SWAT Model for Water Components Separation in Iran*, Springer Hydrogeology,
DOI 10.1007/978-4-431-55564-3_2

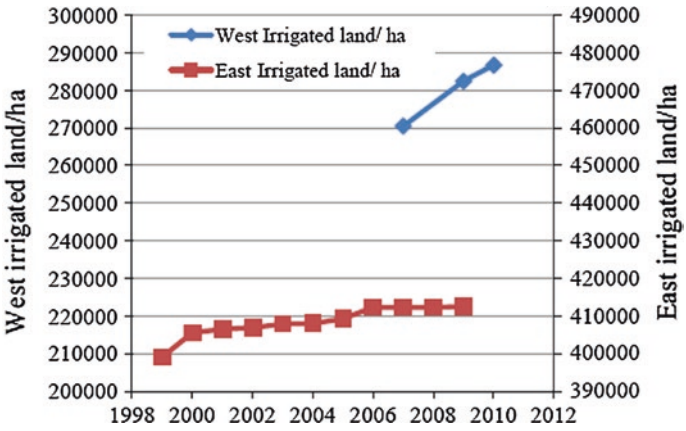

Fig. 2.1 East Azerbaijan and West Azerbaijan agricultural land, Lake Urmia Basin (Zulkifley et al. 2014)

2.1.1 Gorganrood Catchment

Gorganrood is mountainous catchment located in the northern Iran, Caspian coast (Fig. 2.2). Effect of land use changes on water balance and its components in Gorganrood catchment, Iran was comprehensively examined developing a spatially distributed hydrologic model (WetSpa) for the period of last two decades. This model comprises of topography, soil and landuse maps (Fig. 2.3) to predict discharge hydrographs and spatial distribution of hydrological factors. Figures 2.4 and 2.5 represent two resultant parameter maps, which are imperative for model simulation, i.e. potential runoff coefficient and flow travel time maps, respectively. For each grid cell the model holds water balance in the root zone by analyzing variations in soil moisture because of continuous alterations in infiltration of precipitation, runoff, initial absorption, evaporation transpiration, interflow, and percolation to the groundwater zone. The model provides all flow modules at any cell, comprising surface flow, interflow and groundwater flow.

The deliberated hydrological processes in the model are evapotranspiration, precipitation, depression storage, interception, surface runoff, percolation, interflow, infiltration, groundwater flow, and water balance in each layer. A schematic representation of the considered hydrological processes can be seen in Fig. 2.6.

Isolated water balance for the vegetated, bare-soil, open water and impermeable share of each cell accounts for entire water balance for each raster cell. For each grid cell, the modeling of root zone water balance is performed constantly by associating inputs and outputs determined by Eq. (2.1).

$$D\Delta\theta/\Delta t = P–I–V–E–R–F \tag{2.1}$$

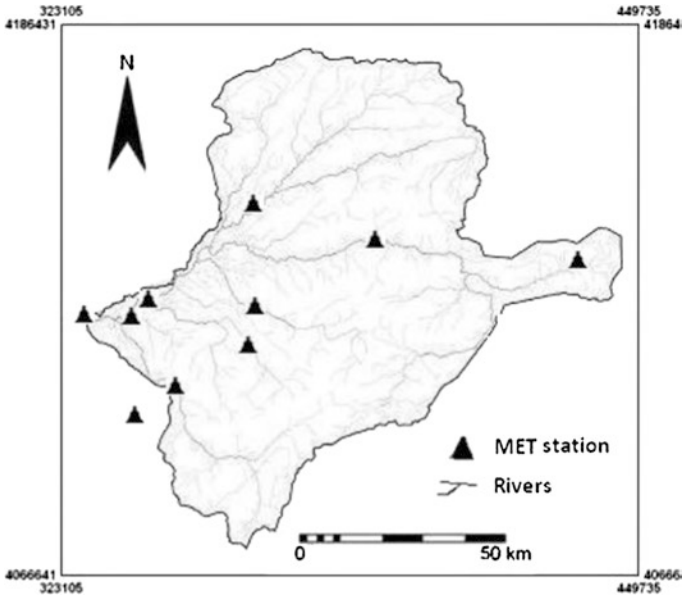

Fig. 2.2 Location of Gorganrood basin, with main tributaries and stations

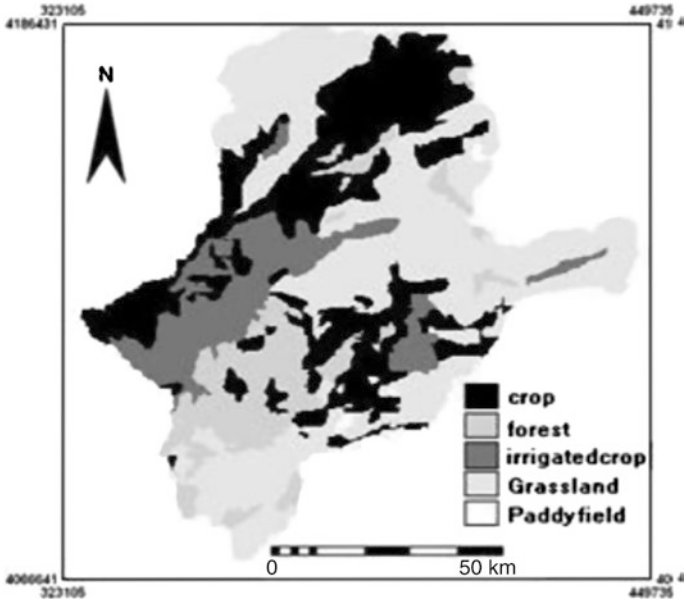

Fig. 2.3 Land use map of the Gorganrood basin

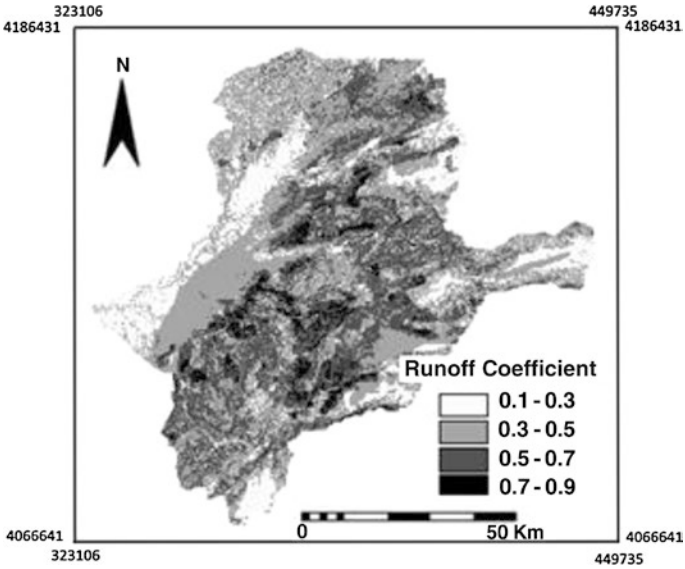

Fig. 2.4 Potential runoff coefficient map of the Gorganrood basin

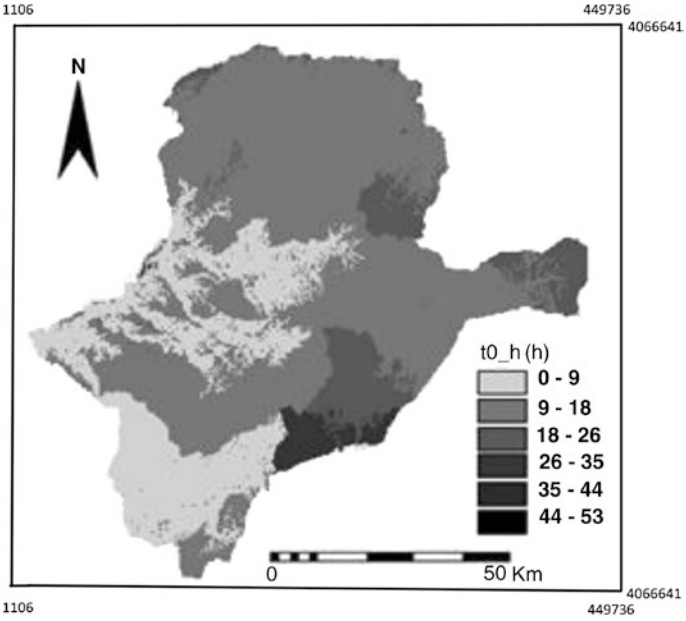

Fig. 2.5 Flow travel time of the Gorganrood basin

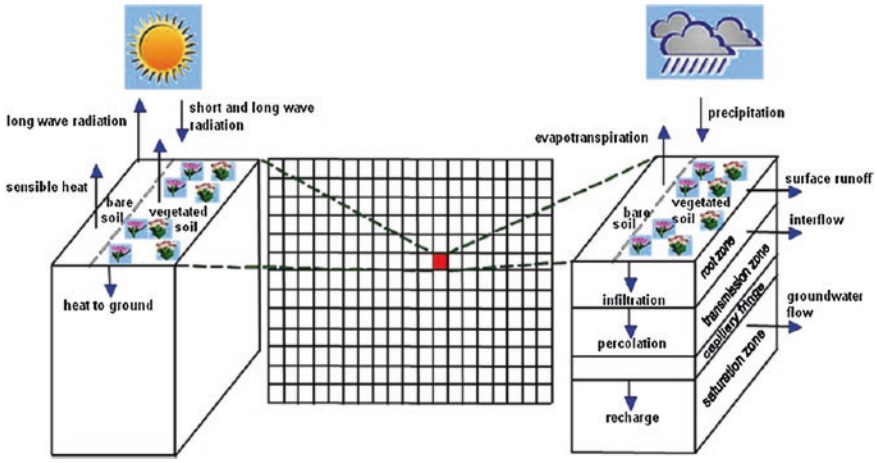

Fig. 2.6 WetSpa model structure

where D [L] is the root depth, $\Delta\theta$ [L3L-3] is the alteration of soil moisture, Δt [T] is the time interval, I [LT-1] is the initial perception comprising interception and depression losses within time step Δt, V [LT-1] is the rate of surface runoff or rainfall excess, E [LT-1] is the actual evapotranspiration from the soil, R [LT-1] is the filtration out of the root zone, and F [LT-1] is the concentration of interflow in depth over time. The rainfall excess is measured applying a moisture-related altered rational technique with possible runoff coefficients reliant on land cover, soil type, slope, the extent of rainfall, and the precursor soil moisture. In the case of surface layer, actual evapotranspiration is calculated as an area-weighted mean of the land use percentage. The course-plotting of overland flow and channel flow is employed by the process of the diffusive wave approximation of the St. Venant equation (2.2):

$$\frac{\partial Q}{\partial t} = d\frac{\partial^2 Q}{\partial x^2} - c\frac{\partial Q}{\partial x} \tag{2.2}$$

where Q [L^3T-1] is the discharge at time t and location x, t [T] is the time, x [L] is the distance along the flow direction, c [LT-1] is the location dependent kinematic wave celerity and is interpreted as the velocity by which a disturbance travels along the flow path, and d [L^2T-1] is the location dependent dispersion coefficient, which expresses the tendency of the disturbance to disperse longitudinally as it travels downstream. supposing that the hydraulic range lines the deepness of the average flow for overland flow and waterways, c and d can be estimated by c = (5/3)v, and d = (vH)/(2S0), where v [L/T-1] is the flow velocity measured by the Manning equation, and H [L] is the hydraulic range or average flow depth. Model was calibrated for the investigated catchment area for the duration of 1983–1989, whereas the duration from 1990 to 1995 was implemented for model validation.

Assessment of the result illustrates that the plant canopy interrupted 6.22 % of the precipitation, 90.19 % penetrates to the soil, 84.41 % evapotranspiration to the atmosphere, 12.43 % recharges to the groundwater reservoir, and 15.83 % converts into runoff, of which 2.71, 1.15 and 11.97 % forms the surface flow, interflow, and groundwater flow, respectively. Furthermore, these calculated amounts are equitable related to the hydrological properties of catchment.

Annual changes in water balance and its modules (mm) have been described comprehensively in Table 2.1. The flow (R) involves the surface runoff (RS), interflow (RI) and groundwater flow (RG). Different modules of the computed flow in association with rainfall are presented in Fig. 2.7 (Kabir and Bahremand 2011).

2.1.2 Zanjanrood Catchment

The hydrological impacts of land-use change in Zanjanrood basin, Iran were explored in order to make useful strategies for sustainable availability of water resources. The simulation of water balance was performed employing the Soil and Water Assessment Tool (Ashraf et al. 2014). Model calibration and uncertainty assessments were conducted applying sequential uncertainty fitting (SUFI-2). Data obtained by simulation study from January 1998 to December 2002 were provided for further parameter calibration, and after this the model was certified for the period of January 2003 to December 2004. The expected monthly streamflow coincided with the observed values: throughout calibration the correlation coefficient was 0.86 and the Nash–Sutcliffe coefficient 0.79, compared with 0.80 and 0.79, respectively, during validation. With the intention of investigation of impacts of land-use changes in 1967, 1994 and 2007, the model was employed to simulate the key modules of the hydrological cycle. The results illustrate that throughout 1967 a 34.5 % reduction of grassland with simultaneous upsurges of shrubland (13.9 %), rain-fed agriculture (12.1 %), bare ground (5.5 %) irrigated agriculture (2.2 %), and urban area (0.7 %) resulted in a 33 % rise in the magnitude of surface runoff and a 22 % drop in the groundwater recharge. Additionally, the area of subbasins which was affected by intensive runoff enlarged from 14 to 28 mm. The consequences point out that the hydrological retort to overgrazing and the substituting of rangelands (grassland and shrubland) with rain-fed agriculture and bare ground (badlands) is nonlinear and manifests a threshold impact. The runoff intensifies radically when clearing of rangeland exceeds 60 %. Conversely, groundwater suppressed by 80 % in rangeland (Ghaffari et al. 2009).

2.1.3 Lake Urmia Basin

The Lake Urmia basin is located in the North West of Iran with high mountain areas, foothills, and plains. It is a closed drainage basin (i.e. no outlet) with an area

Table 2.1 Modules of water balance estimated for each year

Year	Rainfall (mm)	Interception (mm)	Soil moisture (mm)	Infilteration (mm)	Evapotranspiration (mm)	Percolation (mm)	RS (mm)	RI (mm)	RG (mm)	R (mm)
1983	278	25.75	250	256	304	12.9	5.2	1.45	26.94	34
1984	301	21.31	245	367	358	31.8	10	3.73	30.43	44
1985	256	25.96	248	291	285	33.1	7	2.77	31.48	41
1986	301	26.1	252	384	372	37.5	9.1	3.38	32.17	45
1987	355	32.67	257	434	385	81.3	17	7.92	67.74	92
1988	336	29.53	257	440	400	61.9	14	6.18	62.75	83
1989	257	22.11	250	355	319	43.7	8.4	3.84	41.86	54
1990	296	25.34	248	321	327	38	8.3	3.39	36.82	49
1991	325	23.28	247	389	360	50.5	11	4.45	45.01	60
1992	377	34.32	258	566	461	131	24	12.7	110.9	147
1993	310	26.28	250	419	389	53.2	13	5.14	54.14	72
1994	287	27.1	256	397	350	57.3	11	4.76	57.02	73
1995	267	28.2	249	329	347	29.5	7.6	2.34	33.3	43

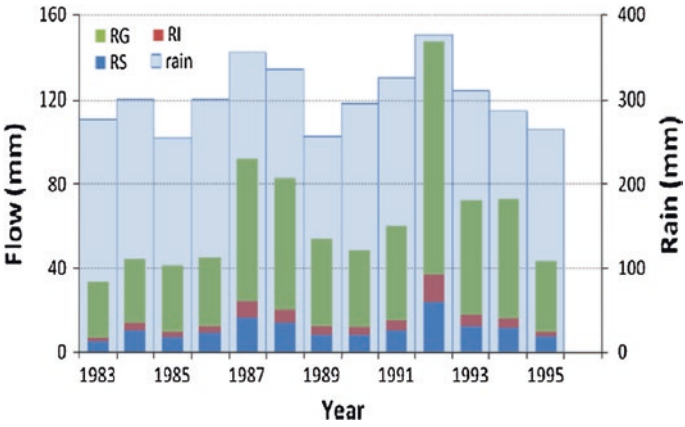

Fig. 2.7 Comparison between different estimated flow modules and rain quantity

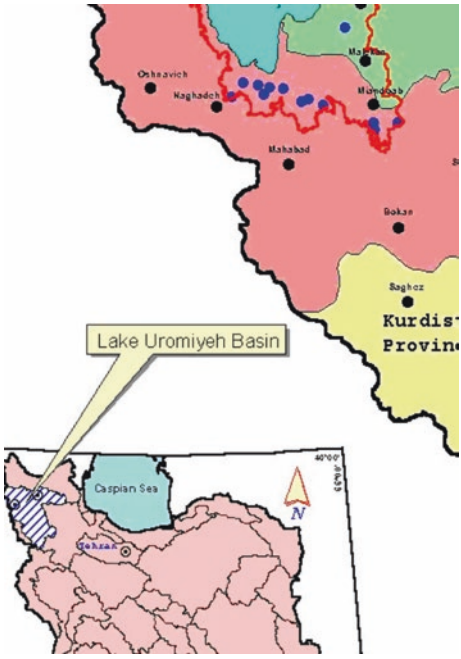

Fig. 2.8 Lake Urmia basin map (Sima and Tajrishy 2013)

of about 51,876 km^2 (Fig. 2.8). Lake Urmia basin is just about 3 % of the total area of Iran (FAO 2008), with about 51,876 total km^2 and 18,702.86 km^2 agricultural lands in East Azerbaijan and West Azerbaijan, respectively (Ardakanian 2005). In the Lake Urmia Basin, increasing population, socio-economic progress and the enlargement of farming land to supply foodstuff have resulted water scarcity.

As irrigation has intensified in both West Azerbaijan and East Azerbaijan, so the water accessibility in the downstream regions has been rigorously reduced. The intensive cultivation on acreage after the hydrometric stations could be deliberated as one of the key complications to calculate the volume of water delivered to the Lake (Sima and Tajrishy 2013). Release of water from the rivers and canals are problematic as well, and the recent droughts in the area have had substantial influence on rivers influx and lake water balance. For example, in recent years, no water inflow to the lake from the Mardogh Chai River was noticed after establishment of Baba roud station (Sima and Tajrishy 2013).

From 1969 to 1998, the area of lake surface has been comparatively persistent (5300 km^2) (Fig. 2.9) (UNEP 2012). Since 1998, the lake size has been reduced to the less than its half size. According to satellite data, its area condensed to around 2366 km^2 in August (Fig. 2.9) (UNEP 2012). In 1995 highest water level was recorded in Lake Urmia and exceeding 1277.49 m of sea level (Fig. 2.10) (Natural Resources and Watershed Management Organization 2011). As it is clear in an aerial photographs in Fig. 2.10, the surface area of Lake Urmia basin has reduced in generally at the south and east position during 2006 and 2011. Decreasing of the Lake surface area could be address to the reduced water influx to the lake exactly from mid 1990s which water level affectedly has declined up to present-day (Fig. 2.10 and Table 2.2).

The entire watercourses and streams reach to this lake has been desiccating at very fast rate since 1990. The maximum lake water level noted was 1277.80 m in 1994 whereas it was dropped up to 1271.58 m in 2008. The lake water capacity has altered throughout the investigation period and displays a reduction from 32 to 14.5 million m^3, while the lake salinity went up from 205 to 338 g L^{-1} because of the high evaporation rate and low water influx. Regarding Lake Urmia basin, there has been an increase in public wakefulness of the emerging water scarcity, environment and all the challenges that could definitely become crisis for the native people of that area.

2.1.4 Karkheh Catchment

An inclusive spatio-temporal evaluation of the surface water resources of the semi-arid Karkheh basin, Iran was performed which subsequently facilitates policy makers to do efforts for sustainable water development in that area. The investigation is on the basis of the consideration of statistical parameters, flow interval features, base flow separation and trend analysis and for this purpose data collected from seven main gauging stations (Fig. 2.11) were employed from 1961 to 2001. In addition, basin level water accounting was done for the water year 1993–1994. The results illustrates that detected daily, monthly and annual streamflows are extremely flexible in space and time within the basin (Fig. 2.12). The streamflows have not been altered considerably when measured at annual basis; nevertheless major trend has been exhibited for few months, most particularly a drop for the

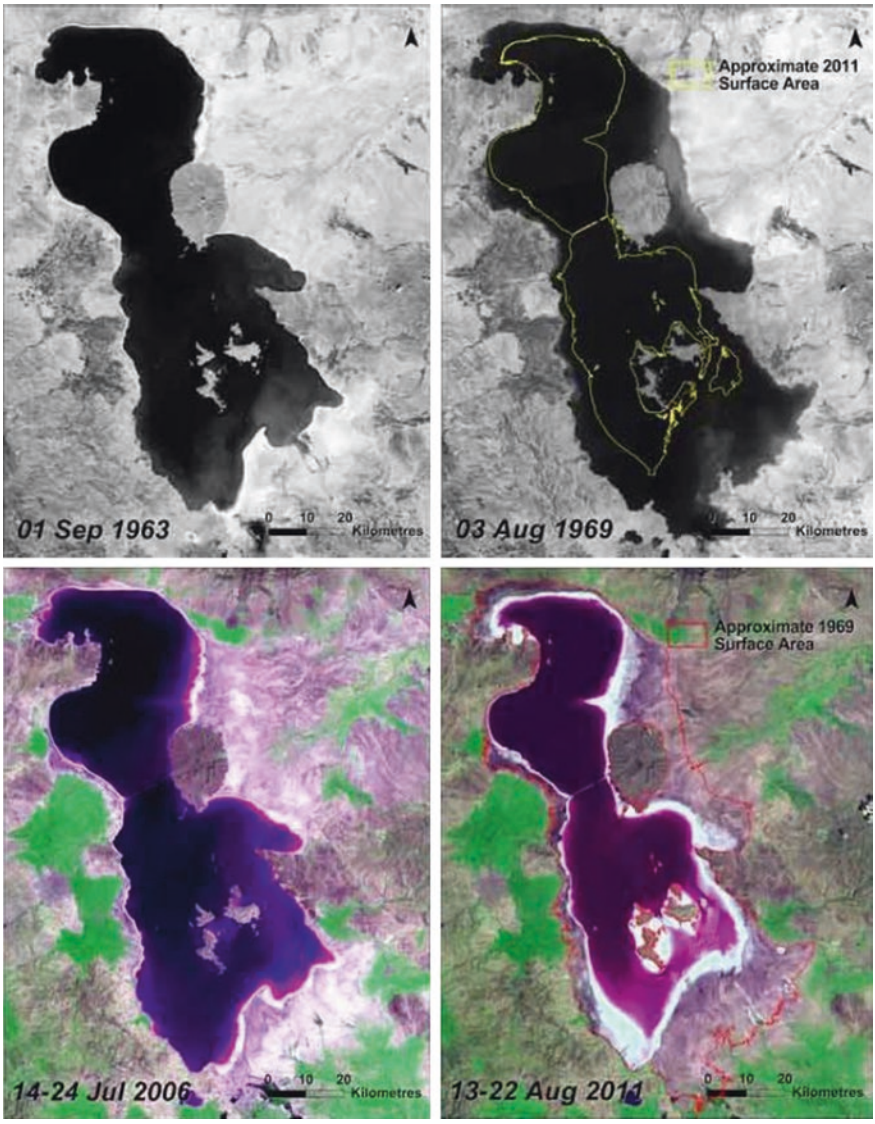

Fig. 2.9 Landsat image of Lake Urmia (*Source* 1963 Image: ARGON data from USGS; 1969 image: Corona data from USGS, visualization by UNEP GRID Sioux Falls; 1972–2011 images: Landsat data, 2011 image: visualization by UNEP GRID Sioux Falls

period of May–June and a rise for the duration of December–March. Figure 2.13 shows that hydrograph peaks occur in March and April roughly one month in the lag of precipitation. Snow melting in the winter season and contribution of water after passing through different waterways such as ground water is a major source of streamflow. The key reasons involved the climatic variations, land use and

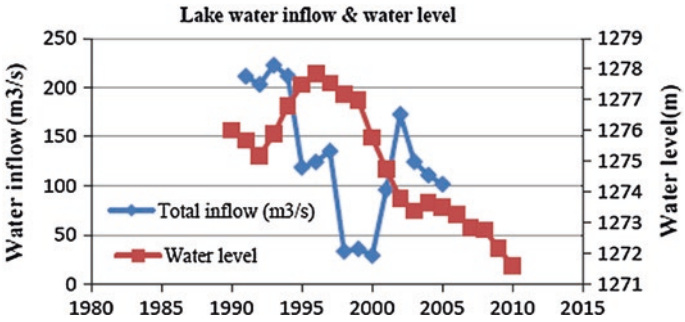

Fig. 2.10 Lake water inflow and Lake water level. Data from Natural Resources and Watershed Management Organization (2011)

Table 2.2 The water inflow to the Lake Urmia Data from (Sima and Tajrishy 2013)

Year	1978	1986	1993	1998	1999	2000
Water inflow to the Lake (MCM)	13,526.7	10,725.82	8845.49	586.34	439.97	341.2

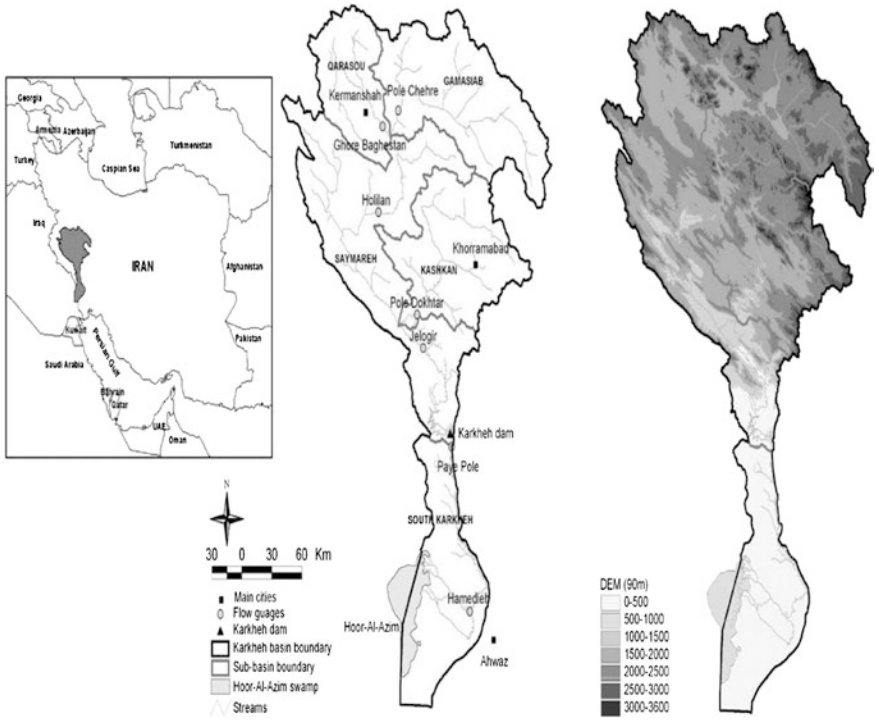

Fig. 2.11 Location of Karkheh basin with seven gauging stations

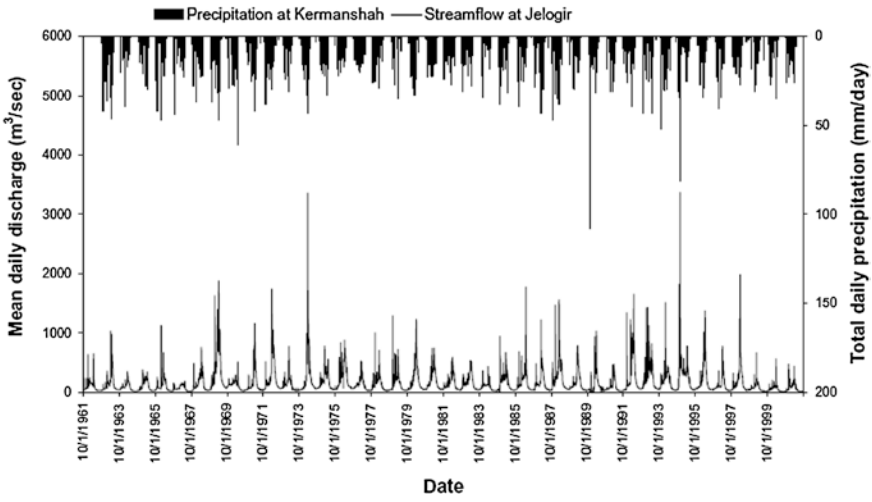

Fig. 2.12 Average yearly variability daily streamflow during 1961–2001

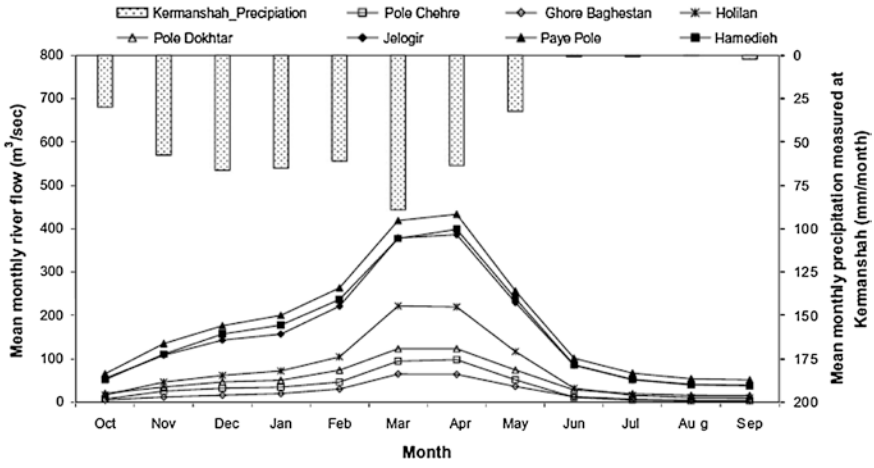

Fig. 2.13 Average monthly discharge in study area of Karkheh basin, Iran

reservoir practices. The study accomplishes that the water distributions to various sectors were lesser than the entirely accessible resources throughout the investigation period (Fig. 2.14). Though, regarding the large variability of streamflows, climatic variations, land use and current water resources development practices, it will be enormously challenging to full fill the requirements of all sectors in the upcoming years, predominantly in the course of dry season (Masih et al. 2009).

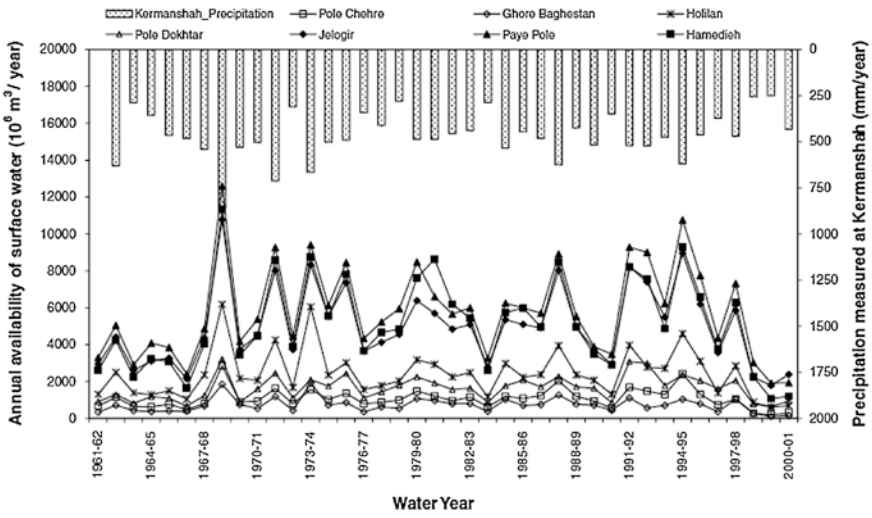

Fig. 2.14 Long-term variability in yearly surface water availability in Karkheh basin, Iran

2.2 Response of Sedimentation to Land Use Changes in Iran

One of the most important concerns in arid and semi-arid areas, Iran is water erosion and sediment transport. Soil particle transmission from farm and orchards to other areas causes the fertility of such lands decreases gradually (Sarmadian et al. 2010). Deforestation in Iran has been more rapid in the past 50 years than at any time in Iran's history. Intensive cultivation and mismamnagement have caused environmental problems and soil degradation (Bakar et al. 2015). Moreover, sedimentation in water channels clogs the water ways; it may also transfer pollutants into farm lands and dams, which are used for irrigation and drinking purposes (Sarmadian et al. 2010).

Erosion causes serious consequences for economy as well as the environmental productivity. The important influences of soil erosion are manifest in areas which don't have erosion but suffer from its consequences by sediment deposition in watercourses and reservoirs, water quality and flow rate decreasing (Gharibreza et al. 2014). All these results have a negative impact on water of river regimes. There are many erosion classifications available in the literature review. Since water erosion is the most significant problem in western Iran, Surface erosion and mass movements in the catchment body, produce the soil loss which is due to its moving to another area as sediment. Development strategies led to changes in land use which exposed sensitive geological formations, consisting largely of shale and marl, to soil erosion. Moreover, poor vegetation cover in the Zagros Mountains was one of the main factors which caused millions of tons of soil to be transported by water to downstream catchments. Surface erosion and sediment yield are important factors that should be taken into account in planning renewable natural resource

projects. The Zagros mountain range begins in northwestern Iran and roughly corresponds to Iran's western border, and it spans the whole length of the western and southwestern Iranian plateau, ending at the Strait of Hormuz.

2.2.1 *Sub-catchments (Amrovan, Atray, Ali Abad, Ebrahim Abad, Royan)*

Several experimental models were used for predicting the erosion severity and sediment yield in a sub-catchment area. Response erosion severity and suspended sediment yield to land use changes of five small catchments (Amrovan, Atray, Ali Abad, Ebrahim Abad, Royan), Semnan Province, Iran (Fig. 2.15) were assessed implementing PSIAC model using consistent sediment yield data dumped in reservoir built in the outlet of these catchments (Gharibreza et al. 2013a). A strong positive correlation was found between Upland erosion and Specific Sediment Yield i.e. $r_2 = 0.86$.

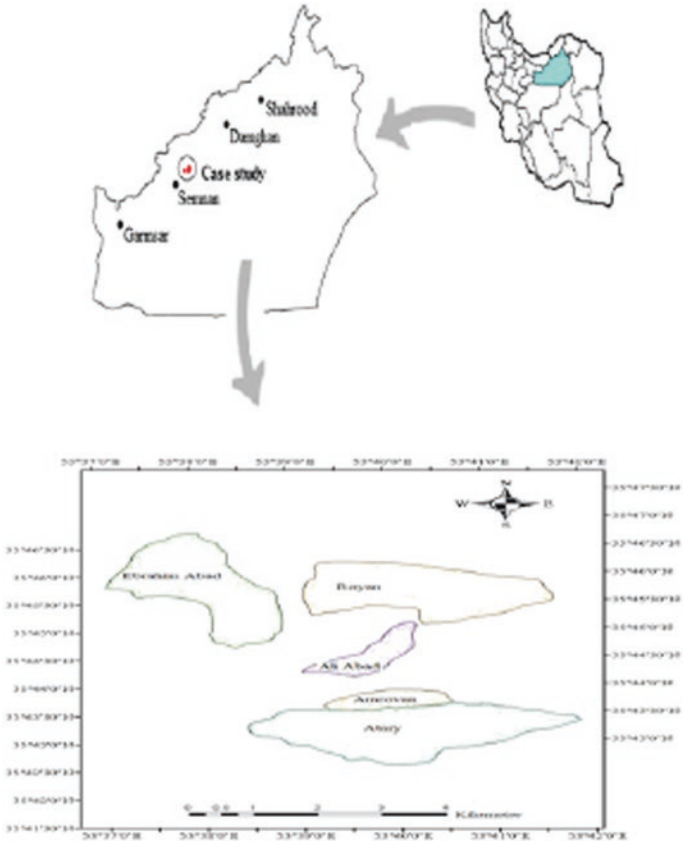

Fig. 2.15 Location of five sub-catchments (Amrovan, , Ali Abad, Ebrahim Abad, Royan)

Table 2.3 Scores and coefficient of different PSIAC factors and the quantity of predicted SSY in the study catchments

PSIAC factors	Catchments				
	Amrovan	Atray	Ali Abad	Ebrahim Abad	Royan
Surface geology (y1)	5.99	5.76	5.74	5.18	5.66
Soil type (y2)	4.28	3.43	1.97	4.35	4.65
Climate (y3)	1.12	1.12	1.12	1.12	1.12
Runoff (y4)	0.71	1.21	0.72	1.14	1.20
Slope (y5)	3.76	5.26	5.35	9.67	7.90
Ground covers (y6)	16.03	13.80	15.36	13.90	11.4
Land use (y7)	17.67	16.77	18.58	17.95	17.41
Upland erosion (y8)	16.58	6.20	7.08	5.40	7.85
Channel erosion and sediment transport (y9)	4.09	0.00	1.51	0.00	5.03
Total score (Pt)	70.23	53.55	57.43	58.71	62.22
Rating class	3	3	3	3	3
Predicted SSY (t ha^{-1} $year^{-1}$)	3.171	1.74	1.99	2.09	2.35

This method involves nine parameters that rely on surface geology, soils, climate, runoff, topography, ground cover, land use, channel erosion, and upland erosion. Each parameter is divided into various definite categories, and dependent on the extent of influence of each parameter category; a weighting value is allotted to each category using the model tables (PSIAC 1968).

Nine PSIAC parameters have been rated on the basis of PSIAC Guide Tables for investigation of catchments which can be seen in Table 2.3. The totalities of the calculated values for the suitable properties of the nine parameters generated the total score (Pt) and rating class for the catchments, and then followed by putting of a linear regression between Pt and the detected value of suspended sediment yield to calculate predicted suspended sediment yield. Equation 2.3 can be used to calculate specific sediment yield.

$$SSY = 4.119\,Pt + 55.31 (R2 = 0.755) \tag{2.3}$$

where, specific sediment yield is denoted as SSY (t ha^{-1} $year^{-1}$), PSIAC total score as Pt which is found by summing each discrete parameter (Table 2.3).

The findings of this investigation point out that all of the catchments are associated with modest rating class of suspended sediment yield i.e. class 3. Amrovan sub-catchment was found to have maximum magnitude of PSIAC predicted suspended sediment yield (3.171 t ha^{-1} $year^{-1}$), on the other hand it was minimum (1.74 t ha^{-1} $year^{-1}$) for Atray sub-catchment.

In order to evaluate relationship between nine PSIAC parameters and suspended sediment yield for different catchments, linear regression and correlation analysis was performed for detected suspended sediment yield and the score of each parameter for the catchments (Fig. 2.16). Surface geology has significant influence (Fig. 2.16a), due to great distinctions in erodibility of geological

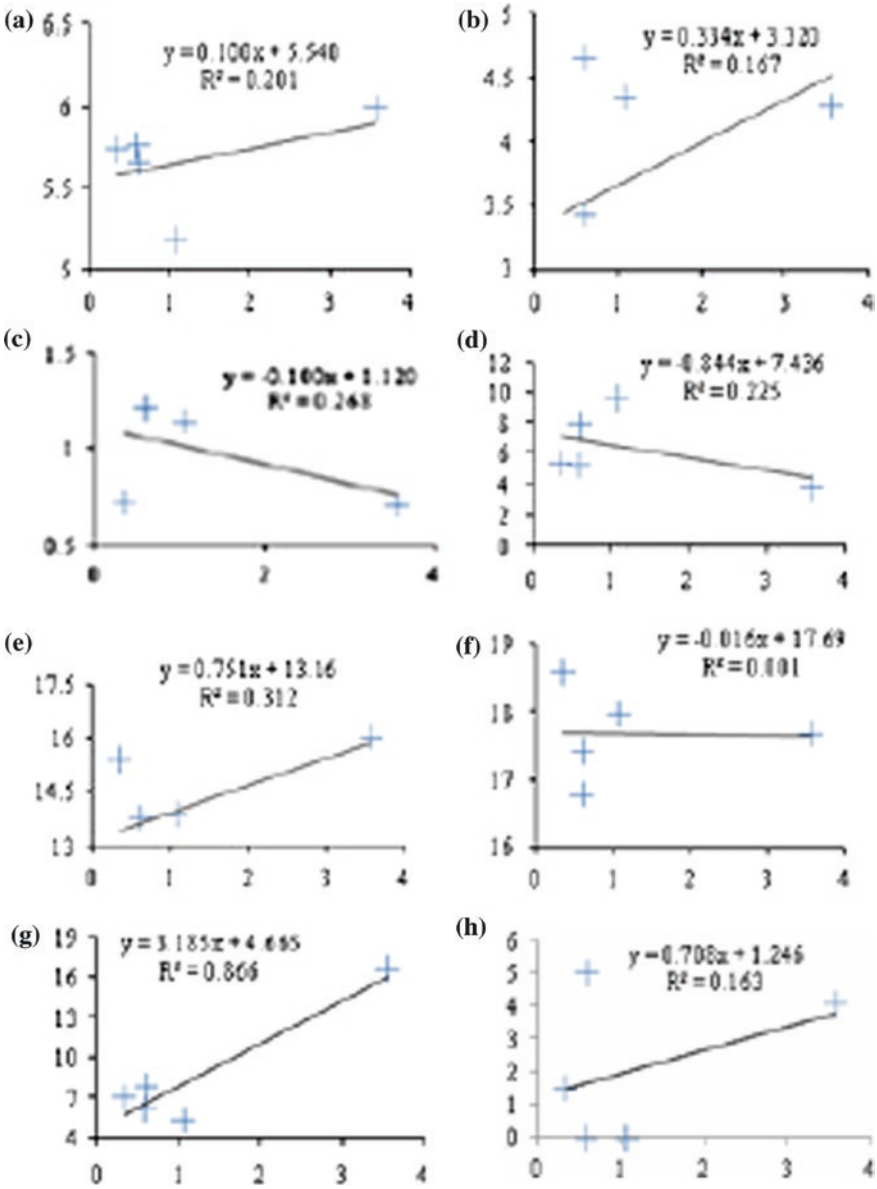

Fig. 2.16 Relation concerning each PSIAC scores and observed suspended sediment yield. Horizontal diagrams are observed suspended sediment yield (t ha^{-1} $year^{-1}$) and vertical diagrams are individual PSIAC scores. **a** Surface geology, **b** soil type, **c** runoff, **d** slope, **e** ground cover, **f** land use, **g** upland erosion and **h** channel erosion and sediment transport

materializations in the catchments. For instance, Amrovan and Royan catchments contain highly weathered constituents such as marl and quaternary whereas rest of the catchments (Ebrahim Abad, Atray) have a more resilient geology for example Azarin rocks.

The catchments under investigation showed distinction based on soil texture (Fig. 2.16b). Therefore, impact of soil is in range of low to moderate in zones where there is maximum to minimum stone coverage and moderate to high in zones where there is a soil that is categorized between moderate to single grained textured soils. The erodibility of a soil is affected by stony layer (Poesen et al. 1994; Nyssen et al. 2001) and grain dimension (Morgan 1986; Evans 1980).

Furthermore, runoff is an imperative factor in clarifying suspended sediment yield variability between the catchments (Fig. 2.16c). Runoff is further influenced by other factors (land use, soil and water conservation practices, slope, lithology and soil conditions) (USDA-SCS 1964). Topography exhibits comparatively strong impact on the changeability of specific sediment yield (Fig. 2.16d); though most of the regions of Amrovan, Ali Abad and Atray catchments are categorized based on steep upland slopes i.e. >20 % and in the Ebrahim Abad and Royan these are higher slopes i.e. <20 %. The effect of topography may be partially concealed by collaboration of impacts. Since stoniness may be anticipated to upsurge with degree of slope, the impacts of slope steepness and soil cover on erosion may neutralize each other (Haregeweyn et al. 2005).

The land cover is highly interrelated with suspended sediment yield (Fig. 2.16e). The influence on suspended sediment yield changeability is strong as a number of catchments stay ploughed and bare during rainy season (e.g. Amrovan), Though others are significantly safe because of being well covered. The impact of vegetation cover in decreasing soil erosion has been proved by conducting research related to vegetation cover: for instance cover associated with interception and cover in directly connected with the soil layer such as the impact of remains of crops (Morgan 1986) and stones (Nyssen et al. 2001). Besides interception, land cover disperses the energy of surface runoff by enhancing unevenness (Morgan 1986).

A weak correlation exists between land use and SSY (Fig. 2.16f), primarily due to insignificant land use changes across the catchments; above 90 % of the zone of most of these catchments consist of rangeland. Upland erosion and suspended sediment yield are highly interrelated (Fig. 2.16g) in these catchments, erosion takes place by rill, inter-rill and some gully erosions. Even though rates of erosion are suppressed in the catchments having prevailing shrub land and well stone cover: for example Ebrahim Abad and Atray catchments, a number of catchments like Amrovan the proportion of shrub and stone cover is very poor. Channel erosion is also representing some variable clarifying suspended sediment yield (Fig. 2.16h) in our study catchments there are no large waterways. Conversely in the Amrovan and Royan there are some small and not well developed waterways. The sediment yield from waterways is generally due to the occurrence of very erodible parental constituents such as marl in the case of this catchments and because of the vertices property of clay developments (Gharibreza et al. 2013b)

that are vulnerable to penetrating that results in bank flop and vigorous head cuts (e.g. Amrovan). Henceforth, importance should be given to recovering the waterways and the routed sub catchments while planning soil and water management practices in the catchments.

The analysis illustrates that suspended sediment yield differs considerably between catchments, i.e. from 3.57 to 0.35 t ha^{-1} $year^{-1}$. The remarkable spatial variability in suspended sediment yield is primarily related with dissimilarities in lithology, runoff, topography, ground cover and upland erosion.

2.2.2 Karkhe Catchment

In recent times, Karkhe watershed (KW) with size above 5 million ha faced many complications in the natural, social and man-made habitats. Improper land practices, soil erosion and shortage of rainfall are the most critical issues in this watershed disturbing the entire area basically. As anticipated, these complications have resulted in a substantial decrease in biodiversity in fauna and flora, a decline in capacity and excellence of water resources in watershed and intensification in possibility of destructive overflows. With the aim of investigation related to land use variations and soil erosion in 5 sub-regions of Karkhe watershed, LANDSAT images were developed for two periods of time '1988 and 2002'. The impacts of these operations on the physico-chemical properties of water like cation and anion level, acidity and salinity were determined. It was concluded that erosion variations in Karkhe Watershed are negligible from 1988 to 2002. The range of urban area and irrigated agricultural lands in Karkhe sub-regions (Gamasiab, Gharresu Kashkan) are about 1000 and 2000 km^2 correspondingly, the drop in river discharge almost 121.6 m^3 s, is the highly effective parameter for the drop in acidity from 7.9 in 1988 to 8.1 in 2002, an increase in salinity from 1.6 mg L^{-1} in 1988 to 3.6 mg L^{-1} in 2002 as average quantity of SAR in all sub-regions of watershed and the high density of the anions from 8.1 mg L^{-1} in 1988 to 16.4 mg L^{-1} in 2002 and cations from 8.8 to 16.5 mg L^{-1} in Karkhe River. According to the deputy of watershed management, Jihad agriculture in Iran, in 2004 the key concern in this area is the conversion of lands into geologically erodible lands which forms over 79 % of the entire watershed consequently generating sediment at about 1.5 million m^3 $year^{-1}$ that discharges directly into the Karkhe catchment (Mahmoudi et al. 2010).

2.2.3 Chamgardalan Catchment

Chamgardalan catchment is one of the sub-catchments of Karkheh watershed with the size 583.7 km^2 (Fig. 2.17). This watershed is positioned between latitudes 33° 23′N to 33° 40′N and longitudes 46° 16′E to 46° 40′E. GIS (ArcGIS9.3) was used for erosion intensity maps and the quantification of sediment yield/transport as

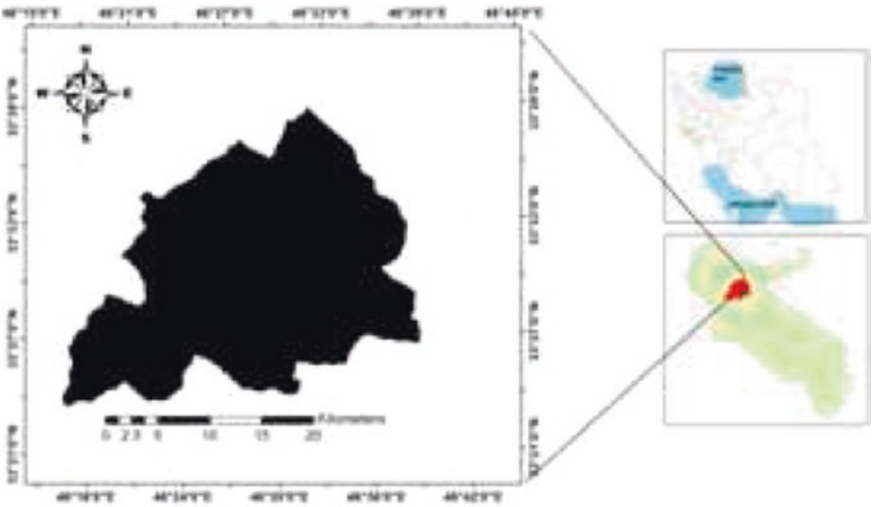

Fig. 2.17 Location of Chamgardalan catchment

well (Fig. 2.18). Description of the coefficient maps (Xa, Y, φ and j) was on the basis of spatial input data, viz. land use/land cover map (Fig. 2.19), DEM (Digital Elevation Model) (Fig. 2.20), geology of area (Fig. 2.21), and satellite images of area. The Y coefficient map represents the soil confrontation to erosion which is developed on the basis of geology and soil data.

By using EPM method, average yearly catchment Degradation Wsp (average yearly sediment yield) is determined by means of the following Eq. (2.4):

$$Wsp = T \times h \times \pi \times (aZ^3 \times F)(\mathrm{m}^3\ \mathrm{year}^{-1}) \tag{2.4}$$

where h (mm) indicates average yearly rainfall, F represents catchment area (km^2) and T signifies the temperature coefficient and t is average yearly air temperature (°C).

Erosion coefficient Z can be calculated by Eq. (2.6).

$$T = \left(\frac{t}{10} + 0.1\right)^{1/2} \tag{2.5}$$

$$Z = Y \times Xa \times (\varphi + j) \tag{2.6}$$

where Y: indicates Coefficient of the soil confrontation to erosion (functions of geology and soil type), X: indicates Land use/land cover coefficient, a: represents conservation coefficient after an erosion estimates (here a = 1), φ: indicates coefficient of the observed erosion process (takes into consideration clearly detectible erosion processes), j: indicates average slope of the catchment.

$$R = \frac{4(P \times D)^{1/2}}{L + 10} \tag{2.7}$$

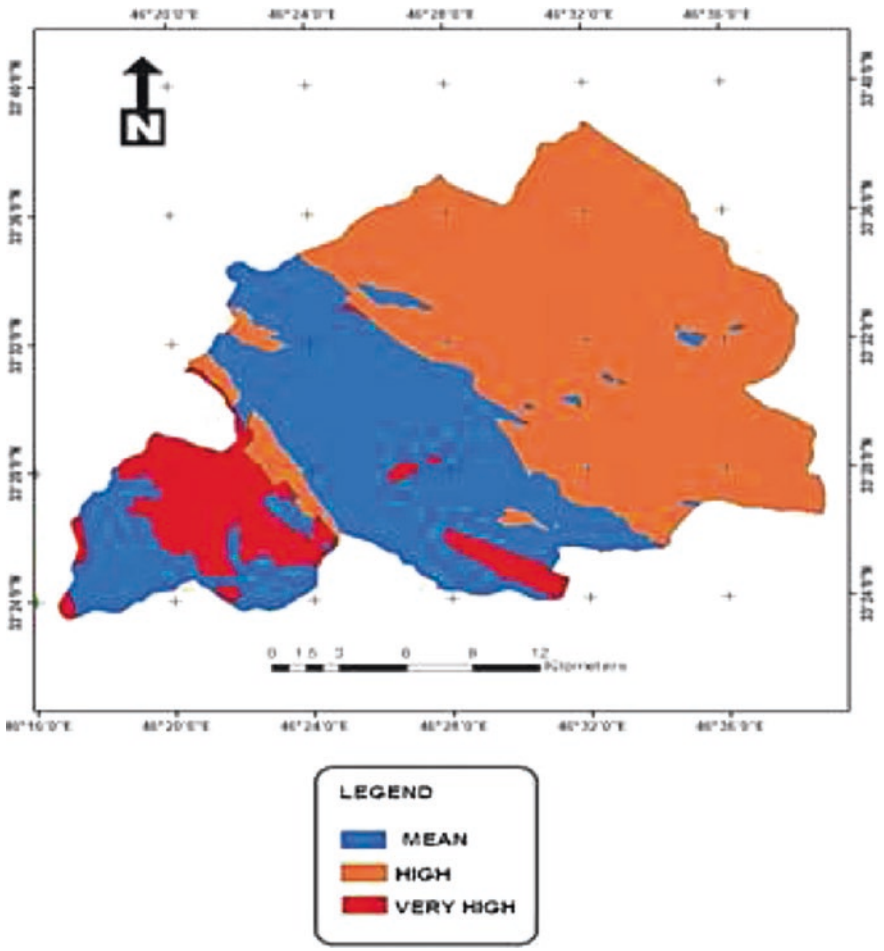

Fig. 2.18 Erosion quality map of Chamgardalan catchment

R is coefficient of sediment formed in any homogenous units,
P Perimeter of the homogenous unit (km),
L Length of the homogeneous unit (km),
D Average altitude gradient (km).

Finally, *Gs* symbolize the average yearly sediment amount that enters the detected cross-section which is calculated by multiplying Eqs. (2.4), and (2.7) as indicated by Eq. (2.8).

$$G_s = T \times H \times (Z^3) \times F \times R \ (\mathrm{m}^3 \ \mathrm{year}^{-1}) \tag{2.8}$$

All EPM functions are determined in homogeneous unit (Fig. 2.22).

The main objective of the study was qualitative and quantitative estimation of the erosion and sediment yield of Chamgardalan watershed, Ilam Iran by applying

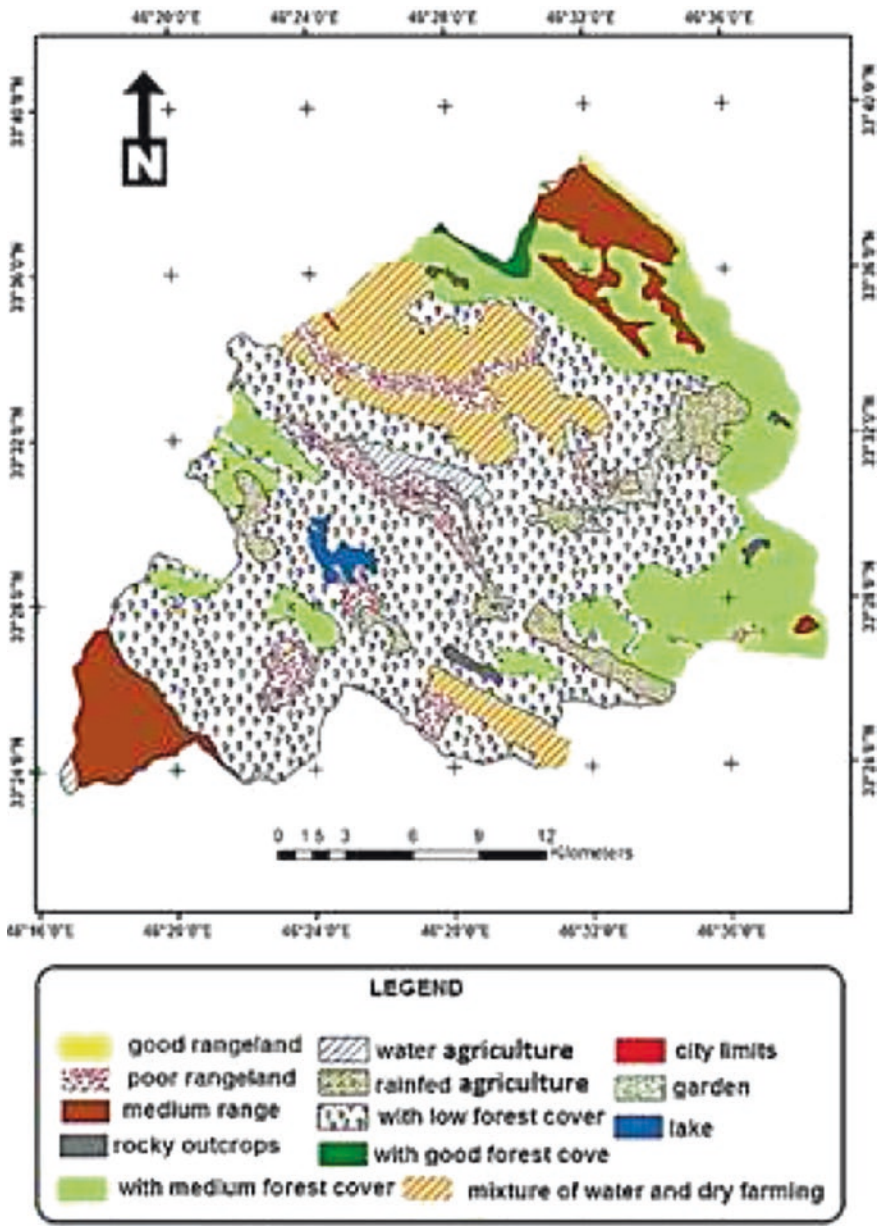

Fig. 2.19 Land use map of Chamgardalan catchment

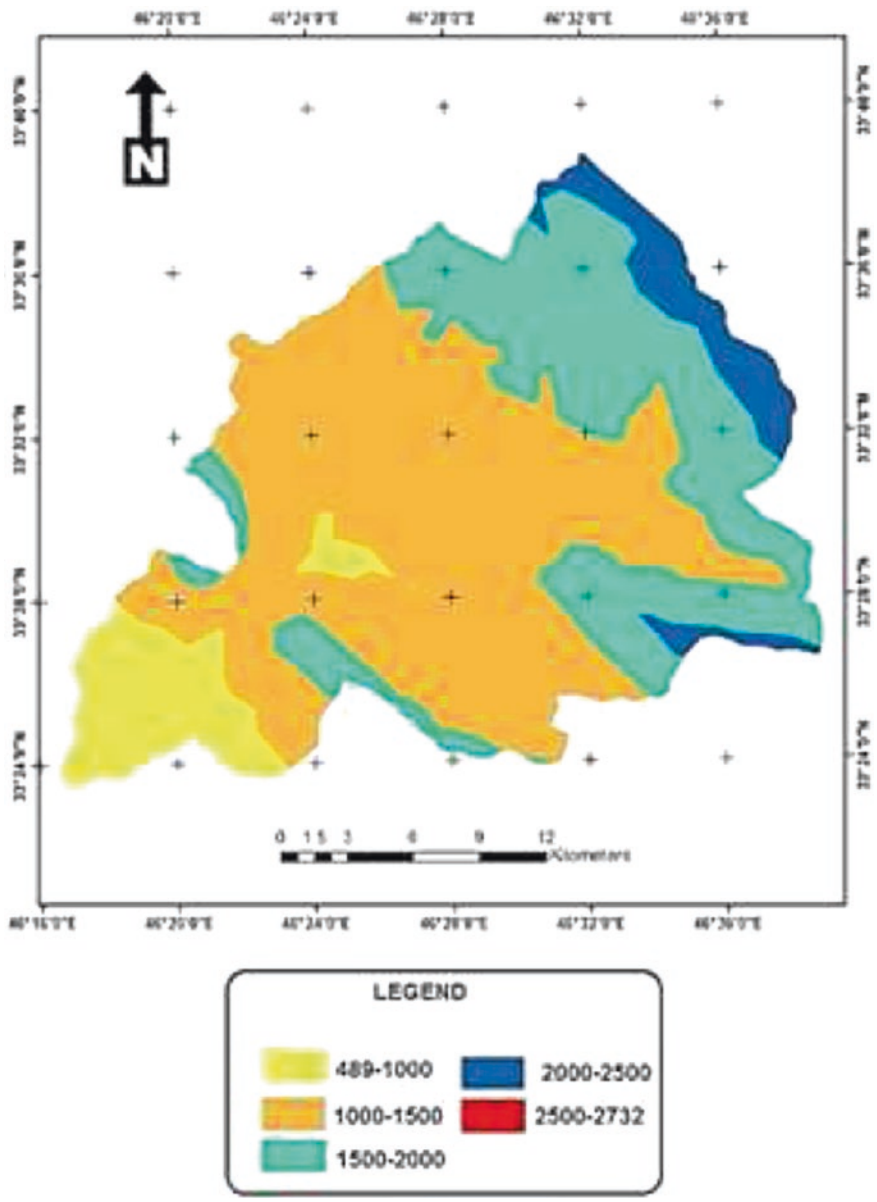

Fig. 2.20 Digital elevation map (DEM) Chamgardalan catchment

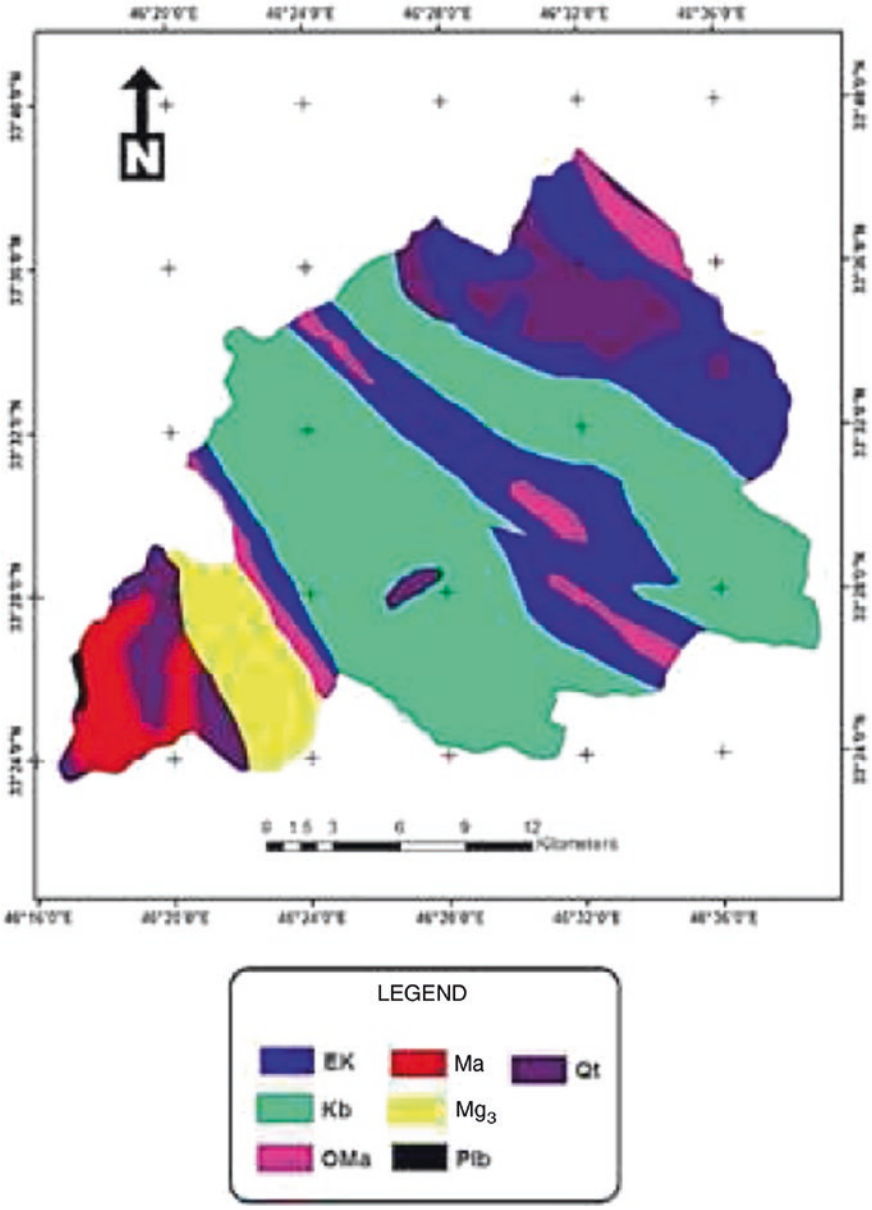

Fig. 2.21 Geology map of Chamgardalan catchment

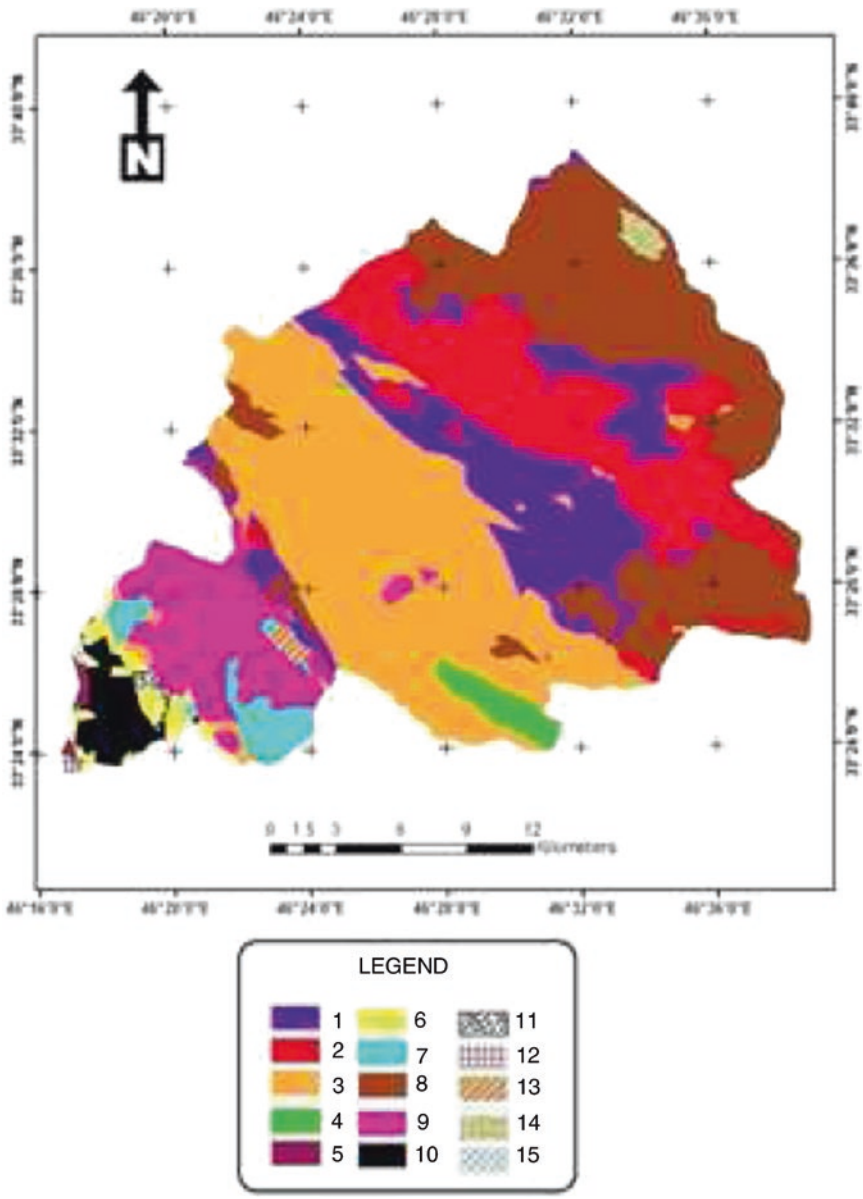

Fig. 2.22 Homogenous units map of Chamgardalan catchment

EPM (Erosion Potential Method) and field data in GIS software. A grid-based distributed model EPM well-matched with ArcGIS9.3 Geographic Information Systems (GIS), was employed to 583.7 km^2 Upper Ilam Dam River in Ilam province. Model considerations were derivatives of digital elevation model (DEM), land use and soil type map of the basin. These considerations and the obtained regular climatological data (1998–2010) were applied (1) to examine the presentation of the EPM model in order to assess the entire sediment yield, (2) to classify various erosion modules. The conclusions shows that observed overall sediment was 22.60 t h^{-1} $year^{-1}$, while the overall estimated sediment concentration using model was 19.97 t h^{-1} $year^{-1}$. The predicted concentration of overall sediment was close to the observed concentration in the stations at basin outlet. Erosion Potential Method (EPM) can be developed for other homogeneous units which don't contain hydrological stations, as the erosion modeling and watershed controlling practices cost lesser than constructing and establishing hydrological stations (Gharibreza et al. 2013b).

2.2.4 Shar-Chi Catchment

The Shar-chi catchment is in the north-western part of Iran and in west Azarbyjan province positioned between the 37° 19′ 34″ to 37° 31′ 29″ east latitude and 44° 34′ 02″ to 45° 00′ 50″ north latitude and its size is 413.9 km^2. Almost 88 % of catchment comprises of hills and mountains and remaining 12 % lies in gentle slope. Impact of land use changes on suspended sediment yield in Shar-chi catchment was predicted on the basis of data available for the duration of 1974–1999. Figure 2.23 is demonstrating the process of sediment generation in Shar-chi catchment.

The major issue regarding this catchment is transformation of rangelands into rainfed crops in hilly areas with lack of management practices. This contributes to maximum erosion for the reason that a large proportion of the fields are positioned on steep slopes and the ploughing is done in the direction of the slope.

So as to identify the land use changes of these regions two unlike Landsat image (ETM, June, 2000 and TM, Aug, 1990), an ASTER image (24.July, 2000) and aerial photographs (1956) were applied. A correlation between release and the

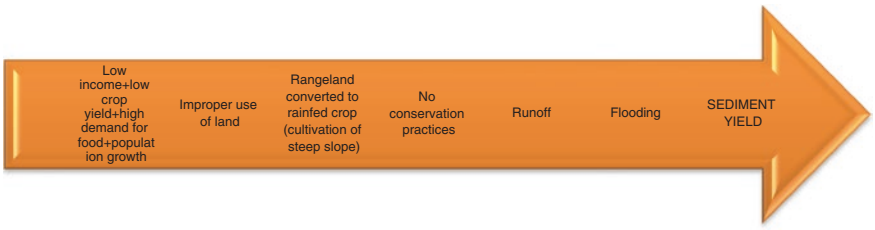

Fig. 2.23 Process of the generated sediment yield in Shar-chi catchment

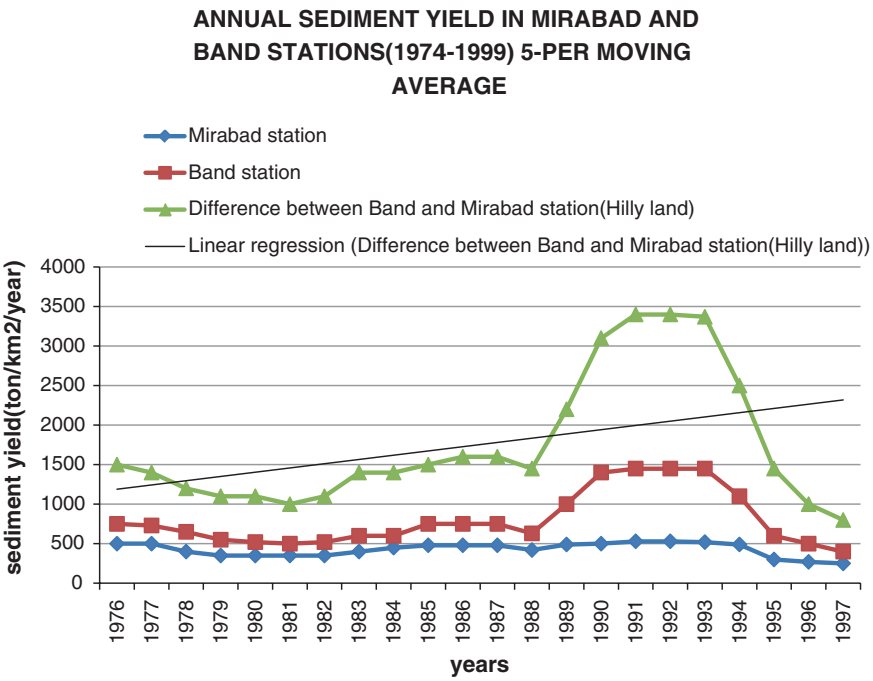

Fig. 2.24 Yearly sediment yields in Mirabad and Band stations and mountainous region

sediment carriage was finally applied. In the case of less release the mean values of the sediment amounts were used, however for the excessive release an exponential function.

Generally, the land use variations occur in the lower part of the catchment, named the Hills, and the impact on the sediment yield was investigated by deducting the sediment yield of the upstream station (Mirabad) from the downstream station (Band). The assessed yearly sediment yield variations of the Hills ranged from 390 to 6529 ton km^2 year^{-1} between 1989 and 1996 the yields ranged from 14,446 to 1298 ton km^2 year^{-1} then during the dry periods from 1997 to 1999 the obtained yields were 390 ton km^2 year^{-1} (Fig. 2.24). A trend line shows that from the period of 1974–1999 there was an upsurge in the sediment yield from the hills, while no such tendency was observed for the upper catchment. Therefore, in the later case amount of sediment yield was taken as a control value due to absence of land use maintenance (Fig. 2.25).

The large amount of sediment yield from the Hills is the evidence of a thoughtful environmental issue, which has resulted in deserting of various lands as well as disturbs the sedimentation in the recently constructed reservoir and in the Lake Uromich wetland. Potential strategies should be implemented for soil maintenance and restrain farming of the land with steep slopes.

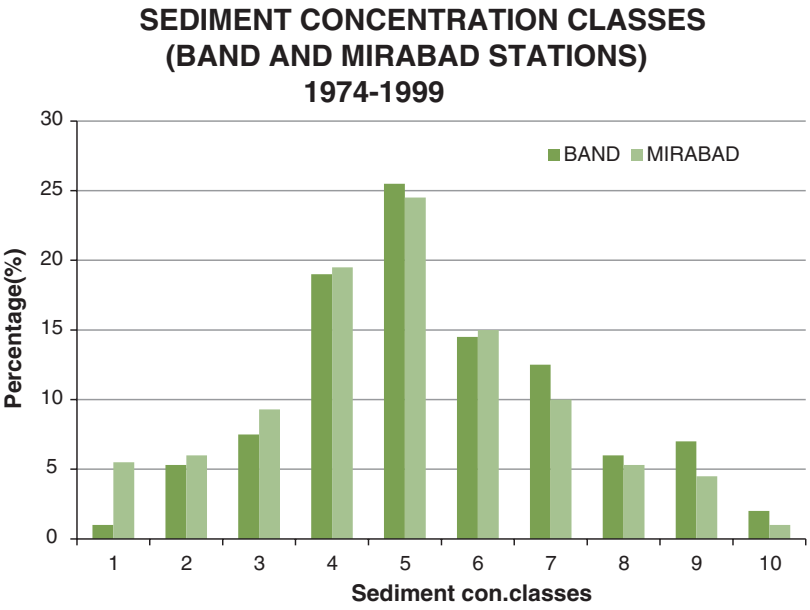

Class	Sediment concentration(mg/litr)
1	0-10
2	10-20
3	20-30
4	30-50
5	60-100
6	100-200
7	200-500
8	600-1000
9	1000-50000
10	>50000

Fig. 2.25 Percentage of sediment concentration classes in Band and Mirabad stations

The division of sediment data into ten classes histogram designed for the frequency analysis of data which is represented by Fig. 2.25. For the less quantities, up to 50 mg L^{-1}, the upper Mirabad station has rather large quantities than that of the lower Band station and vice versa. This proves the extremely erosive nature of the soils and less vegetated cover in the Hills, compared to Mountain unit. The overall and average yearly sediment yields for Band station were 20,172 and 776 ton km^{-2} $year^{-1}$, respectively throughout the period from 1974 to 1999, conversely it was 10,829 and 417 ton km^{-2} $year^{-1}$ for Mirabad station (Gharibreza et al. 2013c).

References

Ardakanian R (2005) Overview of water management in Iran. The National Academies press, Washington, DC

Ashraf MA, Ahmad M, Aqib S, Balkhair KS, Bakar NKA (2014) Chemical species of metallic elements in the aquatic environment of an ex-mining catchment. Water Environ Res 86(8):77–728

Bakar AFA, Yusoff I, Ng TF, Ashraf MA (2015) Cumulative impacts of dissolved ionic metals on the chemical characteristics of river water affected by alkaline mine drainage from the Kuala Lipis gold mine, Pahang, Malaysia. Chem Ecol 31(1):22–33. doi:10.1080/02757540.2014.950569

Evans R (1980) Mechanics of water erosion and their spatial and temporal controls: an empirical viewpoint. In: Kirkby MJ, Morgan RPC (eds) Soil erosion. Wiley, Chichester, pp 109–128

FAO Water Reports (Food and Agriculture Organization) (2008) Irrigation in middle east region in Figure AQUASTAT Survey—2008

Ghaffari G, Keesstra S, Ghodous J, Ahmadi H (2009) SWAT-simulated hydrological impact of land-use change in the Zanjanrood basin, Northwest Iran. Hydrol Process 24(7):892–903

Gharibreza M, Raj JK, Yusoff I, Ashraf MA, Othman Z, Zakaria W, Tahir WM (2013a) Effects of agricultural projects on nutrient levels in Lake Bera (Tasek Bera). Peninsular Malaysia. Agric Ecosyst Environ 165(1):19–27

Gharibreza M, Raj JK, Yusoff I, Othman Z, Zakaria W, Tahir WM, Ashraf MA (2013b) Historical variations of Bera Lake (Malaysia) sediments geochemistry using radioisotopes and sediment quality indices. J Radioanal Nuclear Chem 295(3):1715–1730

Gharibreza M, Raj JK, Yusoff I (2013c) Sedimentation rates in Bera Lake (Peninsular Malaysia) using 210Pb and 137Cs radioisotopes. Geosciences J 17(2):211–220. doi:10.1007/s12303-013-0013-3

Gharibreza M, Raj JK, Yusoff I, Othman Z, Zakaria W, Tahir WM, Ashraf MA (2013d) Land use changes and soil redistribution estimation using 137Cs in the tropical Bera Lake catchment. Malaysia. Soil Till Res 131(1):1–10

Gharibreza M, Habibi A, Imamjomeh SR, Ashraf MA (2014) Coastal processes and sedimentary facies in the Zohreh River Delta (Northern Persian Gulf). CATENA 122(1):150–158. doi:10.1016/j.catena.2014.06.010

Haregeweyn N, Poesen J, Nyssen J, Verstraeten G, de Vente J, Govers G, Deckers S, Moeyersons J (2005) Specific sediment yield in Tigray-Northern Ethiopia: assessment and semi-quantitative modeling. Geomorphology 69:315–331

Kabir A, Bahremand A (2011) Water balance of Gorganrood river basin East of Iran. Afr J Agric Res 6(25):5591–5599

Mahmoudi B, Bakhtiari F, Hamidifar M, Danehkar A (2010) Effects of land use change and erosion on physical and chemical properties of water (Karkhe Watershed). Int J Environ Res 4(2):217–228

Masih I, Ahmad M, Uhlenbrook S, Turral H, Karimi P (2009) Analysing streamflow variability and water allocation for sustainable management of water resources in the semi-arid Karkheh river basin, Iran. Phys Chem Earth Parts A/B/C 34(4–5):329–340

Morgan RPC (1986) Soil erosion and conservation. Longman Scientific and Technical, Wiley, New York

Natural Resources and Watershed Management Organization (2011)

Nyssen J, Mitiku H, Moeyersons J, Poesen J, Deckers J (2001) Removal of rock fragments and its effect on soil loss and crop yield. Soil Use Manag 17:179–187

Poesen J, Torri D, Bunte K (1994) Effects of rock fragments on soil erosion by water at different spatial scales: a review. Catena 23:141–166

PSIAC (1968) Report of the water management subcommittee on sectors affecting sediment yield in the pacific southwest area and selection and evaluation of measures for reduction of erosion and sediment yield. ASCE, 98, report no. HY12

Sarmadian F, Rahimy P, Keshavarzi A (2010) Modeling of sediment yield and bicarbonate concentration in Kordan Watershed. Iran J Agric Sci Technol 12:121–131

Sima S, Tajrishy M (2013) Using satellite data to extract volume–area–elevation relationships for Urmia Lake, Iran J Great Lakes Res 39:90–99

UNEP United Nation Environmental Program/Global Resource Information Database/The Drying of Iran's Lake Urmia and its Environmental Consequences (2012)

USDA-SCS (1964) Hydrology. Section 4 part I, catchment planning. National engineering handbook. US department of agriculture, Soil conservation service, Washington, DC

Zulkifley MTM, Ng TF, Raj JK, Hashim R, Ashraf MA (2014) The effects of lateral variation in vegetation and basin dome shape on a tropical lowland stabilization in the Kota Samarahan-Asajaya area, West Sarawak, Malaysia. Acta Geol Sin-Eng 88(3):894–914

Chapter 3
Application of SWAT Model in Taleghan Catchment

Abstract In Tehran province of Iran, Taleghan basin is one of subsidiary basin of sefidrood catchment basin consist of 19 subsidiary basins. Each of which reflected as a self regulating hydrological branch. Taleghan catchment alienated into 28 hydrological sub-basins. By using GIS method inclined regions of catchment categorized into five classes. Geology, morphology, climatic conditions, temperature, snow pack, climatic regime, relative humidity, potential evaporation also studied and discussed in this chapter. Soil of Taleghan categorized into 11 classes. Water resources reflected as one of the key resource of providing water for several practices like agriculture, drinking and industry. Three orogenic and tectonic uplifts during Pre-Cambrian (some 350 million years ago), Mesozoic (150 million years ago), and Cenozoic (72 million years ago) Periods have shaped existing structural topographies of the Taleghan Catchment, parting sedimentary and volcanic rock systems in the region.

Keywords Taleghan · Subsidary basins · GIS method

3.1 Catchment Area

3.1.1 Location

Taleghan catchment basin is in the Tehran province, Iran located on the south east of Alborz range in Iran with average yearly precipitation and temperature 591 mm and 4.48 °C, respectively, and at 120 km distant from the northwest Tehran (Fig. 3.1). Taleghan catchment basin is one of the subsidiary basins of Sefidrood catchment basin which is confined by Alamoot in the north, the region of Ziaran and Samgh Abad in the south, one segment of Karaj a mountainous area with sharp steepnessess having many stone outcrops, and the uppermost

M. Hosseini and M.A. Ashraf, *Application of the SWAT Model for Water Components Separation in Iran*, Springer Hydrogeology,
DOI 10.1007/978-4-431-55564-3_3

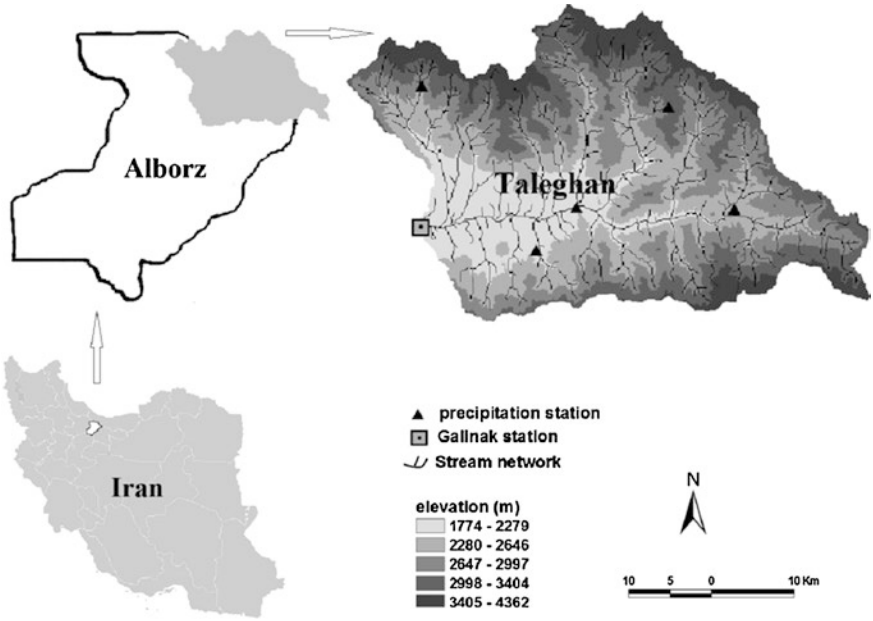

Fig. 3.1 The location of Taleghan catchment

and lowermost segments have 300 and 1776 m elevation, correspondingly, from the sea level.

The basin comprises of 19 subsidiary basins, each one reflected as an self-regulating hydrological branch in a way that Minavand subsidiary basin contains smallest size i.e. 2.14 % of the entire basin, and Mehran subsidiary basin contains the maximum size, i.e. 13.26 % of Taleghan catchment basin. The acreage of this basin contains pastures, lands for dry agriculture, water lands, and areas with no use. So, the major fraction of the acreages in this area i.e. 89.37 % of the entire basin, entails rich and poor pastures together.

3.1.2 Hydrological Subbasins

Taleghan catchment is alienated into 28 hydrological subbasins (Fig. 3.2). The physiographic properties of each one have been described in Table 3.1. It is indicated by this table that the subbasin of largest size is number 5 sub-basin whereas the subbasin number 11 is smallest one. The former and latter

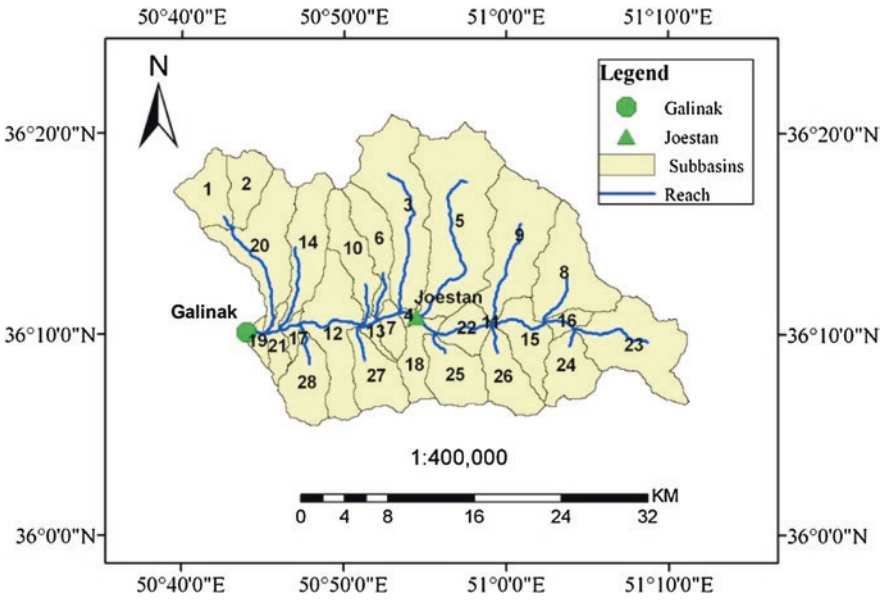

Fig. 3.2 Map of the hydrological subbasins of Taleghan catchment

Table 3.1 Frequency distribution of the slope classes of Taleghan catchment

Slope class (%)	Area (ha)	Area (%)
0–5	982	1.22
5–10	1882	2.34
10–20	7166	8.92
20–40	27,859	34.69
>40	42,425	52.82

correspondingly encompass 12.49 and 1 % of the entire catchment region. The highest part of the catchment is Joestan subbasin which consist of 25 subbasins (Fig. 3.3).

The inclined region of the catchment has been categorized into five classes by means of GIS methods (Table 3.2). This table discloses that the major proportion of the catchment i.e. 52.82 % includes "in excess of 40 %" class. Conversely, the smallest proportion of the catchment i.e. 1.22 % goes to the 0–5 % class. The weighted mean gradient is around 41.3 %.

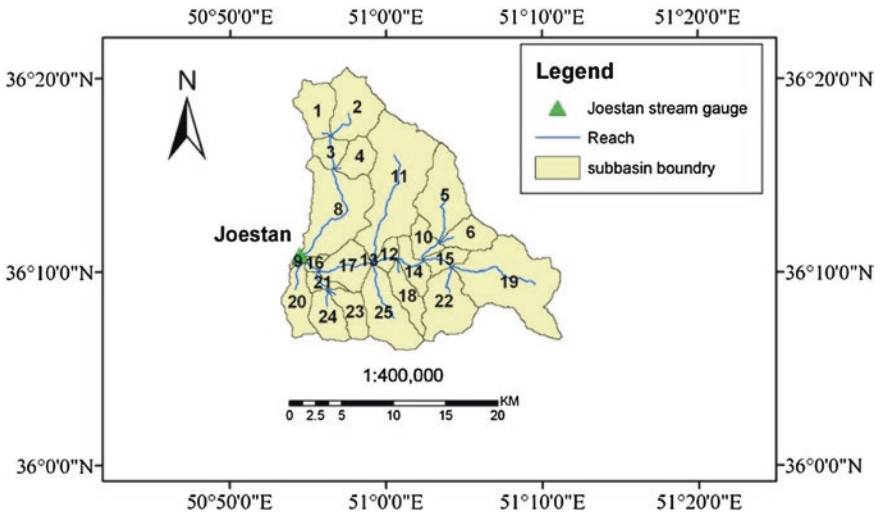

Fig. 3.3 Map of the hydrological subbasins of Joestan catchment

Table 3.2 The physiographic properties of the hydrological subbasins of Taleghan catchment

Subbasin	Number of HRU[a]	Elevation (m)			Area	
		Min	Max	Average	Hectares	%
1	8	2238	4027	2962	2329	2.89
2	7	2243	4112	3166	2004	2.49
3	5	1941	4047	2859	7133	8.86
4	3	1934	2397	2113	235	0.29
5	9	1968	4362	2935	10,061	12.49
6	15	1911	3919	2823	2457	3.05
7	25	1910	2641	2190	960	1.19
8	9	2245	4149	2853	4812	5.97
9	8	2122	4114	2895	6138	7.62
10	10	1896	3926	2782	2740	3.40
11	5	2115	2303	2180	10	0.01
12	25	1826	3307	2284	4838	6.01
13	10	1891	2672	2117	457	0.57
14	8	1810	3979	2740	3702	4.60
15	6	2118	4002	2733	2587	3.21
16	6	2247	2989	2547	684	0.85
17	13	1809	2419	1985	478	0.59
18	10	1967	3420	2611	1771	2.20
19	11	1775	2421	1941	534	0.66
20	8	1792	3804	2524	5031	6.25

(continued)

Table 3.2 (continued)

Subbasin	Number of HRU[a]	Elevation (m)			Area	
		Min	Max	Average	Hectares	%
21	14	1790	2703	2089	960	1.19
21	14	1790	2703	2089	960	1.19
22	4	2018	3070	2415	1554	1.93
23	6	2322	3922	3016	5665	7.03
24	4	2331	3558	2742	2502	3.11
25	4	2024	4059	3169	2814	3.49
26	4	2117	4038	2941	2658	3.30
27	23	1892	3268	2499	2655	3.30
28	14	1827	3127	2416	2778	3.45
	Average	1775	4362	2753	80,549	100

[a]Hydrologic response units

3.2 Geology

Taleghan Catchment is sited in Central Alborz Mountain Range which reveals west-east trend. Actually, this catchment is part of one of the eminent Iran's doubled over mountainous series having 2000 km length, 140 km breadth and 3600–4800 m altitude. Three orogenic and tectonic uplifts during Pre-Cambrian (some 350 million years ago), Mesozoic (150 million years ago), and Cenozoic (72 million years ago) Periods have shaped existing structural topographies of the Taleghan Catchment (Tehrani 2005), parting sedimentary and volcanic rock systems in the region. Mosha-Fasham, North Tehran and North Qazvin main faults are the consequences of stated orogenic activities which have been established along confines of structural regions. Taleghan River is one of the key Central Alborz Rivers which discharge water westward to the Caspian Sea.

3.3 Morphology

Taleghan Basin is one of the mountainous regions which incidence of its morphological units was verbalized by geological, climatologically and topographical influences. Generally, the most morphological units of Taleghan Catchment are mountains, hills and plains. These units have been alienated to various morphological categories with respect to geological developments. It clarifies that morphological units were organized by form of geological developments.

Morphological units have been alienated into morphological subunits. The very common morphological subunits are the rocky outcrops in many degree, volcanic

necks, sills, and batholiths in mountainous regions in Taleghan Catchment. Moreover, the most prevailing features of mountainous region are rocky outcrops, regular and irregular hillsides, alluvial fans, old and new. In conclusion, the common subunits in plains are flood plains and fluvial plain. Erosional characteristics like gully, rill, and sheet erosions are common in hilly and plain areas.

The morphological units, as well as drainage configuration in Taleghan Catchment primarily are organized by physical phenomenon such as faults and folding axes. Field examination displayed that dendritic pattern is very common pattern in Taleghan basin. With respect to topographical trend, Taleghan River keep an eye on physical trend headed for west and is ended to the dam.

3.4 Climate

As said by the author (Hosseini 1997) the climate of south Alborz Mountains region, so the catchment, is affected by the Caspian Sea. Generally, the precipitation regime of the Taleghan catchment is the consequence of the Mediterranean regime with one main extreme precipitation spell on the termination of winter and initial spring monitored by one extended dry period in the summer. In fall there is one more rain spell in which precipitation is affected by humid air having interaction with northern Siberian air masses. The effect of the monsoon from the Indian Ocean is very infrequent all through the year. The Taleghan catchment has an unbalanced average yearly precipitation with maximum coefficients of variation; the least i.e. 454 mm occurs at Galinak while the extreme i.e. 814 mm occurs at Dizan. With respect to regional precipitation distribution, the Taleghan catchment is categorized as semi-wet. Figure 3.4 represents the Locations of the Hydrometeorologic Stations in Taleghan Catchment.

3.4.1 The Climatic Regime

So as to find the climate type of the Taleghan catchment the De Martonne technique can be applied. The technique of De Martonne uses the average temperature (°C) and concentration of annual rainfall (mm) to categorize the climate rendering to Eq. (3.1) (De Martonne 1926):

$$AI = \left[P \big/ (T + 10) + 12p(t + 10)\right]_{/2} \tag{3.1}$$

where AI is the dryness coefficient, T is the average temperature (°C), and P is the average yearly rainfall (mm), t is the average temperature of the driest month in

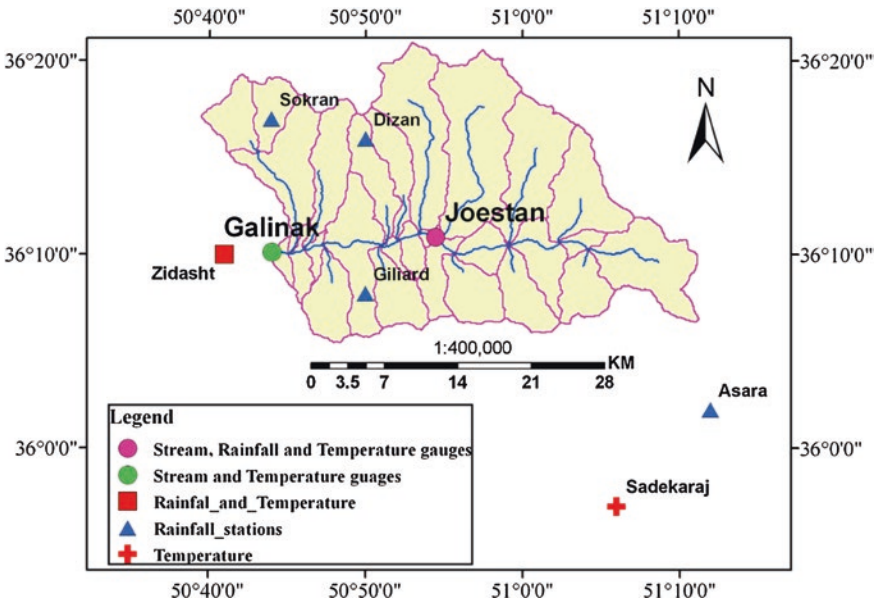

Fig. 3.4 Locations of the hydrometeorologic stations in Taleghan catchment

Table 3.3 Classification of climate by means of De Martonne's aridity index

AI value	Climate class
≤5	Arid
5–12	Semi-arid
12–20	Dry sub-humid
20–30	Moist sub-humid
30–60	Humid
≥60	Wet

(°C), and p is the precipitation of the driest month in mm. Table 3.3 describes the categorizations of the aridness on the basis of De Martonne's Aridity Index.

While locations of the rain gage stations of the investigated region and the average yearly precipitation therein averaged during the period 1992–2004 indicated in Table 3.4.

In Taleghan catchment *AI* is equivalent to 19.08. Conferring to De Martonne technique, this shows that the region categorizes in the dry-sub humid climate class. The lapse rate is utilized to regulate precipitation for altitude bands in the subbasin. To regulate the precipitation, the altitude of recording station is identified for the altitude band (Neitsch et al. 2005).

Table 3.4 Locations of the rain gage stations of the investigated region and the average yearly precipitation therein averaged during the period 1992–2004

Station	Longitude (°)	Latitude (°)	Elevation (m)	Mean annual precipitation (mm)
Zidasht	50.68	36.17	1750	478.17
Galinak	50.77	36.17	1750	454.49
Asara	51.2	36.03	1950	562.86
Joestan	50.9	36.2	1990	547.16
Giliard	50.83	36.13	2150	560.31
Nesa	51.33	36.08	2210	660.88
Dizan	50.83	36.27	1950	814.49
Sokran	50.73	36.28	1588	502.55

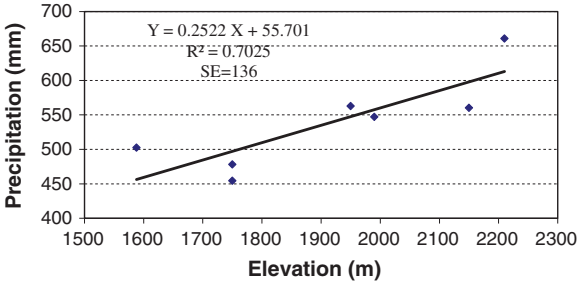

Fig. 3.5 The relationship concerning elevation and average yearly precipitation for the investigated region averaged during the period 1992–2004

Table 3.5 The average yearly precipitation depth from 1987 up to 2004 at Galinak station

Year	Precipitation (mm)	Year	Precipitation (mm)
1987	1267.7	1996	691.4
1988	1126.2	1997	626.9
1989	463.8	1998	826.7
1990	535.7	1999	398.2
1991	880.7	2000	437.6
1992	1112.6	2001	447.6
1993	955.6	2002	894.2
1994	1403.8	2003	992.3
1995	725.8	2004	953.1

Water Resource Company (WRC)

The correlation between average yearly precipitation and altitude represents an excellent coefficient determination ($R^2 = 0.7$) in Taleghan catchment (Fig. 3.5). The lapse rate procedure commonly relates for overwhelming absence of precipitation data for hilly region. The correlation of precipitation and altitude calculates that the precipitation lapse rate is equivalent to 252.2 mm km^{-1}. The average yearly precipitation averaged for the duration of 1987–2004 at Galinak station is 818.9 mm (Table 3.5).

Table 3.6 The average monthly rainfall depth in Taleghan catchment averaged during the period 1987–2004

Month	Jan	Feb	Mar	Apr	May	Jun	Jul	Aug	Sep	Oct	Nov	Dec	Ave.
Prec. (mm)	78	91	139	136	76	19	14	6	5.8	64	100	94	68

Water Resource Company (WRC)

The average monthly precipitation in Taleghan catchment averaged for the duration of 1987–2004 is précised in Table 3.6. According to this table the least and extreme rainfall rates take place in September and March, correspondingly. The last column reports the mean rainfall rate (68.4 mm) averaged above months and years.

3.4.2 Snowpack

In the Taleghan region, there are merely six snowpack sites with short duration common data which positioned from 1700 to 2400 m. However extreme altitude is 4362 m. As stated by the Faculty of Agriculture, University of Tehran report (1993), a large proportion of precipitation in Taleghan region is in the form of snow. The proportion of snow to precipitation relies on the climate of the specific year. This report discloses that the least and extreme values of this proportion differ from 33 to 51 % at Armot and Dizan snowpack gauging stations, correspondingly. This report forecast, this value differs from 42 to 62 % in this region.

3.4.3 Temperature

In the Taleghan basin the temperatures are measured simply in the Zidasht and Joestan stations which are located at the altitudes of 1750 and 1990 m, correspondingly. Other temperature stations are sited nearby the Taleghan catchment.

The available indicates the highest and lowest temperatures averaged for the duration of 1987–2004 at the climatological stations in and nearby Taleghan catchment have been précised in Table 3.7. The lapse rate is applied to regulate the temperature for altitude bands in the subbasins. To regulate temperature, the altitude of the recording station is related to the altitude band.

In the Taleghan region, the average yearly temperature drops with elevation at an incline of 8.5 °C km^{-1}. Figure 3.6 represents the average yearly temperature

Table 3.7 Locations of the temperature gage stations of the investigated region and the, minimum, maximum, and average temperatures therein averaged during 1992–2004

Name	Elevation (m)	Longitude (°)	Latitude (°)	Mean temperature (°C)		
				Min	Max	Ave.
Shahrestanak[b]	2150	51.35	35.97	−0.9	15.8	7.45
Sadekara j[b]	1588	51.10	35.95	8	19.6	13.8
Nesa[b]	2200	51.33	36.08	0.2	16.2	8.2
Zidasht[a]	1750	50.68	36.17	4.7	15.3	10
Joestan[a]	1990	50.77	36.23	4.8	17.1	10.95

[a]Inside the catchment
[b]Outside the catchment
Water Resource Company (WRC)

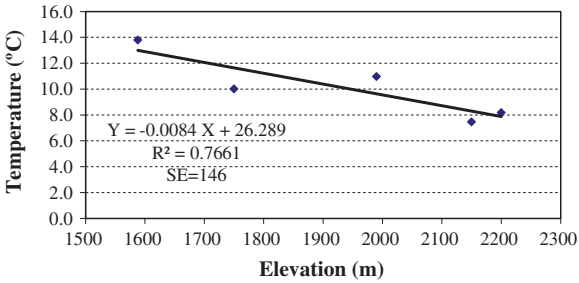

Fig. 3.6 The Relationship concerning elevation and average yearly temperature for Taleghan catchment averaged during 1987–2004

compared to elevation. It designates that the correlation between the two supposes the formula as shown by Eq. (3.2).

$$T = -0.0084\,H + 26.29 \tag{3.2}$$

where T is the temperature (°C) and H is the elevation (m).

3.4.4 The Relative Humidity

The nearby synoptic station to the Taleghan region for assemblage of humidity data is the Ghazvin synoptic station which is sited in the south west region of the Taleghan catchment. The average monthly relative humidity of the Ghazvin station for 18-year data has been described in Table 3.8. The minimum and maximum have been described to be occuring in August and January and resemble to 35 and 68 %, correspondingly. Averaged over months and years (1987–2004), the average yearly relative humidity at Ghazvin station is 47 %.

Table 3.8 The average monthly relative humidity at Ghazvin synoptic station averaged during 1987–2004

Month	Oct	Nov	Dec	Jan	Feb	Mar	Apr	May	June	Jul	Aug	Sep	Ave.
Mean (%)	43	53	63	68	63	52	49	42	35	35	34	36	47

Table 3.9 Average monthly evaporation at Zidasht station averaged during 1970–1993

Month	Jan	Feb	Mar	Apr	May	Jun	Jul	Aug	Sep	Oct	Nov	Dec	Annually
Pan (mm)	32.2	29.1	39.5	96.5	152.3	239.6	304.3	347.3	279.3	17.3	96.5	47.1	1835
B.P[a] (mm)	–	–	26.1	86.8	136.4	179.8	210.8	235.6	133.3	111	30	–	1250

[a]Balany-criddle method
Faculty of Agriculture (1993)

3.4.5 Potential Evaporation

For the Talaghan basin the potential evaporation is recorded in the Zidasht station and the mean yearly evaporation in the Zidasht station is almost 1835 mm and that it is ranged from a least of 1415.3 mm in the year 1978 to an extreme of 2031.4 mm in the year 1984. Table 3.9 specifies the large variances in average monthly evaporation between pan and Balany–Criddle methods.

3.5 Soil Type and Classification

The soil types of the Taleghan catchment have been categorized into 11 classes by the Faculty of Agriculture, University of Tehran and these classes have been described in Table 3.10. Conversely, distribution of the soil classes within Taleghan catchment is represented in Fig. 3.7.

Table 3.10 Summary of soil properties of Taleghan catchment

Soil type	Depth	Gravel (%)	Soil texture	pH	Organic matter content	Area (ha)
1	Moderately deep	35	Loam	6–7.5	Low	19,392
2	Very slightly to slightly deep	35	Loam	5.6–7.5	Moderate-high	25,300
3	Very deep	15	Clay loam	7.3–8	Low-moderate	7373
4	Slightly-deep	20	Loam	7–7.7	Moderate	4070
5	Slightly deep to very deep	35	sandy loam	7.5–7.6	Low	23,840
6	Very deep	35	Sandy loam-loam	7.5–7.6	Low	6
7	Slightly-deep	25	Loam	7–7.2	Low	60
8	Slightly-deep	75	Sandy loam	7.4–8.1	Variable	4658
9	Very deep	35	Loam	7.5–7.7	Moderate	1105
10	Very deep	35	Clay loam	7.5–7.9	1.0<	5430
11	Very deep	0	Clay	7.6–7.7	<0.5 %	360

Faculty of Agriculture (1993)

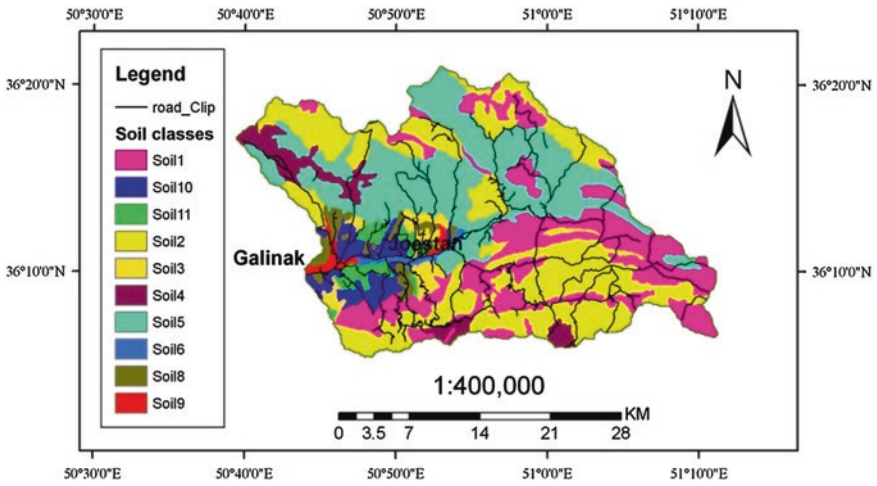

Fig. 3.7 Distribution of soil classes within Taleghan basin (Faculty of Agriculture 1993)

3.6 Water Quality

Water resources are reflected as one of the key resources of providing water for several practices such as agriculture, drinking and industry. As a result of the recent droughts in Iran, knowing and giving qualitative importance to the contaminants of these resources is one of the highly essential responsibilities in environmental organization. For this purpose, various new models in water resources play an imperative role in the monitoring of these resources. With a brief look at the condition of Iranian Taleghan catchment basin, it can be clarified that the intensive growth of population and educating the public welfare affect the land use and risk the natural resources and their reserves. Table 3.11 displays the current condition of land use in Taleghan catchment basin.

In order to give priority to various contaminants within Taleghan catchment, Expert Choice Software was applied on the basis of type of the land use in the basin and contaminants were identified and categorized as well using this software. Basically, this software works on the basis Analytical Hierarchy Process. Figure 3.8 represents the hierarchical structure of contaminative factors in Taleghan catchment basin.

Table 3.11 The present condition of land use in Taleghan catchment basin

Land use	Pasture	Deserted dry farming	Garden and water farming	Rocky rugged areas
Mensuration (ha)	71,928.5	3669.56	1651/16	3238/99
Percentage (mensuration)	89/37	4/56	2/05	4/02
Commutative percent	89/37	93/93	95/98	100

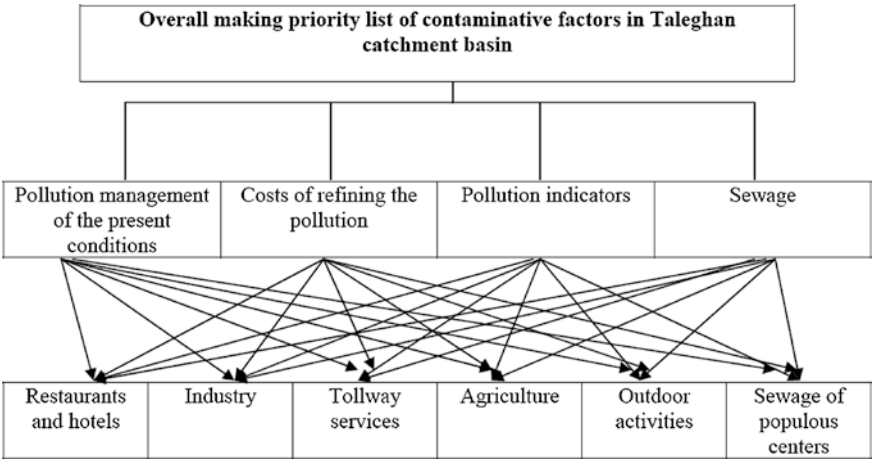

Fig. 3.8 Hierarchical structure of contaminative factors in Taleghan catchment basin

The head to head figures have been used to illustrate that how two variables together are related in association with one standard in order to derive the conclusion. The variable in the leftward is persistent every time and it is employed to be related with other variables. To derive a conclusion, if the leftward variable in association with the present standard has priority over rightward variable, a symbol headed for the leftward can be seen on that standard displaying the rate of priority. If the two variables have identical priority, there is no sign on the variables. The general outcome of these contrasts point out the priority of one variable over alternative variable considering all the present standards to derive the conclusion. Additionally, an association between the priority of each standard and the variable has been clarified in Figs. 3.9, 3.10, 3.11, and 3.12.

According to Fig. 3.13, sewage, agriculture, outdoor activities, industry, industry, tollway services, and restaurant correspondingly have significant contribution for contaminating Taleghan catchment.

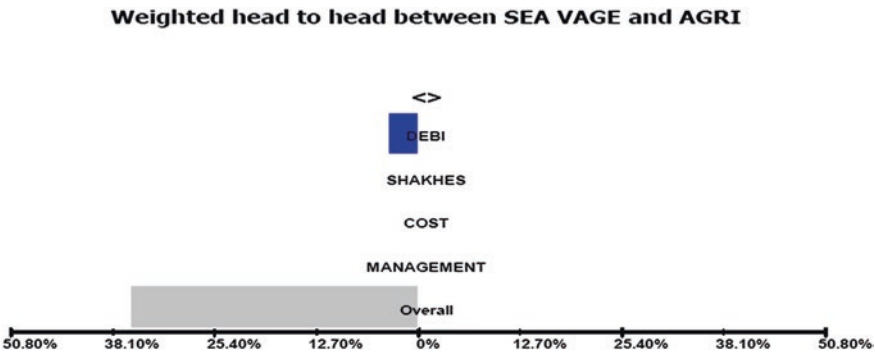

Fig. 3.9 weighted head to head between sewage and agriculture

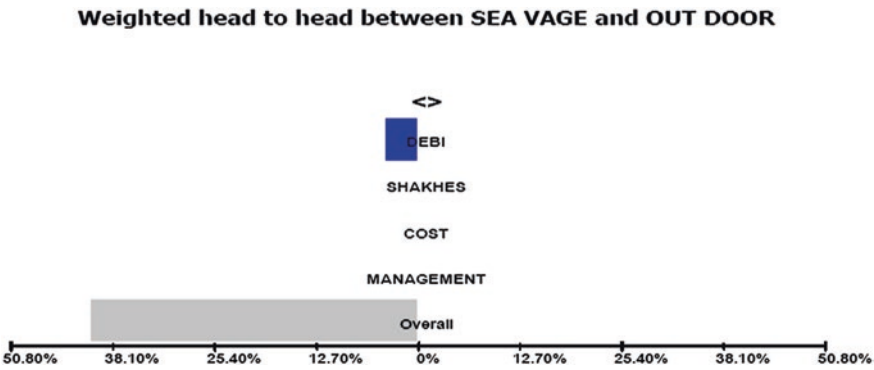

Fig. 3.10 weighted head to head between sewage and outdoor activities

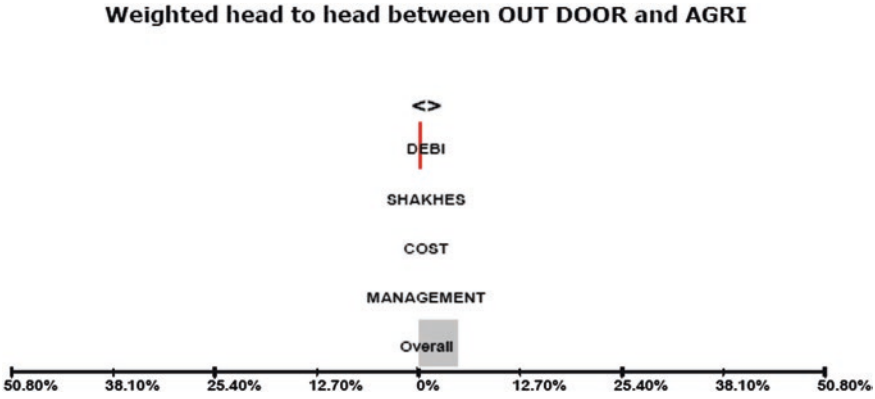

Fig. 3.11 weighted head to head between outdoor activities and agriculture

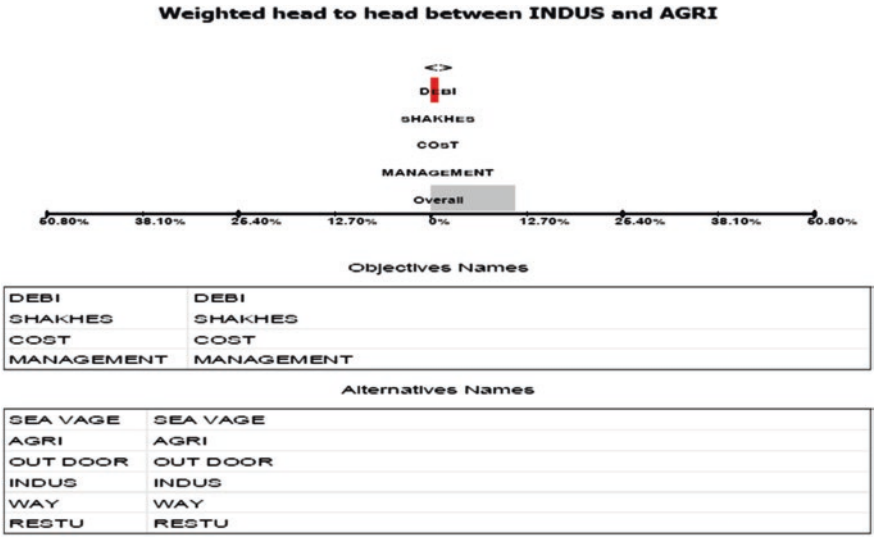

Fig. 3.12 weighted head to head between industry and agriculture

Fig. 3.13 overall making priority list

With the aim of combating the effects of various factors contributing the contamination in Taleghan catchment basin, the subsequent management strategies are suggested:

- Sewage filtering and lessening nutritious constituents of sewage or making a deviating path for sewage.
- Modification or adaptation of farming practices pointing to reduce spraying insecticides, by means of chemical fertilizers, and creating a smaller amount drainage.
- Varying land use or stopping land use variation.
- Monitoring the erosion and sediment.
- Put on watershed management schemes.
- Evaluating the quantity of self-refining of surface water resources and constant protection (Shafiee et al. 2011).

References

Faculty of Agriculture (1993) University of Tehran

Hosseini M (1997) Hydrological analysis of the Roodak Catchment, Iran, and evaluation of flood Simulation model. MSc thesis, ITC, Enschede, The Netherlands

Neitsch SL, Arnold JG, Kiniry JR, Williams JR (2005) Soil and water assessment tool theoretical documentation version. Grassland, soil and water research laboratory, Blackland Research Center, Temple, Texas

Shafiee MRM, Ghanbari F, Sharee FA, Salehi H (2011) Qualitative priority of pollutants in Taleghan catchment using analytical hierarchy process. In: International conference on environment and industrial innovation IPCBEE vol 12 (2011) © (2011) IACSIT Press, Singapore

Tehrani K (2005) Geology of Iran. Kalidar publication, Iran, p 30

Chapter 4
Water Components Separation by SWAT Model in Taleghan, Iran

Abstract Present case study focus on the facts of hydrological processes influenced by land variations in water supply catchment in Iran. In 2006, Taleghan dam envisioned to be used for multipurpose together with visit refreshment, such activities put much pressure on exploitation of land and water resources in Taleghan catchment. Advantageous technique for incorporated management of catchments in the management of sustainability development is inclusion hydrological model i-e soil and water assessment tool model implementing along with GIS. Study consist of three phases (i) the setup (also indicated as warm-up) phase starting from 1992 up to the end of the year 1994 (three years), (ii) the calibration phase which protracted from the commencement of the year 1995 up to the end of the year 2000 (six years), and (iii) a validation phase initiating from 2001 till the end of the year 2004 (four years). Dry agricultural practices lost their constancy and rigorously dropped as a result and the dry agricultural land regions transformed into virgin acreage.

Keywords Base flow assessment · Hydrological yield · Runoff flow water

4.1 Introduction

The present study is an effort to expose certain facet of hydrologic processes influenced by land use variation in a water supply catchment in Iran. The Taleghan catchment, which is positioned in the north west of Iran, is vital for agriculture and water supply, particularly after completing building and starting process of the Taleghan dam in 2006 which is envisioned to be used for multi-purposes together with visit refreshment. These demands and the growing numbers of tourists for refreshment have pose so much pressure on exploitation of land and water resources in Taleghan catchment.

Land use/cover variations have a substantial effect on the generation of runoff and other forms of water fluxes, contaminant transportation to water resources and rates of erosion. So as to have efficient and sustainable use of land and water

M. Hosseini and M.A. Ashraf, *Application of the SWAT Model for Water Components Separation in Iran*, Springer Hydrogeology,
DOI 10.1007/978-4-431-55564-3_4

resources, complete hydrological models need to be implemented to contribute in the monitoring of land and water resources in the catchment. Intensive use of land and water resources in Taleghan catchment and corrosion of suspended sediment yield within have contributed to controlling problems of the water resources and upraised worries over the prominence of the suspended sediment yield. As a result, catchment hydrology assessment is prerequisite for land and water collaborations employing hydrological models with competence to examine land and water management and suspended sediment yield. One of the inclusive hydrological models of this type is the Soil and Water Assessment Tool (SWAT) model (Arnold et al. 1998) implementing along with GIS remote sensing data. These implements may assist as an advantageous technique for incorporated management of catchments in the direction of a sustainable development of a catchment.

This study consists of three phases which are as follow: (i) the setup (also indicated as warm-up) phase starting from 1992 up to the end of the year 1994 (three years), (ii) the calibration phase which protracted from the commencement of the year 1995 up to the end of the year 2000 (six years), and (iii) a validation phase initiating from 2001 till the end of the year 2004 (four years). A general framework of the methodology used in this investigation is summarized in Fig. 4.1. Six major input data sets; digital elevation model (DEM), land use map, soil map, climatological data, and stream gage data were composed and processed.

4.2 The Study Area

Figure 4.2 shows the location of the study area named as Taleghan catchment. The study area is located in the upper part of Taleghan dam catchment in the north west of Tehran, the capital of Iran. It lies within 50° 38′–51° 12′E longitude and 36° 04′–36° 21′N latitude. A summary of some hydromorphological characteristics of the study area are illustrated in Table 4.1. The first stream gauge is located at Galinak which has an area of 800.5 km^2. A second stream gauge, called Joestan station, was selected to compare the results drawn from the former one with. Joestan station lies in the upper part of the catchment and has an area of 412.7 km^2 (Fig. 4.3).

4.3 Results and Discussion

4.3.1 Land Use Assessment

The land use evaluation in Taleghan catchment point out the unbalanced land use conditions throughout the investigation period from 1987 to 2004. Building of Dam and formation of reservoir has vastly influenced land values in this region. Consequently, dry agricultural practices lost their constancy and rigorously dropped as a result and the dry agricultural land regions transformed into virgin acreage.

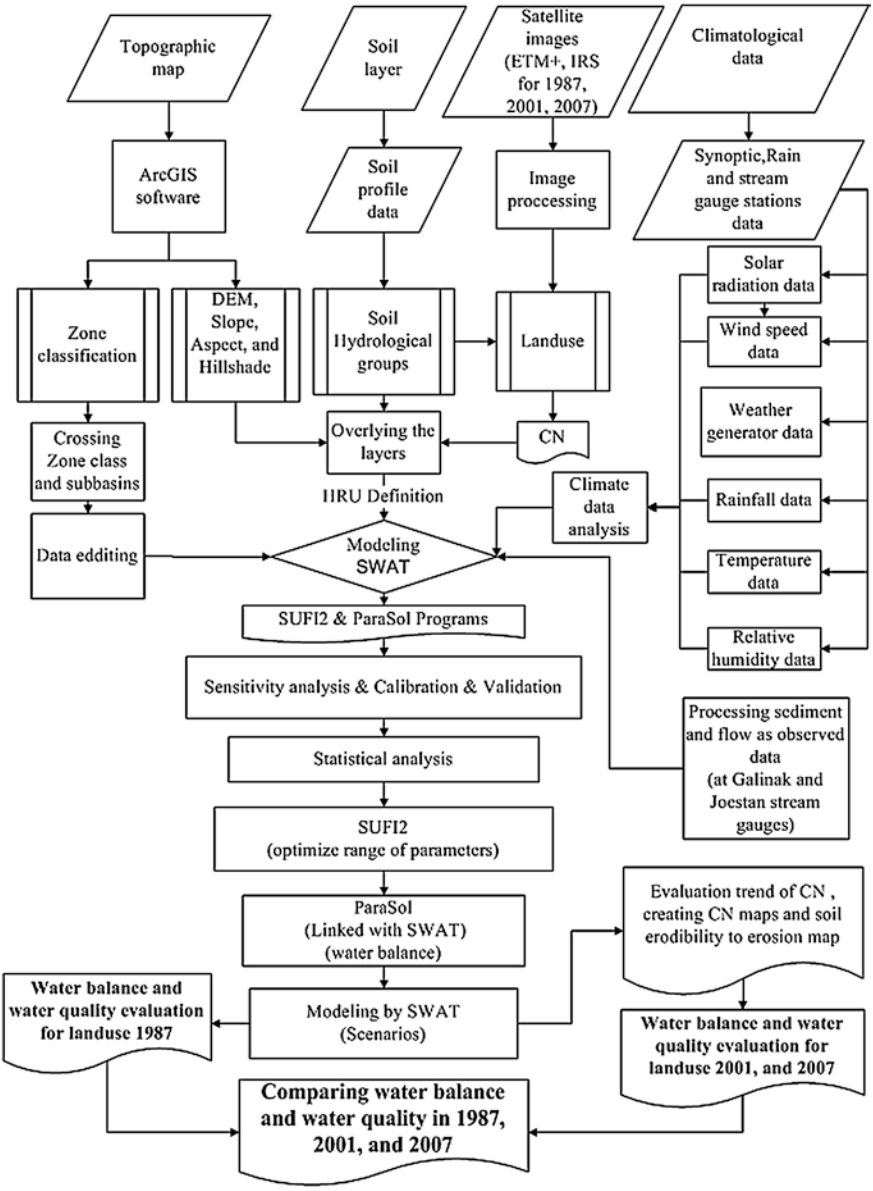

Fig. 4.1 The Overall framework of the methodology of Taleghan catchment study

In order to assess the land use variations throughout the investigation period, two incessant periods for the entire upper part of the catchment i.e. the upstream from 1987 to 2001 and 2001 to 2007. Various land uses like, flood plains, inactive dry farming, garden and irrigation farming, dry land farming, water and dam reservoir, urban and village, and range lands were identified by means of a preliminary sample set and the maximum likelihood (MLC) method (Fig. 4.4).

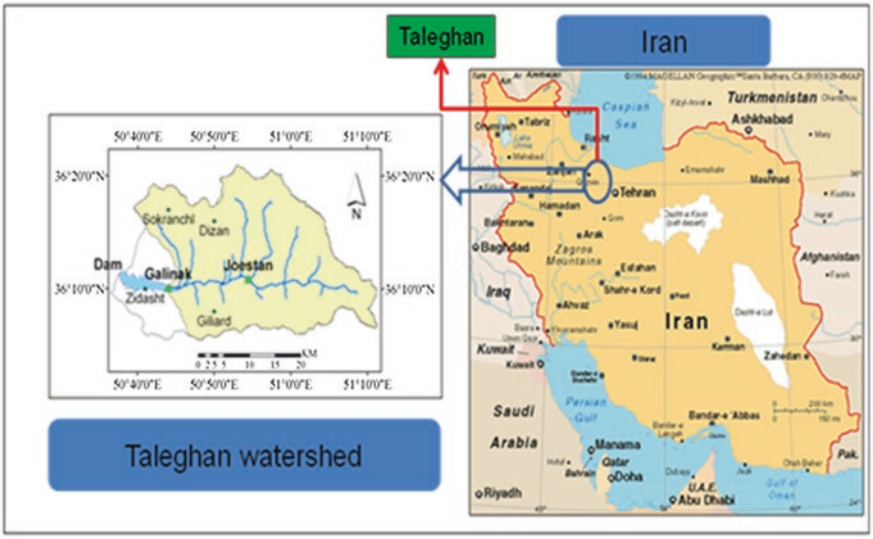

Fig. 4.2 Location of Taleghan catchment

Table 4.1 Specific hydromorphological properties of the investigated region (1995–2004)

Area (km^2)	Slope (%)	Altitude (m)			Mean annual		Runoff coefficient (%)	Drainage density (km/km^2)	Main stream length (km)
		Max.	Min.	Ave.	Precipitation (mm)	Discharge (m^3/s)			
800.5	41.3	4362	1775	2753	701	11.75	66	0.174	140.7

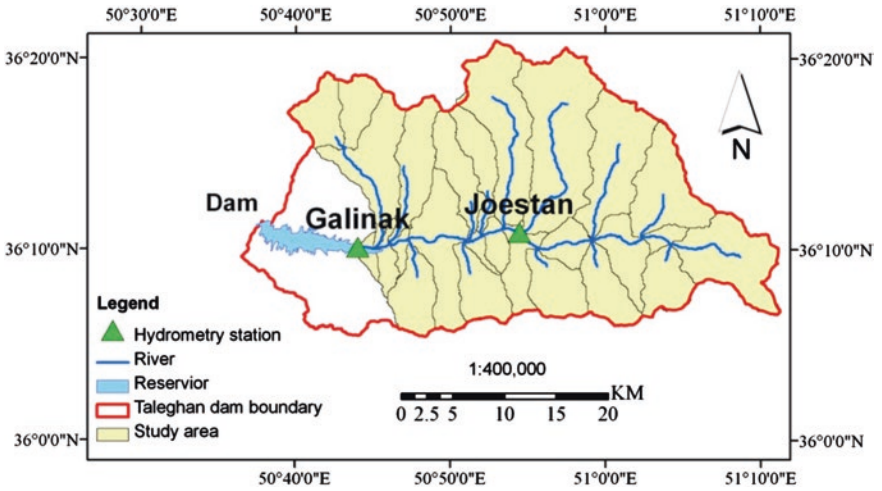

Fig. 4.3 The Taleghan dam boundary and study area

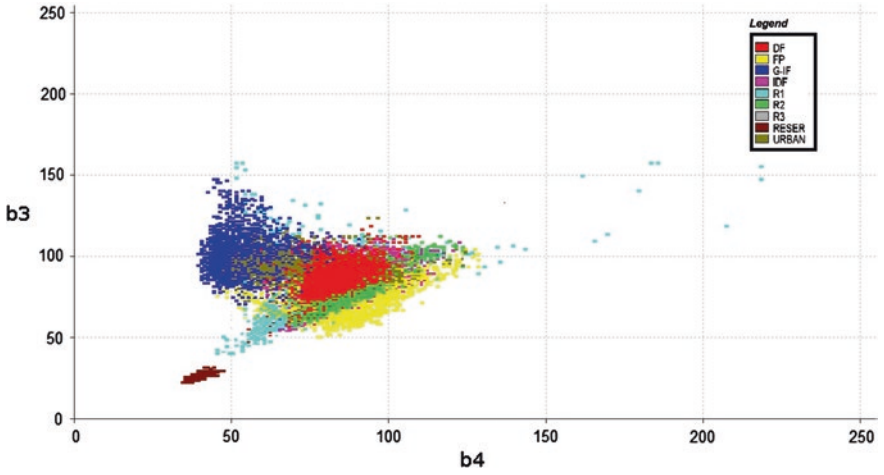

Fig. 4.4 Result of the sample set method employed in classifying the land uses in Taleghan region

From the time when the dam construction approved, gradually the whole rangeland region reduced to the size that a considerable reduction from 82.67 % through the initial phases of building of dam to 35.37 % on the completion of investigation period. Furthermore, inactive dry farming (IDF) intensified from 6.5 % in 1987 to 41.62 % in 2007. These infrequent practices severely enhanced sediment yield and soil erosion. Pressure on the rangeland because of unreliable land management had negative effects on development of landslides as well. Possession of the acreage by migrants increased the size of dry farming (DF) lands throughout the early phases of investigation period from the 2657 to 16,196 ha; i.e. above six times intensification. Nevertheless, in response of the large increase in the size of IDF land, the region of DF land exhibited not as much of decrease in the subsequent phase of investigation period as in the initial.

Growing habilitation posed significant impacts on the orchard-planted regions in the investigation area which reduced rigorously as a result. Hence, the regions of this highly imperative land use experienced 7.33 and 5.35 % reductions throughout the early and subsequent duration of this investigation. The size of well managed rangelands (GR) was 32,287 ha in 1987, and then in the result of overgrazing, poor land use management, and climatic variation, the size shrunk to 5524 ha by late 2007. This means that for the period of the last twenty years, well managed rangeland size reduced from 34.49 to 5.90 %. The transformation is attributed to changing uses of these regions to moderate (MR) or poor (PR) quality rangelands or to inactive dry farming (IDF). Conversely, weak rangeland enlarged from 19.04 % in 1987 to 23.35 % in 2007. The land uses identified by image handling for 1987, 2001, and 2007 can be seen in Figs. 4.5, 4.6, and 4.7. Figure 4.8 depicts the land use variations in a clustered column chart type from 1987 to 2007 in Taleghan region.

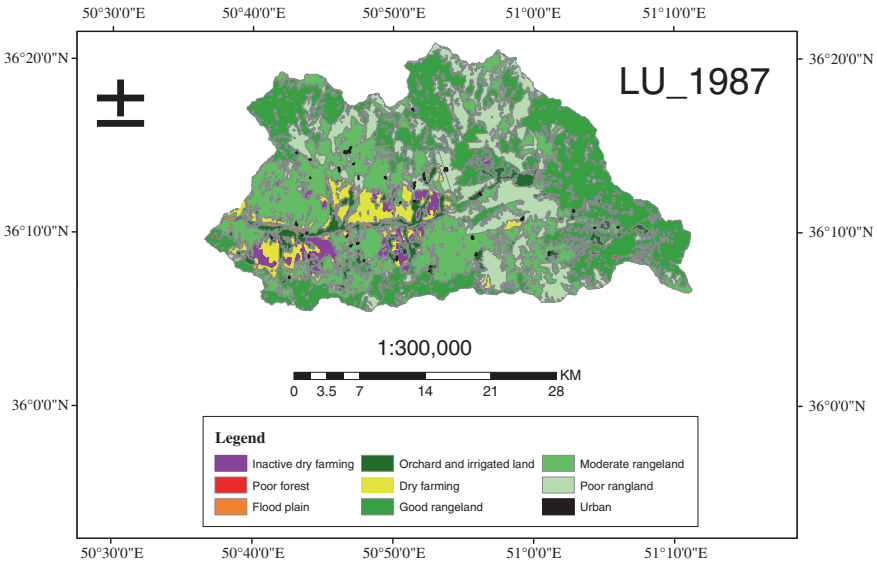

Fig. 4.5 Maps of the identified land uses in 1987 (before dam construction)

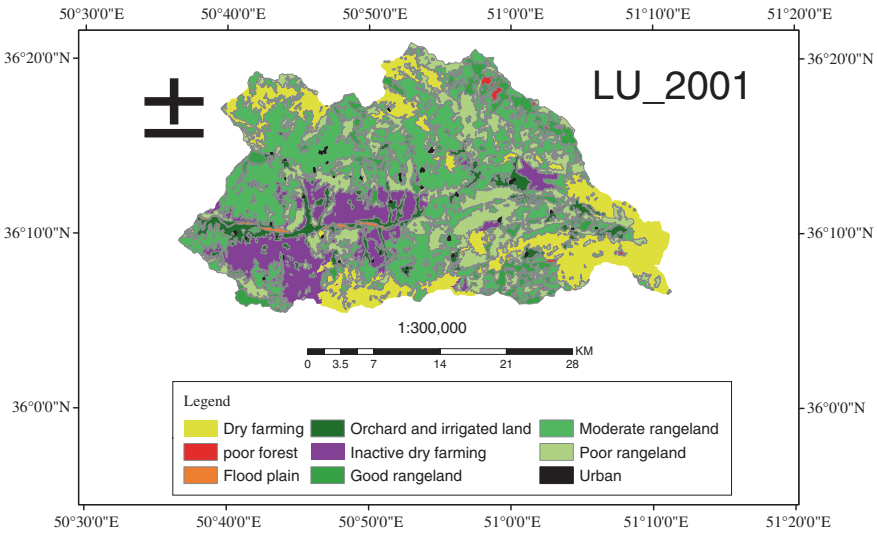

Fig. 4.6 Maps of the identified land uses in 2001 (before dam construction)

4.3.2 Baseflow Assessment

The process of baseflow separation, referred as hydrograph analysis as well, is associated with separating streamflow records into two primary modules; run-off flow and baseflow. Rendering to this technique, waves of high frequency are

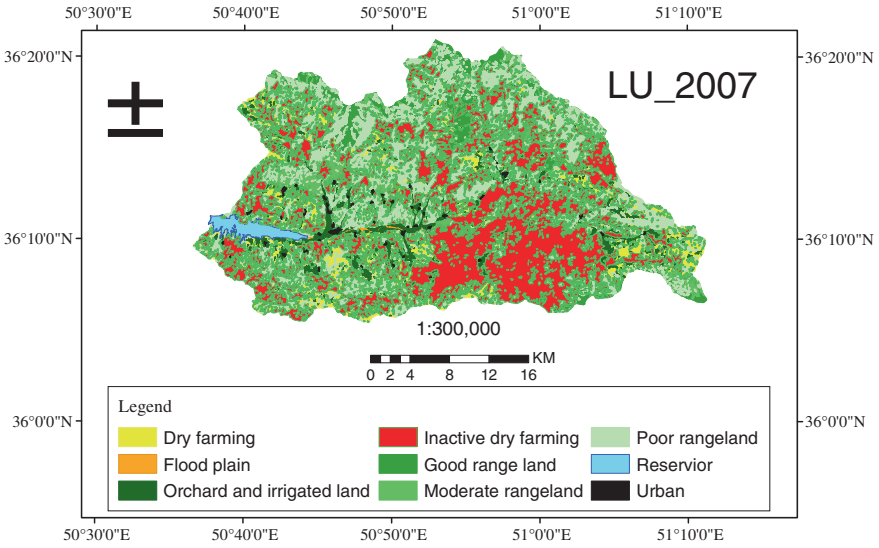

Fig. 4.7 Maps of the identified land uses in 2007 (after dam construction)

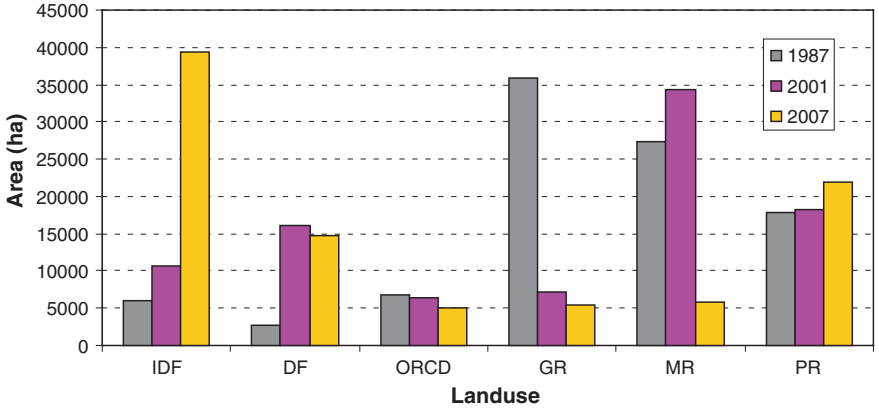

Fig. 4.8 Comparison concerning land use variations and area during 1987–2007 in Taleghan region

related to the direct runoff whereas that of low frequency can be related with the baseflow module. Equation 4.1 represents the digital filter applied for baseflow.

$$q_1 = \alpha \times q_{t-1} + \frac{(1+\alpha)}{2} \times (Q_t - Q_{t-1}) \tag{4.1}$$

where Q_t symbolizes the streamflow at time step t, q_t symbolizes the baseflow, and α symbolizes the filter parameter related to the catchment. α value was taken as 0.03. From 1992 to 2004 daily and direct runoff were used as input data.

The outcomes of baseflow split using the Lyne and Hollick method, reveals that the average yearly separated baseflow for the period from 1992 to 2004

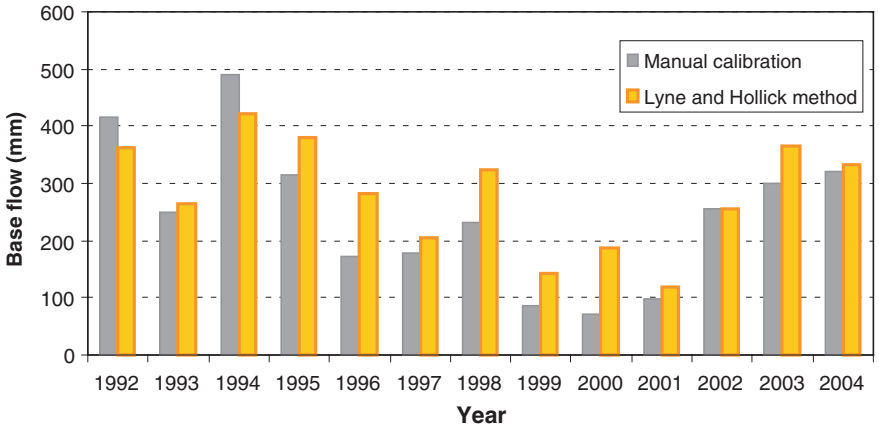

Fig. 4.9 Comparison concerning the baseflow separated by manual calibration and that separated by the Lyne and Hollick Filtering Method during 1992–2004

was 280.2 mm while the yearly average standardized baseflow was 245.2 mm (Fig. 4.9). For that reason, it was concluded that the baseflow estimated using SWAT is reliable well enough to be used in this study.

4.3.3 Sediment Yields Assessment

Assessments of suspended sediment yields were carried out using data collected from time to time applying regression models such as the Quasi Maximum Likelihood Estimator (QMLE). The findings show that daily sediment yield were 680 and 166 according to data at Galinak and Joestan gauging stations, correspondingly (Table 4.2). The discharge data set categorized into 11 classes, on the basis of lowest

Table 4.2 The classes of suspended sediment yield at Galinak and Joestan gauging stations as determined by the QMLE method

Class	Discharge (m^3/s)		Sediment yield (t/d)	
	Galinak	Joestan	Galinak	Joestan
1	10.0	2.5	635	90
2	25.7	7.5	2960	270
3	41.4	12.5	5970	550
4	57.1	17.5	15,233	1447
5	72.7	22.5	21,932	744
6	88.4	27.5	39,667	1845
7	104.1	32.5	0.0	3821
8	119.7	37.5	0.0	12,781
9	135.4	42.5	0.0	7893
10	151.1	47.5	133,308	0.0
11	–	52.5	–	17,353

and highest amount of discharge. The total of the classes was designated by experience. Generally, classes from 5 to 12 containing whole series of discharge were nominated. Then the mean value of sediment yield was estimated for each class. The central discharge class was considered as mean of discharge in the everyone.

A strong positive correlation (R^2) between mean discharge and sediment yields for two stations Galinak ($R^2 = 0.98$) and Joestan ($R^2 = 0.76$) is represented by Figs. 4.10, and 4.11. These figures depicts that an exponential relationship exists between the mean discharge and sediment yield and these can be calculated by means of Eqs. (4.2), and (4.3) correspondingly. Joestan station positioned at high altitude and densely covered with snow contributed to the small R^2 values particularly in the case of large discharge.

$$Y = 5.3611\, X^{1.9702} \tag{4.2}$$

$$Y = 9.917\, X^{1.735} \tag{4.3}$$

where X and Y denote the mean discharge and sediment yield, correspondingly.

The amounts of sediment yield and discharge were calculated on the daily basis using Eqs. (4.2), and (4.3) respectively. Monthly and yearly amount was predicted from these daily ones. And then, the daily sediment yield was implemented in SWAT model in order to obtain observed values.

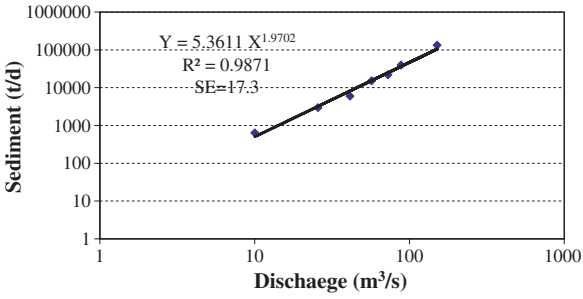

Fig. 4.10 Relationship concerning daily discharge and sediment yield at Galinak station

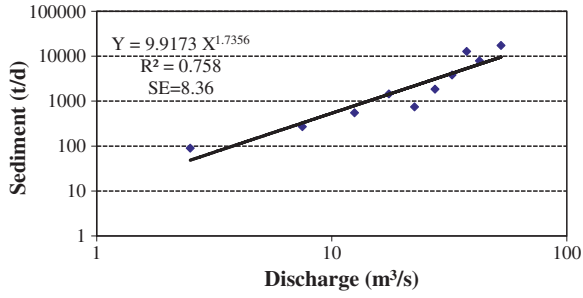

Fig. 4.11 Relationship concerning daily discharge and sediment yield at Joestan station

4.3.4 The Hydrological Yield

4.3.4.1 The Total Water Output

The main statistical standard the investigator applied for assessing the performance of the catchment model was the Deviation of Runoff Volume which is an estimation of a model's capability to predict the overall volume of runoff for the throughout the period of analysis. It is calculated by the following Eq. (4.4):

$$RE = [(X_i' - X_i)/X_i].100 \tag{4.4}$$

where X represents observed value, X′ represents the simulated value, i represents the record, and n represents total number of records. There can be any value for the deviation of runoff volume. Though, zero value specifies exact agreement concerning the observed and predicted runoff. Overall observed and predicted runoff amounts derived from calibration and validation of models at Joestan and Galinak stream gauges throughout the duration from 1995 to 2004 can be seen in Table 4.1. Deviancy of predicted runoff amounts from the observed ones at Joestan station is higher than at Galinak. The deviance at Galinak station for the calibration period is 1.24 % and that for the validation period is −5.34 %. This arithmetical standard was the deviance of runoff amounts (ASCE 1993), which is an estimation of a model's knack to expect the overall amount of runoff for the whole investigation time. Van Liew et al. (2003) stated that deviance of runoff amount ±20 % were reflected good, amount ranging between ±20 and ±40 % were reflected satisfactory and amount higher than ±40 % were reflected unsatisfactory. These series utilized in order to check model performance. In the case of Joestan station, the resultant amounts for the aforementioned duration were 16.07 and 27.26 %, correspondingly. Consequently, overall predictions for water yield at Galinak station were more consistent than those for Joestan station.

4.3.4.2 Yearly Discharge Yield

The overall observed and predicted runoff rates computed using the SWAT for the calibration and validation periods at Galinak and Joestan stations are described in Table 4.3. The findings reveal that the highest and lowest deviances occurred on

Table 4.3 Results of the statistical assessment of model performance on the yearly discharge in the calibration and validation periods at Joestan and Galinak stream gauging stations

Gauging station	Model development stage	Dv (%)	MARE	R^2	SE	E_{NS}
Joestan	Calibration	16	0.17	0.98	0.98	0.45
	Validation	27.26	0.15	0.86	0.79	0.83
Galinak	Calibration	1.24	0.17	0.87	1.54	0.47
	Validation	−5.31	0.20	0.98	0.89	0.84

2001, 1993 with −39.40 and −0.29 % for the Galinak station and this deviancy for Joestan station was 34.83, −0.93 % on 1995, and 1997, correspondingly. The mean deviance for Galinak station is −3.34 however for Joestan station it was 7.07. The deviations in, and between, the observed and predicted discharges during the calibration and validation periods are demonstrated by Figs. 4.12, and 4.13 for Joestan station and in Figs. 4.14, and 4.15 for Galinak stream gauges.

The observed and predicted annual runoff quantity predictions at Joestan and Galinak watercourse gauges demonstrate the big R^2 values correspondingly in the calibration and validation periods (Table 4.3). The coefficient of determination is calculated by the following Eq. (4.5):

$$R^2 = \left[\frac{\sum_{i=1}^{n} (Q_i - \bar{Q})(Q'_i - \overline{Q'})}{\sqrt{\sum_{i=1}^{n} (Q_i - \bar{Q})^2} \sqrt{\sum_{i=1}^{n} (Q'_i - \overline{Q'})^2}} \right]^2 \tag{4.5}$$

where Q denotes the observed streamflow, Q′ the simulated streamflow. $\bar{Q}$ and $\overline{Q'}$ denote the average observed and simulated streamflows, correspondingly. The best model performance is described by an R^2 value of 1 or very approximately so, and vice versa.

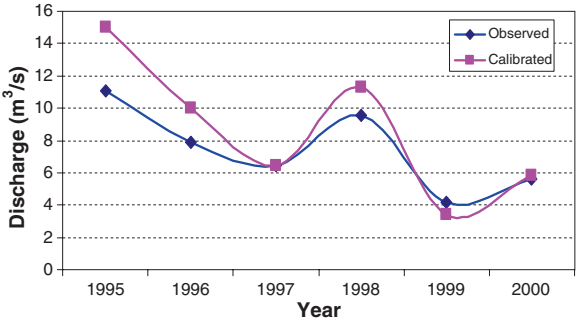

Fig. 4.12 The average annual discharge at Joestan stream Gauging station from 1995 to 2000 in the calibration period according to SWAT

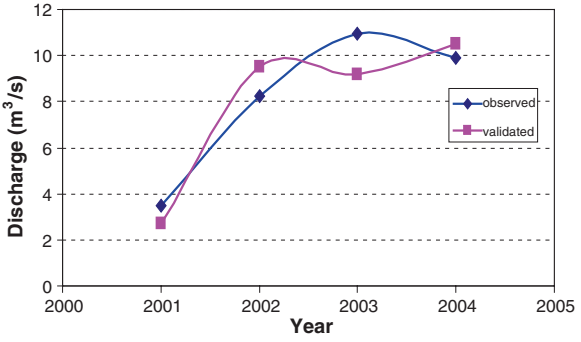

Fig. 4.13 The average yearly discharge at Joestan stream Gauging station in the validation period according to SWAT from 2001 to 2004

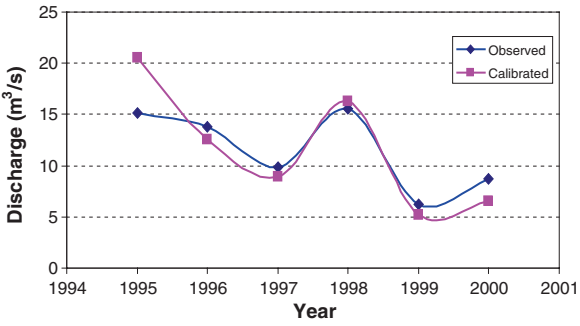

Fig. 4.14 The average yearly discharge at Galinak stream Gauging station from 1995 to 2000 in the calibration period according to SWAT

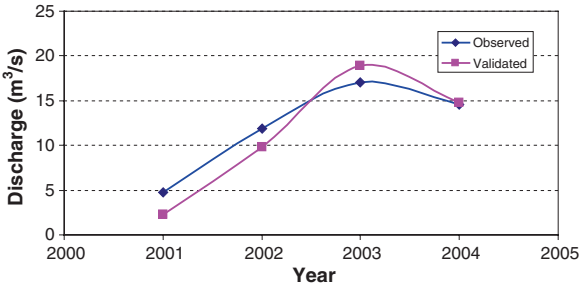

Fig. 4.15 The average yearly discharge at Galinak stream Gauging station in the validation period according to SWAT from 2001 to 2004

Coefficient of efficiency represents the fraction of the variance of the observed runoff that is accounted for by the model (Nash and Sutcliffe 1970). The coefficient of efficiency is calculated by Eq. (4.6).

$$E_{NS} = 1 - \frac{\sum_{i=1}^{n} (Q_i - Q_i')^2}{\sum_{i=1}^{n} (Q_i - \bar{Q})^2} \tag{4.6}$$

where E_{NS} indicates the coefficient of efficiency, Q_i indicates the observed runoff (mm), Q' indicates the predicted runoff (mm), and $\overline{Q}$ indicates the average observed runoff (mm) throughout the simulation period. The values for the coefficient of efficiency can be in range of highly negative values to 1, with 1 demonstrating an exact fit fit concerning the observed and predicted runoff. The coefficient of efficiency for Joestan and Galinak validation periods were 0.83 and 0.84 respectively. As these calculated values were larger than 0.75, therefore this standard indicates excellent results for both stations. The coefficient for calibration periods were 0.45 and 0.47 for both Joestan and Galinak that show satisfactory results. It was reported by Motovilov et al. (1999) that the values larger than 0.75 indicate good simulation of a model and satisfactory for values in the range of 0.75 and 0.36. These ranges were used to categorize model performance.

4.3.4.3 Yearly Sediment Yield Output

Table 4.4 describes the overall yearly observed sediment yields and those predicted by SWAT for the calibration and validation periods at Joestan and Galinak stations. It is indicated by SWAT that the highest and lowest deviances of the predicted sediment yields from the observed ones at Galinak station were 62.31 and 2.11 % 2001 and 1994, correspondingly. SWAT runs shows that the highest and lowest deviances of the predicted sediment yields from the observed ones at Joestan station for 2002 and 2003 were 29.99 % in 2002 and 1.79 % in 2003, respectively. The average deviance between 1992 and 2004 at Galinak station was −6.69 % however it was significantly greater i.e. 9.46 % at Joestan station. Figures 4.16, and 4.17 depicts not only observed and predicted sediment yields but also the resultant deviances of the predicted amount from the observed ones

Table 4.4 The average yearly observed and predicted sediment yields during the calibration and validation periods at Joestan and Galinak stations (1992–2004)

Year	Sediment yield					
	Joestan			Galinak		
	Observed (t)	Predicted (t)	Deviation (%)	Observes (t)	Predicted (t)	Deviation (%)
1992	553,892.2	583,235	5.30	1,338,301	1,374,045	2.67
1993	198,043.2	216,710	9.43	436,619.14	418,262	−4.20
1994	382,292	406,487	6.33	1,145,434.1	1,169,606	2.11
1995	357,362.1	340,791	−4.64	748,467.22	1,191,108	59.14
1996	219,439.4	230,486	5.03	845,973.01	657,498	−22.28
1997	164,359.8	168,821	2.71	399,169.45	349,931	−12.34
1998	306,600.8	360,275	17.51	1,008,521.3	875,314	−13.21
1999	58,027.15	59,896	3.22	113,257.84	117,860	4.06
2000	117,833.7	127,695	8.37	331,353.44	232,828	−29.73
2001	39,889.57	48,363	21.24	64,091.29	24,158.2	−62.31
2002	226,321.9	294,194	29.99	550,236.43	478,045	−13.12
2003	388,506.4	395,476	1.79	1,080,217.9	1,199,546	11.05
2004	261,387	305,217	16.77	749,935.29	684,179	−8.77
Ave.	251,843	272,127	9.46	677,814	674,799	−6.69

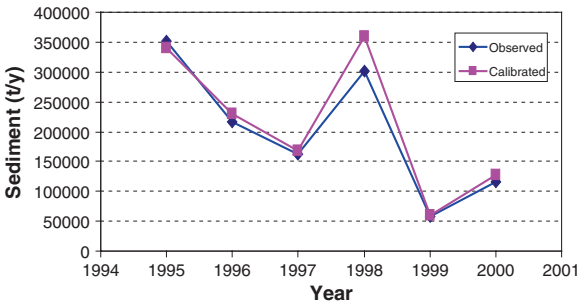

Fig. 4.16 Average yearly sediment yields at Joestan stream Gauging station during the calibration period from 1995 to 2000 as determined from SWAT

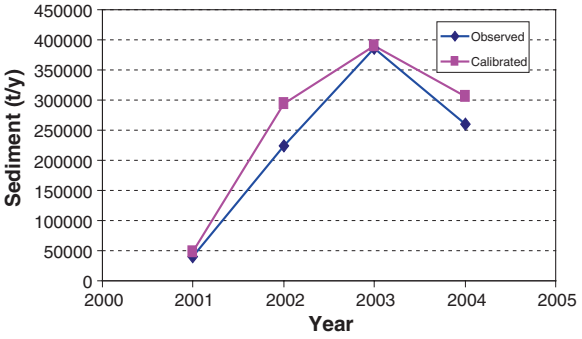

Fig. 4.17 Average yearly sediment yields at Joestan stream Gauging station during the validation period from 2001 to 2004 as determined from SWAT

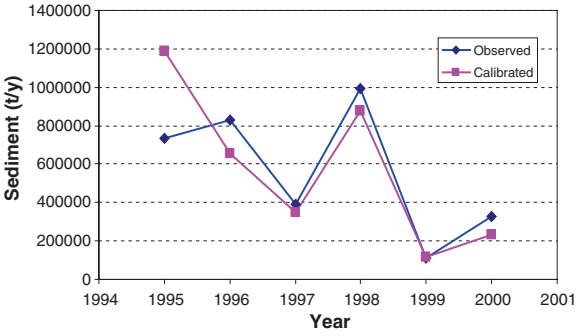

Fig. 4.18 Average yearly sediment yields at Galinak stream Gauging station during the calibration period from 1995 to 2000 as determined from SWAT

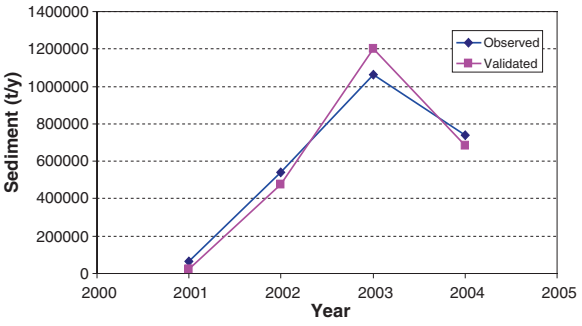

Fig. 4.19 Average yearly sediment yields at Galinak stream Gauging station during the validation period from 2001 to 2004 as determined from SWAT

throughout the calibration and evaluation periods at Joestan station and the same is presented in Figs. 4.18, and 4.19 for Galinak station. Findings related to deviances point out that predicted average yearly sediment at Joestan were acceptable for the years 2001 and 2002 as range of deviances were found between ±20 and ±40 %. Other predicted values were good, as calculated range of deviance was found between −20 and +20. The deviances noted in 1995 and 2001 were 59.14 and −62.31 which shows unacceptable values. These large deviances for average yearly sediment yield at Galinak station imply various parameters like dry year, summer rainfall, overgrazing in low altitude and so on. These large deviances lead to generate average yearly sediment in lower altitudes. This large deviance

revealed unbalanced average yearly sediment at Galinak station. Nevertheless, on the whole, mean deviance in this station predicted −6.69 % that is satisfactory regarding this investigation.

It is evident from statistical studies and examining average yearly sediment yield estimations and predictions for Galinak and Joestan stream gauges that the deviance (Dv) is associated to the model calibration and validation periods for Galinak station.

Calibration of the model was done in two steps:

1. Calibration of the model by SUFI2 and ParaSol programs in monthly period. In this phase ranges of optimized factors were attained by both programs.
2. Statistical examination was applied to relate both programs. SUFI2 and ParaSol were designated for calibration and water balance correspondingly.

This deviance for Joestan is comparatively larger. Though, the coefficient of efficiency is large throughout this phase of model development for Joestan station. The deviance value for model during validation period at Galinak station is equivalent to 0.17 and that the efficiency coefficient is equivalent to 0.95 (Table 4.5), thus was decided that the model is usable and generalizable sufficiently well. The arithmetical consequences direct good and acceptance values at Joestan station in both phases.

The outcomes of the statistical assessments of model presentations on the monthly sediment yields in the calibration and validation phases at Joestan and Galinak stream gauge stations are précised in Table 4.6. Although mean absolute error (MARE) presented comparatively large values throughout both model period phases at Joestan and Galinak stations, both the R^2 and NS coefficient upheld positions in the range of the lower level of good values i.e. 0.75 to 1 values and henceforth they specify good model predictions in this investigation.

Table 4.5 Description of the statistical assessment of model performance on the yearly sediment yield predictions in the calibration and validation periods at Joestan and Galinak stream Gauging stations

Gauging station	Period	Dv (%)	MARE	R^2	SE	E_{NS}
Joestan	Calibration	6.62	0.08	0.96	24,417	0.93
	Validation	14	0.18	0.96	37,063	0.88
Galinak	Calibration	1.01	0.23	0.69	109,776	0.54
	Validation	0.17	0.23	0.98	72,997	0.95

Table 4.6 Description of the statistical assessment of model performance on the monthly sediment yield in the calibration and validation periods at Joestan and Galinak stream Gauge stations

Gauging station	Model development stage	MARE	R^2	SE	E_{NS}
Joestan	Calibration	2.05	0.77	13,868	0.75
	Validation	3.10	0.85	12,813	0.76
Galinak	Calibration	1.30	0.79	42,988	0.74
	Validation	1.26	0.91	29,833	0.90

4.3.4.4 Daily Yield

The calculation and prediction of yearly discharge and rate of precipitation clarify unstable rates of discharge for both stream gauge stations throughout the period from 1992 to 2004 (Fig. 4.20). It is shown in Table 4.4 that yearly runoff rates are influenced significantly by precipitation. However by reason of the impacts of land uses, soil characteristics, topography, and so on, runoff rates do not exactly correspond with those of precipitation.

With the purpose of assessment of daily runoff rates and sediment yields, data consisting of three years for Galinak stream gauge were collected; dry year (2000), normal year (2002), and wet year (2003). The fallouts of detected and predicted mean rates of daily discharge and capacities specify that, as a whole, deviance of the predicted values from the detected ones in the normal year was small i.e. −3.3 % (Table 4.7). It was observed that the deviance of average predicted daily discharges averaged throughout the year from the corresponding detected values was maximum i.e. 45.9 and −19 % in the dry and wet year respectively. For the reason that maximum deviance of average daily discharge in dry year was 45.9 %, so outcomes of average daily discharge were unacceptable in Taleghan investigated region. The small value of coefficient efficiency was confirmed this outcome. The coefficient of efficiency for the wet and dry years specifies unsatisfactory value to predict average daily discharge using model. Figures 4.21, 4.22, and 4.23 portray that less deviance (3.3 %) and satisfactory coefficient efficiency (0.65) for Normal year prove the model proficient to predict average daily discharge in this meteorological condition.

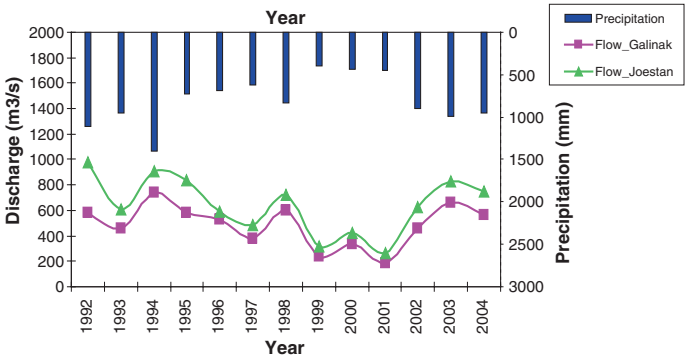

Fig. 4.20 Discharge rates at Galinak stream Gauging station during 1992–2004

Table 4.7 Average observed and predicted average daily discharges and runoff volumes in diverse meteorological conditions averaged on a yearly basis

Year condition	Discharge (m^3/s)		Runoff volume (m^3)		Deviation (%)	E_{NS}
	Observed	Predicted	Observed	Predicted		
Dry (2000)	8.74	4.73	275,692,447	149,068,992	45.9	0.21
Normal (2002)	12.02	12.42	379,192,398	391,817,029	−3.3	0.65
Wet (2003)	17.51	20.83	552,178,752	656,932,684	−19.0	0.42

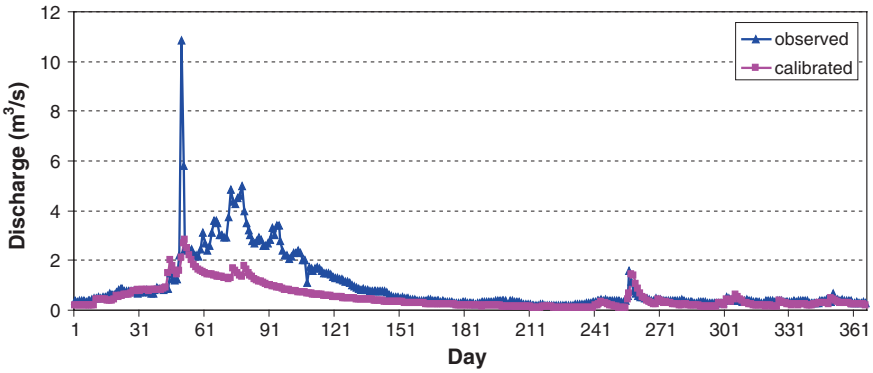

Fig. 4.21 Observed and calibrated daily discharge at Galinak station in the dry period (2000)

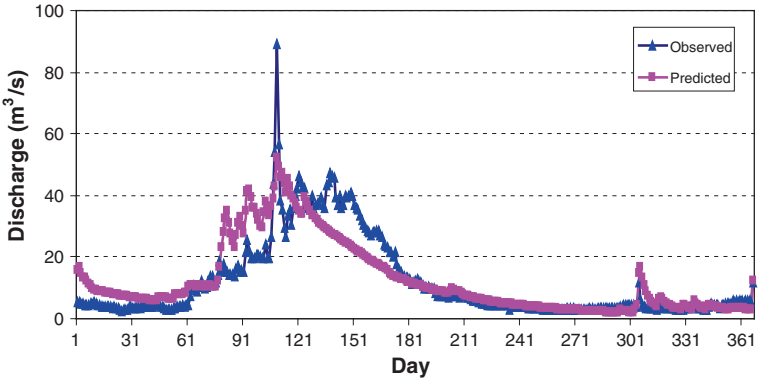

Fig. 4.22 Observed and calibrated daily discharge at Galinak station in the normal period (2002)

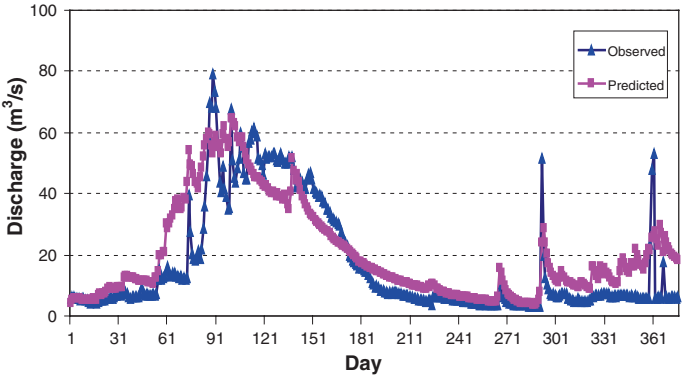

Fig. 4.23 Observed and calibrated daily discharge at Galinak station in the wet period (2003)

4.3.5 Runoff Modules

Assessment of the runoff modules in this investigation required implementation of the relevant considerations adjusted by SUFI2 to examine the enactment of SWAT in both the model calibration and validation phases. The runoff modules comprise of surface runoff, lateral flow, and groundwater flow. As, illustration of dissimilarity between the modules of runoff is random and the origins of the water flowing through a gauging station cannot be observed (Linsley et al. 1949, 1982; Klemes 1986), relating the anticipated fluctuations compared to some observations at the two gauging stations contained by the Taleghan basin is not conceivable.

Ground water flow, lateral flow and monthly surface runoff have been represented in Figs. 4.24, and 4.25 at Galinak and Joestan stream gauges. The

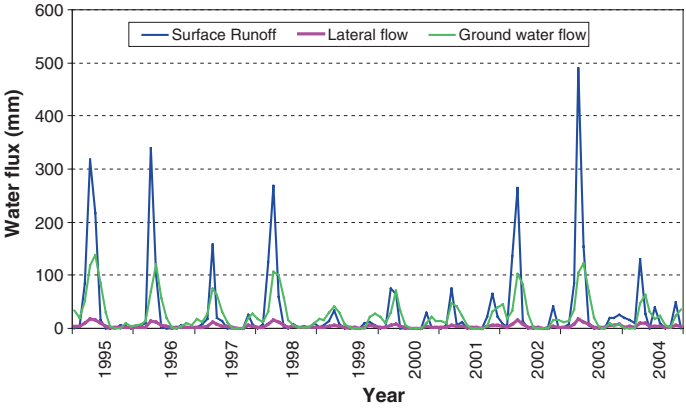

Fig. 4.24 Predicted monthly surface runoff, lateral flow, and groundwater flow at Joestan station (1995–2004)

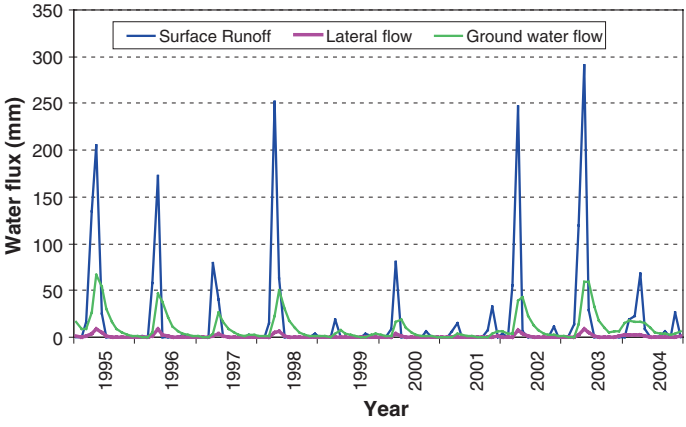

Fig. 4.25 Predicted average monthly surface runoff, lateral flow, and groundwater flow at Galinak station (1995–2004)

fallouts point out strong response of surface runoff during the model calibration (1995–2000) and validation (2001–2004) periods.

That insignificant lateral flow is attributed to the heavy soil texture in both phases. Groundwater flow seems to be rather modest. Consequences relating to Joestan station nearly revealed the pattern in comeback to detect at Galinak station. Nevertheless postponement in groundwater flow was highly prominent in the former than in the latter.

4.3.6 The Water Balance

Table 4.8 summarizes the data regarding water balance at Joestan and Galinak stations expected for the computer-generated Catchment from the 1987 and land use data for the duration of January, 1995, to August, 2004. It is revealed that around 21.16 and 33.16 % of the entire precipitation were surface runoff at Joestan and Galinak stations, correspondingly. Groundwater and lateral flows occur commonly in the upper area of the Catchment, at high elevation. At Joestan and Galinak stations, about 38.24 and 48.85 % of the entire precipitation correspondingly is wasted through evapotranspiration.

The monthly fractions of various water passageways of input to the river flow for Joestan and Galinak stations have been described in Figs. 4.26, and 4.27 for Galinak station, respectively. It can be observed that during the course of April to the end of May, the main sources of the river flow are surface runoff caused by the extreme storms and melting of snow taking place throughout that phase. Maximum proportion of the surface runoff in June is influenced by melting of snow that occurring at regions of high altitude. The average monthly surface modules at Joestan station from April to May were compared and differed to a large extent i.e. 100 %, despite the fact that this contrast at Galinak station represents less deviation of average monthly surface modules i.e. 5 % during these two months. This explains that there is a postponement caused by melting of snow at

Table 4.8 Predicted water balance at Joestan and Galinak stations for the simulated catchment from the 1987 land use data for the period January, 1995–August, 2004

Variable	Joestan		Galinak	
	Total amount (mm)	Fraction of precipitation (%)	Total amount (mm)	Fraction of precipitation (%)
Precipitation	10,056.99	100	7009.68	100
Evapotranspiration	3846.02	38.24	3424.17	48.85
Surface runoff	2128.08	21.16	2324.18	33.16
Lateral flow	1403.17	13.95	117.7	1.68
Groundwater flow	2330.03	23.17	1183.4	16.88
Water loss	349.71	3.48	−39.77	−0.57

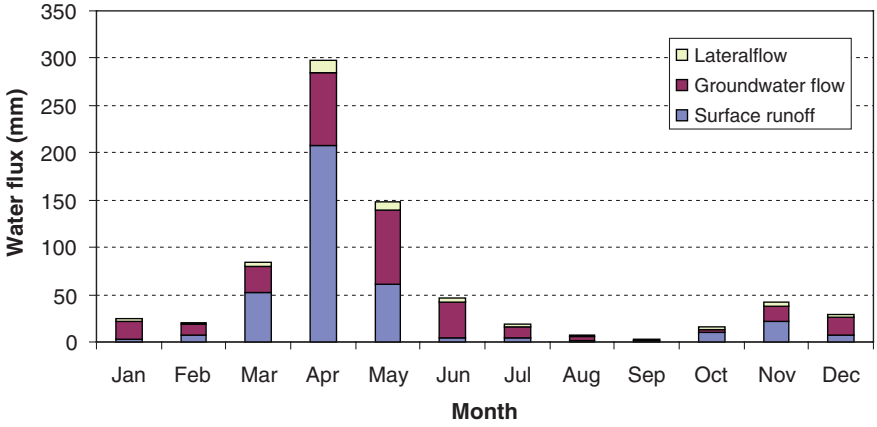

Fig. 4.26 The average monthly ratios of various water passageways of input to the river flow at Joestan station

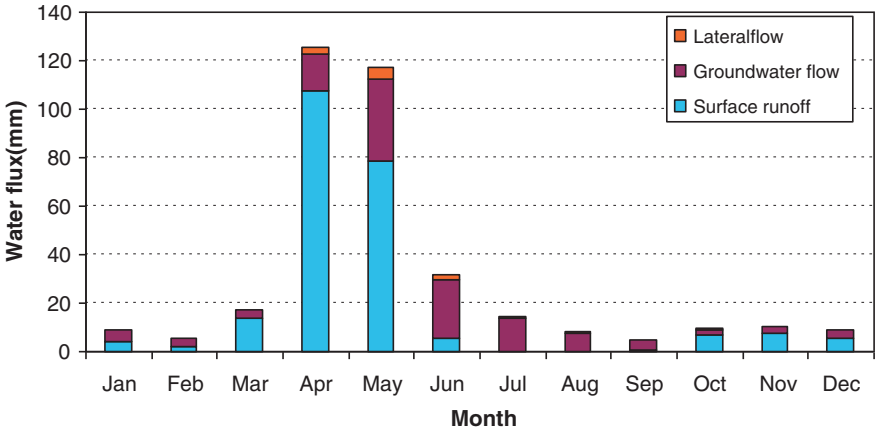

Fig. 4.27 The average monthly ratios of various water passageways of input to the river flow at Galinak station

Joestan station which is positioned at high altitude having extremely cold climatic conditions. This region experiences an extensive dry spell that encompasses from July to the end of subsequent February in the sub-sequential year.

4.3.7 Response of Water Modules and Sedimentation to Land Use Changes

The water balance was stabilized on adjusted values identified by means of calibration and validation with the land uses specified in 1987. To explore the impacts

of land use variations on water balance, two land use scenarios were inspected with the adjusted factors. These land uses were associated with 2001 and 2007.

Figures 4.28, 4.29, and 4.30 portrays that the average yearly water yield modules involving surface runoff, lateral flow, and groundwater flow follow dissimilar pattern, correspondingly. It is illustrated by figures that land use changes lead to

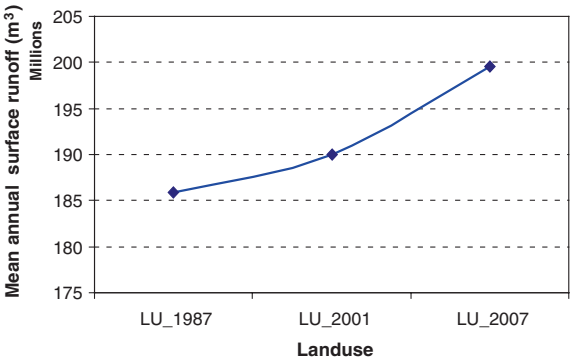

Fig. 4.28 Impacts of land use variations in the years 1987, 2001, and 2007 on the average yearly surface runoff

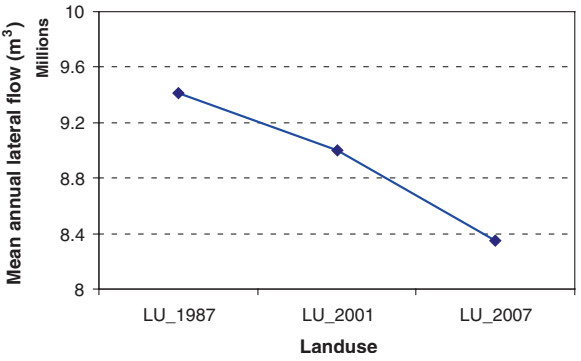

Fig. 4.29 Impacts of land use variations in the years 1987, 2001, and 2007 on the average yearly lateral flow

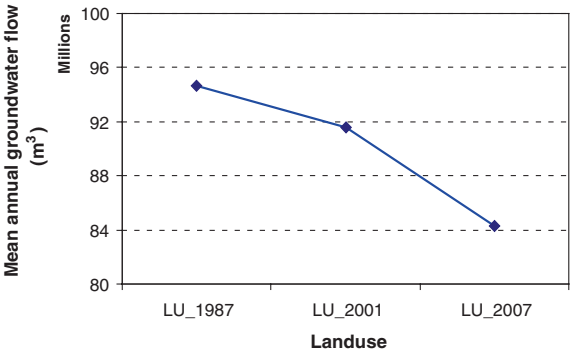

Fig. 4.30 Impacts of land use variations in the years 1987, 2001, and 2007 on the average yearly groundwater flow

pattern of rise in the surface runoff throughout the period of investigation. But the lateral and groundwater flows dropped in the same duration.

A comprehensive comparison of the water balance modules from 1995 to 2004 reveals that the proportion of the entire surface runoff to the entire volume of precipitation at Joestan station rose from 21.16 to 26.13 %. The respective proportion at Galinak station rose from 33.16 to 35.58 % throughout the same period. Within same duration, the overall lateral and groundwater flows declined at both stations. Though, the overall evapotranspiration at both places transformed the least within same duration (Tables 4.9, and 4.10).

The ratio of the entire runoff to the entire lateral and groundwater runs indicates that this proportion elevated by 20 % i.e. from 1.79 to 2.15 at Galinak station. This proportion at Joestan station elevated by 36 % i.e. from 0.69 to 0.94. This proportion is the evidence of elevated values of surface runoff in downstream of Galinak station during past twenty years in the investigated region (Fig. 4.31).

Table 4.11 summarizes the outcomes of suspended sediment yields at Joestan and Galinak stations in 1987, 2001, and 2007. This table represents a comparatively large sedimentation yield at both sites. The amount of sediment yields promoted from 5.81 to 6.68 t ha^{-1} at Joestan station and from 7.26 to 8.28 t ha^{-1} at Galinak station. The changes increase the risk for the aquatic life of the dam. A simple

Table 4.9 The water balance at Joestan station during 1995–2004

Variables	LU_1987		LU_2001		LU_2007	
	Total (mm)	(%)	Total (mm)	(%)	Total (mm)	(%)
Precipitation	10,057	100	10,057	100	10,057	100
Evapotranspiration	3846.02	38.24	3843.66	38.22	3834.36	38.13
Surface runoff	2128.08	21.16	2280.24	22.67	2628.38	26.13
Lateral flow	1403.17	13.95	1376.5	13.69	1269.39	12.62
Groundwater flow	2330.03	23.17	2218.51	22.06	2010.4	19.99
Water loss	349.71	3.48	338.08	3.36	314.46	3.13

Table 4.10 The water balance at Galinak station during 1995–2004

Variables	LU_1987		LU_2001		LU_2007	
	Total (mm)	(%)	Total (mm)	(%)	Total (mm)	(%)
Precipitation	7009.64	100	7009.64	100	7009.64	100
Evapotranspiration	3424.17	48.85	3417.73	48.76	3404.95	48.58
Surface runoff	2324.18	33.16	2375.48	33.89	2493.98	35.58
Lateral flow	117.7	1.68	112.46	1.60	104.35	1.49
Groundwater flow	1183.4	16.88	1145.06	16.34	1053.27	15.03
Water loss	−39.81	−0.57	−41.09	−0.59	−46.91	−0.67

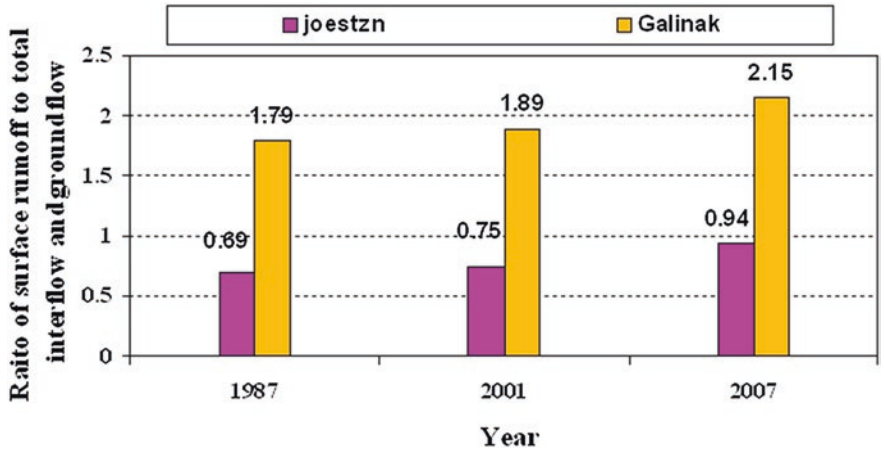

Fig. 4.31 The ratio of total surface runoff to total lateral and groundwater flows from 1995 to 2004

Table 4.11 Mean sediment yield at Joestan and Galinak stations in the years 1987, 2001, and 2007

Station	LU_1987		LU_2001		LU_2007	
	Average (t)	(t/ha)	Average (t)	(t/ha)	Average (t)	(t/ha)
Joestan	232,457	5.81	248,729	6.21	267,325	6.68
Galinak	581,047	7.26	615,909	7.69	662,393	8.28

calculation of sediment yield, supposing that Galinak station encompasses 90 % of the entire dam basin and that the mean soil enormity is equivalent to 2.2 kg m^{-3}, shows that if this pattern lasts even in the upcoming years, at that time, the storing capacity of reservoir will be reduced in excess of 300,000 m^3 for each year.

4.3.8 Susceptibility of Subbasins to Erosion

One of the key requisites of the catchment manager guiding monitoring of sedimentation is categorizing susceptible subbasins. SWAT has capability to calculate input and output of sediment for each subbasin. Figure 4.32 portrays the grading of sub-catchment susceptibilities to erosion. Extreme erosion i.e. 152,300 ton $year^{-1}$ is predictable to occur in subbasin 1. Temporarily, the least erosion occurs in the north hill slopes. The darker the label color is, the less susceptible is the specific subbasin, and vice versa.

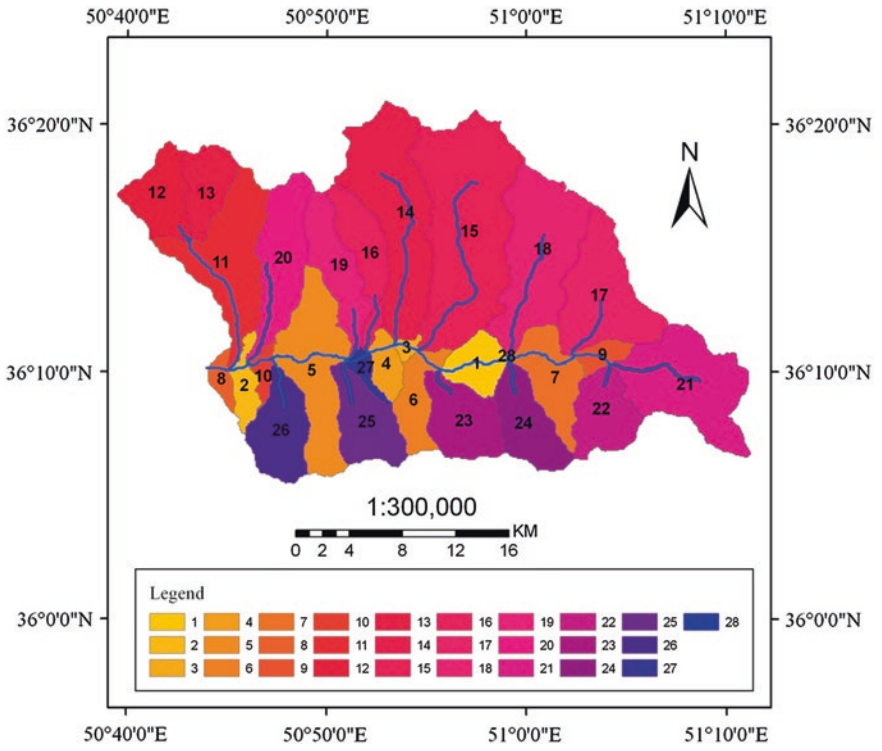

Fig. 4.32 Grading of susceptibilities of Subbasin to erosion

4.3.9 Land Use Scenarios

In this investigation seven scenarios regarding land use variation were examined on different degrees of slope steepness to accomplish the water balance and sediment yield in the forthcoming years (Table 4.12). The scenarios are given below:

1. The last-observed land use (2007)
2. Transmuting rangeland into agricultural land uses in regions of 0–20 % gradient;
3. Transmuting agricultural land uses into urban ones in region of 0–20 % gradient;
4. Transmuting agricultural land uses into urban ones in regions of 0–40 % gradient;
5. Transmuting rangeland into urban land uses in regions of 0–20 % gradient;
6. Transmuting rangeland into bare soil in regions of 0–40 % gradient; and
7. Transmuting all rangeland in the investigation region to bare soil.

Table 4.12 Predictions of the impacts of land use variation scenarios on the average water balance modules and sediment yield during 1995–2004 in the Taleghan area

No.	Scenario	Slope (%)	Precipitation (mm)	Evaporation (mm)	Surface runoff (mm)	Lateral flow (mm)	Groundwater flow (mm)	Sediment yield (t/ha)
1	Current land use (2007)	–	701	340.5	249.4	10.43	105.3	8.28
2	Rangeland to agricultural land	0–20	701	342.7	260.2	9.82	83.54	8.65
3	Agricultural land uses to urban ones	0–20	701	344.4	262.4	9.21	80.25	8.07
4	Agricultural land uses to urban ones	0–40	701	346	268.2	8.4	73.66	7.81
5	Rangeland land uses to urban ones	0–20	701	344.8	270.1	7.3	74.06	8.18
6	Rangeland to bare soil	0–40	701	342.1	274.2	6.1	73.86	9.31
7	Rangeland to bare soil	all	701	346.7	286.9	4.7	57.96	9.87

The results of water balance exhibited less deviation in the average actual rates of evaporation rates subjected to the various scenarios inspected. The lowest and highest positive differences in this module were 2.2 mm in scenario 2 and 6.2 mm in scenario 7, correspondingly. The land use variations in the seven scenarios had unpredictable impacts on the water modules in association with slope gradient. Maximum deviations were detected on water modules when transmuting all land uses in the investigation region into bare soil i.e. scenario 7. Relating scenario 7 with scenario 1 revealed that surface runoff increased by 15 % i.e. 37.4 mm and groundwater flow decreased by 45 % i.e. 47.3 mm. Furthermore, the outcomes exposed that, rendering the Scenario 6, transmuting rangeland to bare soil in gradients 0–40 % (i) generated 10 % i.e. 24.8 mm extra surface runoff than the last land use i.e. scenario 1 and (ii) reduced the groundwater flow up to 30 % i.e. 31.44 mm comparative to the scenario 1. Scenario 5 disclosed that surface runoff increased by 8 % and groundwater flow reduced by 30 %. Scenarios 3 and 4 point out that surface runoff increased by 13 and 18.8 mm in surface runoff and while groundwater flow reduced by 25 and 31.64 mm respectively in corresponding scenario 1. Scenario 2 revealed almost low deviation in surface runoff and groundwater flow with respect to scenario 1 (Land use 2007).

The predicted outcomes of sediment yield related to the seven scenarios revealed that the least and extreme upsurges in sediment yields, in contrast with scenario 1, were 4.4 % i.e. 0.37 t ha^{-1} rendering for scenario 2 and 19.2 % i.e.

1.59 t ha^{-1} (19.2 %) rendering for scenario 7. According to Scenarios 3 and 6, there were upsurges in sediment yields up to 5.3 and 12.4 % each year, correspondingly, when related with scenario 1. Upsurges up to 2.3 and 1.2 % disclosed by scenarios 4 and 5 correspondingly once related with scenario 1. Table 4.10 portrays the differences in the water modules and sediment yields considering the various examined scenarios.

The outcomes of examination of scenarios regarding water balance displayed changed scenarios on different gradients steepness have slightest deviation on evapotranspiration in the investigated region. Additional deviation on water modules occurred regarding scenarios 7, where entire rangelands transformed into bare soil. One more precarious water module with cumulative surface runoff and declining groundwater flow occurred where rangelands transforming into bare soil in gradient steepness 0–40 %.

The predicted outcomes of sediment yield were related to the seven land use scenarios. The extreme upsurge in sediment yields related to the last observed land use (2007) was 19 % i.e. 1.6 t ha^{-1} regarding scenario 7 (all rangeland is bare). Scenario 2 i.e. rangeland to agriculture, 0–20 % and scenario 6 i.e. rangeland to the bare, 0–40 % revealed upsurge up to 4 and 12 % correspondingly. Scenario 3 i.e. agriculture to urban 0–20 % gradient, scenario 4 i.e. agriculture to the urban, 0–40 % gradient, and scenario 5 i.e. rangeland to the urban, 0–20 % gradient revealed reductions in sediment yields up to 2.5, 5.7 and 1.2 % correspondingly.

4.4 Conclusion

A database technique for exploring the water balance and water quality variations across different land uses within the Taleghan catchment was effectively settled. The prediction of water balance at Joestan and Galinak stations was performed for the simulated catchment for the duration January from 1995 to August 2004. Groundwater and lateral flows occurred generally in the highly elevated hilly region of the catchment. The foremost cause for this progression was the slow melting of snow packs at upper altitudes. Low temperatures at higher altitudes promote infiltration; consequently, further interflow occurred at these altitudes. Moreover, the good rangeland frequently positioned in the higher regions of the catchment was unreachable to the people grazing animals. Cumulative land cover downstream of Joestan station was highly significant subsidize to the many water modules.

The monthly magnitudes of altered water passageways point out that mostly surface runoff is the main source of the river flow consequently extreme storms and snow melt taking place throughout April and May. A large proportion of the surface runoff in June relies on snow melt that occurs at high altitude regions. A contrast of average monthly surface modules at Joestan station flanked by April and May exhibited highly considerable dissimilarities between them i.e. 100 %,

however low distinction i.e. 5 % at Galinak station. This proves a postponement by reason of snow melt at Joestan station which is at high altitude with low temperatures.

A growing trend in surface runoff was followed by degradation of land use. Nevertheless the lateral and groundwater flows deteriorated in the same duration. A positive trend was obtained for surface runoff and negative trend for interflow throughout the investigation period, particularly for the subsequent phase (2001–2007). Consequently, one of the leading programs for organizers is to monitor this enhanced degradation that occurred in the past ten years.

The suspended sediment yields at Joestan and Galinak stations in 1987, 2001, and 2007 were comparatively high. The sediment yields amplified from 5.81 to 6.68 t ha^{-1} at Joestan station and from 7.26 to 8.28 t ha^{-1} at Galinak station. The upsurge is a source for anxiety about the natural life of the dam reservoir. Meanwhile Galinak station comprises the 90 % of the entire dam catchment and that the mean density of soil is 2.2 t m^{-3}, following this pattern there will be a loss of in excess of 300,000 m^3 of the stored reservoir each year. This great quantity of sediments is a basis of thoughtful alarm to the government and policy makers, in future demanding healthier catchment management practices.

This investigation has effectively established a modified SWAT model for the investigated region to be employed by managers and water engineers in the catchment in their policies of upcoming land improvements. Managers will be able to explore the impacts of different land use variation scenarios on the existing water quantity and sediment yield in the catchment. By means of the modified model, organizers and policy makers will have right to use an established model for predicting sediment yield and water supply for the future. The modified model can be implemented for ungagged catchments in semi-arid areas for the prediction of flow rate and sediment yield. Thanks to the efficacious employment of the SWAT model for Taleghan region, it can be suggested for regions with the alike climatic conditions.

References

Arnold JG, Srinivasan R, Muttiah RS, Williams RJ (1998) Large area hydrologic modeling and assessment part I: model development. J Am Water Resour Assoc 34(1):73–89

ASCE (1993) Criteria for evaluation of watershed models. J Irrig Drain Eng 119:429–442

De Martonne E (1926) Une nouvelle fonction climatologique: l'Indice d'Aridité. La Météorologie 2(2):449–458

Klemes V (1986) Dilettantism in hydrology: transition or destiny? Water Resour Res 22(9):177–188

Linsley JRK, Kohler MA, Paulhus JLH (1949) Applied hydrology. McGraw-Hill, USA

Linsley JRK, Kohler MA, Paulhus JLH (1982) Hydrology for engineers. McGraw-Hill, USA

Motovilov YG, Gottschalk L, Engeland K, Rodhe A (1999) Validation of a distributed hydrological model against spatial observations. Agric For Meteorol 98–99:257–277

Nash JE, Sutcliffe JV (1970) River flow forecasting through conceptual models 1. A disscussion of principales. J Hydrol 10(3):282–290

Van Liew MW, Arnold JG, Garbrecht JD (2003) Hydrologic simulation on agricultural watersheds: Choosing between two models. Trans. ASAE 46(6):1539–1551